EPA-650/2-74-045

June 1974

Environmental Protection Technology Series

KINETIC MECHANISM OF METHANE/AIR COMBUSTION WITH POLLUTANT FORMATION

Office of Research and Development
U.S. Environmental Protection Agency
Washington, DC 20460

EPA-650/2-74-045

KINETIC MECHANISM OF METHANE/AIR COMBUSTION WITH POLLUTANT FORMATION

by

C. H. Waldman, R. P. Wilson, Jr., and K. L. Maloney

Ultrasystems, Inc.
2400 Michelson Drive
Irvine, California 92664

Contract No. 68-02-0270
ROAP No. 21ADG-10
Program Element No. 1AB014

EPA Project Officer: W. S. Lanier

Control Systems Laboratory
National Environmental Research Center
Research Triangle Park, North Carolina 27711

Prepared for

OFFICE OF RESEARCH AND DEVELOPMENT
U.S. ENVIRONMENTAL PROTECTION AGENCY
WASHINGTON, D.C. 20460

June 1974

This report has been reviewed by the Environmental Protection Agency and approved for publication. Approval does not signify that the contents necessarily reflect the views and policies of the Agency, nor does mention of trade names or commercial products constitute endorsement or recommendation for use.

ABSTRACT

A large set of chemical reactions describing methane/air combustion was evaluated to determine the significant reactions at atmospheric pressure, $1500 < T < 2500^{\circ}K$, and equivalence ratio in the range $0.8 < \phi < 1.25$. The reactions were screened to eliminate (a) reactions whose net contribution to heat evolution or pollutant formation was negligible, (b) species which had no discernable effect on either major species or temperature, and (c) groups of reactions constituting only species exchange loops. A set of 26 reactions/17 species was derived which can duplicate to $\pm$ 5% the predictions of the 134 reaction/25 species master set. Ten additional pyrolysis reactions are cited for low-temperature and fuel-rich applications. The Zeldovich mechanism is the principal route to NO for stoichiometric combustion, but under lean conditions, a path to NO involving N_2O is also active. For fuel-rich conditions, comparison with stirred reactor data suggest that NO formation cannot be explained by the Zeldovich mechanism alone, and an alternate path involving species of the type RN may be of importance. Finally, prompt NO arising from O-atom overshoot was not predicted for an idealized plug flow ignition case.

This report was submitted in partial fulfillment of Contract No. EPA 68-02-0270 by Ultrasystems, Inc. under sponsorship of the Environmental Protection Agency. Work was completed as of February 1974.

TABLE OF CONTENTS

Section		Page
	ABSTRACT	iii
	LIST OF FIGURES	vii
	LIST OF TABLES	viii
	ACKNOWLEDGEMENTS	ix
	CONCLUSIONS	x
	RECOMMENDATIONS	xii
I.	INTRODUCTION	1
	A. Chemical Kinetics--An Important Factor in Combustion-Generated Nitrogen Oxides	1
	B. Detailed vs. Global Hydrocarbon Kinetics	1
	C. Objectives	2
	D. Methods for Determining the Kinetic Mechanism	3
II.	A SYSTEMATIC METHOD OF ANALYZING COMPLEX REACTION MECHANISMS	5
III.	SELECTION OF SPECIES, REACTIONS, RATES, AND CONDITIONS	7
	A. Problem Statement: Flame Conditions in Gas-Fired Combustors	7
	B. Species, Reactions, and Rates	9
	C. Screening Criteria	13
IV.	RESULTS FOR PERFECTLY-STIRRED COMBUSTION	16
	A. Stoichiometric ($\phi = 1$) Perfectly-Stirred Reactor	16
	B. Fuel Rich ($\phi = 1.25$) Perfectly-Stirred Reactor	25
	C. Fuel Lean ($\phi = 0.8$) Perfectly-Stirred Reactor	29
	D. Simplifications to the Methane Oxidation Mechanism	32
V.	RESULTS FOR PYROLYSIS, IGNITION, AND POST-FLAME REACTIONS	34
	A. Pyrolysis and Ignition at Stoichiometric ($\phi = 1$)	34
	B. Post-Flame Reactions at Stoichiometric ($\phi = 1$)	46

TABLE OF CONTENTS (Cont)

Section		Page
VI.	SYNTHESIS OF THE SCREENED REACTION SET	51
	A. Union Reaction Set for Five Test Cases	51
	B. Corroboration with Three New Cases	51
VII.	EVALUATION OF REACTION SET AGAINST STIRRED REACTOR DATA	56
	A. Purpose	56
	B. Representation of Experimental Conditions with KAP	57
	C. Predictions Based on Screened Reaction Set	60
	D. Kinetic Revisions to Reconcile Theory with Data	62
	REFERENCES	72
Appendix		
A	Description of the Numerical Program	78
B	Approximation Techniques for Arrhenius Rate Coefficients	85
C	Thermochemical Properties of Methoxyl, CH_3O	87

LIST OF FIGURES

3.1	8-Case Screening Matrix	7
4.1	Methane Oxidation Paths, WSR ($\phi = 1$)	22
4.2	Nitric Oxide Formation Paths, WSR ($\phi = 1$)	24
4.3	Methane Oxidation Paths for Fuel-Rich Stirred Reactor [WSR ($\phi > 1$)]	28
4.4	Methane Oxidation Paths for Fuel-Lean Stirred Reactor [WSR ($\phi < 1$)]	31
5.1	Schematic of Ignition Model	34
5.2	Comparison of Formaldehyde Profiles for IGN ($\phi = 1$)	36
5.3	Effect of Methoxyl (CH_3O) on Ignition Delay [IGN ($\phi = 1$)] (Temperature and Oxygen Mass Fraction)	39
5.4	Methane Oxidation Paths for Ignition [IGN ($\phi = 1$)]	42
5.5	Mass Fraction Profiles for Ignition [IGN ($\phi = 1$)]	43
5.6	Nitric Oxide Profile for Ignition of Preheated Reactants ($\phi = 1$)	44
5.7	Detailed Structure of Ignition Runaway	45
5.8	Profiles for Post-Flame Case (Plug Flow, $\phi = 1$)	46
5.9	Methane Oxidation Mechanisms in Simulated Post Flame Conditions, PFR ($\phi = 1$)	49
5.10	Nitric Oxide Mechanisms in Simulated Post Flame Cases, PFR ($\phi = 1$)	50
6.1	Nitric Oxide Decomposition Observed for PFR ($\phi > 1$)	55
7.1	Jet-Stirred Reactor	57
7.2	Comparison of Experimental Data from Jet-Stirred Reactor with Predictions Based on Various Reaction Sets	61
7.3	Parameter Study on $CH_2 + N_2 \rightarrow CHN + HN$	68

LIST OF TABLES

3.1	Species Included in Present Study	10
3.2	Master Reaction Set	11
4.1	Selected Test Cases for WSR ($\phi = 1$)	16
4.2	Comparison of Results for WSR ($\phi = 1$) Case	17
4.3	Marginal Species [WSR ($\phi = 1$)]	18
4.4	Screened Reaction Set (22 Reax) for Stoichiometric Stirred Reactor [WSR ($\phi = 1$)]	20
4.5	Screened Reaction Set (21 Reax) for Fuel-Rich Stirred Reactor [WSR ($\phi > 1$)	26
4.6	Screened Reaction Set (23 Reax) for Fuel-Lean Stirred Reactor (WSR ($\phi < 1$)	30
5.1	Controlling Reaction Sets for Ignition Case [IGN ($\phi = 1$)]	40
5.2	Screened Reaction Set (23 Reax) for Adiabatic Plug Flow Reactor ($\phi = 1$)	47
6.1	Union of Controlling Reaction Sets	52
6.2	Comparison of Controlling Reaction Set with Those of Previous Investigators	53
7.1	Thermal Conductivity of Firebrick	59
7.2	Determination of Heat Transfer Coefficient for Jet-Stirred Reactor	60
7.3	Rate Revisions Intended to Boost O-Atom Levels	65
7.4	Candidate $R + N_2 \rightarrow R \cdot N + N$ Reactions	66
7.5	Empirically Adjusted 33-Reaction Set for CH_4/Air with Revisions to Table 6.1 Noted (*)	70
B.1	Bond Dissociation Energies	86
C.1	Thermodynamic Functions for Methoxyl (CH_3O)	89

ACKNOWLEDGEMENTS

The authors gratefully acknowledge many helpful discussions with Dr. Victor S. Engleman of ESSO Research and Engineering Co. and Dr. Robert Shaw of Stanford Research Institute.

The research was financed under Contract 68-02-0270 with the U. S. Environmental Protection Agency; Messrs. David W. Pershing and Steve Lanier served as most helpful contract monitors.

CONCLUSIONS

1. Twenty-six reactions can duplicate to $\pm$ 5% the predictions of a 134-reaction master set for methane/air combustion at P = 1 atm, $1500 < T < 2500^{o}K$, and $0.8 < \phi < 1.25$ (see Table 6.1). (page 52)

2. Stirred reactor measurements suggest that NO formation can occur via reactions of the form $R + N_2 \rightarrow RN + N$ which were not included in the 134-reaction set. The possibility that such reactions may be active is corroborated by observations of HCN [Bachmaier et al. (1973)]. A list of potential candidate reactions is given in Table 7.4. (page 66)

3. The controlling mechanism for methane oxidation appears to be similar to that postulated by Fenimore (1964) and Fristrom and Westenberg (1965) and later exercised by Bowman (1970, 1971). There are three departures: (a) The O-radical rather than OH appears to be the major oxidation agent X in reactions $CH_3 + X \rightarrow$, and $CH_2O + X \rightarrow$. (b) Five parallel paths [reactions (36), (44), (47), (52), and (143)] are available between CHO and CO. (c) In CO oxidation, termolecular recombination may be significant.

4. Methane pyrolysis at intermediate temperature ($1200 < T < 1500^{o}K$) appears to be controlled by reactions of the form $CH_n + CH_2O = CHO + CH_{n+1}$. Ten additional reactions appear to be significant (see Table 6.1). (page 52)

5. The bottleneck in NO formation is the rate of breaking up molecular nitrogen, and from our study it appears that the Zeldovich mechanism ($N_2 + O \rightarrow NO + N$) appears to be controlling. Two alternative mechanisms have surfaced: N_2 can collide with an active radical such as CH_2 or OH (see item 2 above) or N_2 can combine with O in a three-body reaction to form N_2O, a fraction of which subsequently goes to NO via $N_2O + O \rightarrow NO + NO$.

6. For ignition idealized as plug flow, the O-atom overshoot is too brief (~.1 msec) to generate nitric oxide and therefore cannot explain "prompt NO" (see, however, item 2 as an alternate explanation of "prompt NO").

7. The following backward rate of the $O + N_2 \rightarrow NO + N$ reaction gives best fit for comparison with stirred reactor data:

$$k_b = 6.31 \times 10^{11} T^{1/2} \quad \text{[Baulch (1969)]}$$

This rate is a factor of X2 greater than that widely used.

8. Nitric oxide appears to decompose in the prolonged presence of formaldehyde at high temperatures, a curiosity which upon further study may have obvious practical applications.

9. Eight species appear to be insignificant to methane oxidation: CH, CN, NO_2, CH_2, HN, CH_3O, CHN, and HNO. Four of the species may have to be restored to account for NO formation, especially under fuel-rich conditions (CH_2, CHN, CN, HN).

RECOMMENDATIONS

1. The NO-formation mechanisms in fuel-rich flames should be characterized with further numerical studies and experiments. Particular attention should be paid to detection of species CH_x and RN which may participate in alternate (non-Zeldovich) mechanisms.

2. Experiments to reduce the uncertainties in the rates of certain key reactions (e.g., $CO + HO = CO_2 + H$, $O + N_2 = NO + N$, and $N_2 + O + M = N_2O + M$) should be undertaken.

3. The sensitivity of the screening method to variations of the reaction rates should be determined.

4. Chemical reaction mechanisms capable of scavenging NO_x should be identified and tested in appropriate experiments.

5. The 26-reaction set derived herein should be exercised on other stirred reactor data and shock-tube data on the CH_4/air system.

6. The screening procedure should be reapplied periodically as rates of individual reactions become better defined.

7. Nitric oxide measurements in well-stirred reactors fired by CH_4/air should be repeated with direct measurements of the heat-transfer rate (which is currently the greatest source of uncertainty in existing data).

8. The effect of stirred-reactor unmixedness upon NO emissions should be studied in order to more authoritatively fit rate constants.

9. In order to provide an extremely simple CH_4 oxidation mechanism for complex fluid models such as the Gosman or UARL codes, the 26-reaction set should be screened with relaxed criteria.

I. INTRODUCTION

A. CHEMICAL KINETICS--AN IMPORTANT FACTOR IN COMBUSTION-GENERATED NITROGEN OXIDES

It is well known that NO and CO production in flames is rate-limited, and is strongly coupled to hydrocarbon oxidation through the heat release and radical-generation mechanisms. Limited knowledge of the mechanism of hydrocarbon combustion has impeded an understanding of the kinetics of NO_x formation in flames. Of course, heterogeneous effects, flowfield mixing processes and radiation must be described before the kinetic mechanisms can be used for any given flame.

Whatever complexities attend the description of the combustion flowfield, there is no doubt but that the coupled rates of chemical processes ultimately determine the pollutant formation rates. It is with the kinetic mechanisms of combustion with pollutant formation that the present study is concerned. We have selected the methane/air system for study, since it is crucial to see if combustion of this simplest of hydrocarbons can be adequately modeled kinetically before attempting more complex gaseous fuels, not to mention those in liquid form with bound nitrogen.

B. DETAILED VS. GLOBAL HYDROCARBON KINETICS

Approximate kinetic schemes have been used to describe the oxidation of nearly all practical hydrocarbon fuels. The models generally assume a relatively fast partial oxidation of the hydrocarbon to yield CO, followed by the presumably well-known detailed kinetics ascribed to the $H_2/O_2/CO/N_2$ system [Mellor (1972)]. These "global" methods have previously proved useful for calculations of system performance and stability [Edleman and Fortune (1969)].

However, these approximate kinetic models have been shown to be unreliable to predict pollutant formation [Mellor (1972)]. Global reaction rates may be adequate for simulation of energy release, but detailed kinetic calculations are needed for pollutant formation because small changes in the hydrocarbon chemistry model strongly influence local temperature and composition. Serious disagreement has been found between detailed and approximate techniques for calculation of NO_x formation. For example, various partial equilibrium models for the $H_2/O_2/CO/N_2$ system give widely differing results as shown by Bowman and Kesten (1971).

The weakness of approximate kinetic methods are clearly demonstrated by recent results using a well-stirred reactor. Engleman et al. (1973) first tested the reliability of a postulated $H_2/O_2/CO/N_2$ reaction set by calculating NO formation in H_2/air and moist CO/air mixtures; they obtained good agreement with stirred reactor measurements at 1 atm. They then compared their predictions with experiments using propane, adding a global $C_3H_8 \rightarrow CO$ partial oxidation step to the kinetic mechanism. On the lean side, they underpredicted NO formation by a factor of 2; moreover, an order of magnitude disagreement existed under fuel-rich conditions. On the other hand, earlier predictions obtained from the same reaction set compared favorably with experimental results for NO formation in a shock tube for CH_4/air at 3 atm over a wide range of equivalence ratios [Seery and Bowman (1970)]. Clearly it will be necessary to establish the detailed mechanism of hydrocarbon combustion in order to accurately predict NO formation.

C. OBJECTIVES

In order to elucidate the role of chemical kinetics in pollutant formation in gas-fired combustors, we have attempted to determine the necessary and sufficient set of species, reactions, and rates to describe the heat release and pollutant formation from methane/air combustion. In the course of studying the CH_4/air system, the following additional questions were analyzed:

1. What reactions control the pyrolysis of CH_4?
2. What reactions control the oxidation of CH_4 and what are the intermediate species?
3. What reactions control the formation of NO? Is the Zeldovich mechanism ($O + N_2 \rightarrow NO + N$) the only significant path? How important is the hydroxyl radical ($N + OH \rightarrow NO + H$)?
4. In addition to NO, are other nitrogen-bearing pollutants formed during combustion, and if so, which reactions are responsible?
5. Is NO formed predominantly in the flame (during radical overshoot) or mainly in the post-flame region?

The final objective of the present study is to examine whether the screened reaction set is complete and able to predict the heat release and pollutant emissions experimentally measured in laboratory flames.

D. METHODS FOR DETERMINING THE KINETIC MECHANISM

The following difficulties present themselves:

(i) The selection of intermediate species requires knowledge of undetermined critical reaction paths.

(ii) The set of conceivable elementary reactions is extremely unwieldy and its complexity defies attempts to use intuition to arrive at the necessary and sufficient subset.

(iii) The paucity of measured rate data makes it difficult to select rate coefficients.

(iv) Once the problem is set up, coupled non-linear rate expressions must be solved subject to widely differing time constants.

Our approach has been to develop and apply a procedure for reaction screening to deal with problems (i) and (ii) in a systematic fashion. Engineers are often confronted with complex chemical systems; without a convenient way to select the reaction paths of importance for a particular application, the reaction sets chosen usually will omit one or more reactions of importance and/or include unnecessary ones. Such incorrect reaction sets may lead to

incorrect results and/or wasted computation time. In order to alleviate this problem, a formal procedure is developed for the systematic examination of reactions in order to reduce their numbers while retaining any desired degree of accuracy. In this way the necessary and sufficient set of reactions and species to describe the phenomenon of interest can be obtained with the minimum effort. The rate uncertainties [item (iii)] can be reduced by adjusting rates in the screened set until it can predict experimental stirred-reactor cases.

As for the computation problem [item (iv)], modern numerical analysis techniques [Tyson and Kliegel (1968)] and high-speed computers permit computations with very large numbers of reactions and so can remove the guesswork involved in intuitively selecting reaction subsets of complicated chemical systems.

The remainder of this report is arranged as follows. The chapter to follow presents the description of a systematic method for screening large numbers of reactions (Chapter II). Following this we deal in succession with the selection of flame conditions and reaction data (Chapter III), with the detailed screening on perfectly-stirred combustors (Chapter IV), and on ignition, pyrolysis, and post-flame relaxation (Chapter V). Finally, these results are synthesized into a master set (Chapter VI), and some comparisons with stirred-reactor measurements are presented (Chapter VII).

II. A SYSTEMATIC METHOD OF ANALYZING COMPLEX REACTION MECHANISMS

The screening analysis is carried out in a systematic manner as described in the eight steps outlined below:

(1) Problem Statement: The non-equilibrium combustion problem is defined in terms of the reactants and ranges of stoichiometry, pressure and temperature. Sample cases are set up to cover this three-dimensional matrix (ϕ, P, T). The mixing and heat transfer models for these sample cases are idealized (e.g., adiabatic plug flow or stirred reactor) so that the chemical evolution of the system will be readily apparent.

(2) Species and Reaction Inventory: Given the reactants, a large list of conceivable species which could act as intermediates or products is composed. A comprehensive list of bimolecular reactions and additional first-order and three-body reactions is composed. About 50% to 70% of these reactions can be screened out because they are not elementary, because they are highly endothermic, or because of steric improbability.

(3) Rate Assignments: The available rate data on the remaining reactions is collected; estimates of rates are made where necessary (see Appendix B). A "best rate" is assigned to each reaction and a range of uncertainty is defined.

(4) Reaction Screening: Each sample case is run using the kinetics code, (see Appendix A), which calculates the fractional contribution of each reaction to the production and destruction of each species at pre-assigned points in the system evolution. Reactions are eliminated if their influence on the production or destruction of key species is less than prescribed screening criteria. For example, one may find it useful to eliminate a reaction contributing less than 5% to the change of any important variable. This screening step is the core of the analysis procedure.

Certain reactions which survive this numerical screening and appear significant are in fact negligible: Reactions which affect the destruction of

a species are unimportant if the production of that species far exceeds the destruction (i.e. the reaction is far from equilibrated).

(5) Species Screening: The Jacobian elements $\partial \dot{X}_i / \partial X_j$ (see Appendix A) are examined to find species j which seem to have a negligible effect on the rate of change of any species or temperature. Such species can be screened out if a rerun of the sample case confirms no sensitivity to their presence.

(6) Analysis of Reaction Groups: Frequently a group of reactions has no significance other than to form a species-exchange loop which makes its member reactions appear active [preventing their detection in step (4)]. By systematic inventory of the paths involved with species, it is possible to recognize and eliminate these non-productive reaction groups.

(7) Synthesis: A "master" set of reactions is synthesized by taking the union of all reaction sets which describe sample cases. Further refinements and corroboration can be made by exercising this "master" set on new sample cases. It is revealing and useful to identify subsets such as the intersection (reactions important in all cases) and special reaction groups which need only be included for low-temperature pyrolysis, low pressure, or fuel-rich conditions.

(8) Rate Adjustment: Given the reduced master reaction set, values of the more uncertain rate coefficients are selected on the basis of best-fit of data taken from idealized kinetically controlled experiments such as the stirred reactor and shock tube.

The systematic procedure outlined above formalizes the steps taken by past investigators, and supplements the intuition with an efficient numerical screening tool. Portions of the procedure have been used by prior investigators to suggest reactions of importance in calculating rocket engine performance [Kliegel et al. (1969)] and to analyze ethane/air combustion [Chinitz and Bauer (1966)].

III. SELECTION OF SPECIES, REACTIONS, RATES, AND CONDITIONS

A. PROBLEM STATEMENT: FLAME CONDITIONS IN GAS-FIRED COMBUSTORS

A matrix of test cases was designed to reflect conditions corresponding to ignition, burning, and post-flame zones, as shown in Figure 3.1.

Figure 3.1

8-CASE SCREENING MATRIX

Schematic of Reaction Progress:

$(CH_4, O_2) \longrightarrow$ (Radicals and Intermediates) $\longrightarrow (CO_2, H_2O)$

	IGNITION/COMBUSTION Without Backmixing (Plug flow)	COMBUSTION With Backmixing (2msec Stirred reactor)	POST FLAME Without Backmixing (Plug flow)
Φ = 1.25	IGN ($\phi > 1$)*	WSR ($\phi > 1$)	PF ($\phi > 1$)
Φ = 1.00	IGN ($\phi = 1$)*	WSR ($\phi = 1$)	PF ($\phi = 1$)
Φ = 0.80		WSR ($\phi < 1$)	PF ($\phi < 1$)*

Those cases denoted * were made at high enthalpy ($\Delta T_o = 300^oK$) to test the effect of preheat.

Ignition presumably occurs in combustors after reactants are injected into the primary zone and mixed with hot products. For this study, ignition is modeled as a plug flow (zero backmixing), with initial composition taken to be a mixture of reactants and equilibrium combustion products. The exact reactant/product fraction was found unimportant in the present application; it only affected the delay to ignition but not the detailed mechanism of the chemical runaway. It is essential to recognize that methane/air reactants are not heated to the ignition point ($\sim 1200^oK$) without dilution.

For gas-fired combustors, the extent of backmixing of hot products with unburned reactants during the heat release process is not well established. Characteristic heat-release times are known to be on the order of .1 msec, so backmixing is expected to be negligible on a scale much more than $L = \sqrt{Dt} \approx 10^{-2}$ cm, for example in a diffusion flame of 10^{-1}-cm thickness. On the other hand, the very thin deflagration waves characteristic of premixed flames would permit backmixing and indeed require it in order to propagate.

In the present study we consider two extremes of backmixing: plug flow and perfect backmixing. The plug flow extreme is analyzed by observing the ignition case after the chemical runaway. The stirred reactor extreme is set up as separate cases as noted in Figure 3.1. Starting conditions are critical in the numerical solution of the WSR, since the first iteration must "ignite". However the steady state WSR solution has only CH_4/air as input and retains no memory of the starting concentrations.

These WSR cases were run with a residence time of 2 msec. Using screening criteria to be described in the next section, we examined residence time of two to three times as great as this for the WSR ($\phi = 1$) case. As shown below, we found only one extra reaction screened out at 4 msec, compared to the 2 msec case, and four additional reactions eliminated at 6 msec (out of 134 reactions)*

	Reaction	X Indicates Screened Out at Residence Time of 4msec	6msec
(31)	$CN + H_2 = CHN + H$		X
(82)	$H_2 + NO = H + HNO$		X
(83)	$H_2 + O = H + HO$		X
(93)	$H + NO_2 = HNO + O$	X	X

It appears that the reaction set obtained for a 2 msec residence time should be more general than the sets obtained at longer residence times. Reactions (31), (82), and (93) were later determined to be insignificant at 2 msec as well because the species CN, CHN, HNO, and NO_2 were eliminated as unimportant.

*Reaction numbers refer to Table 3.1 (page 11).

Finally, plug-flow cases were set up to represent the hot combustion gases in the post-flame zone. For some combustors, it is in this "cooking" period that most of the pollutants are formed; certainly most of the $CO \rightarrow CO_2$ conversion occurs here. The post-flame zone of a real combustor is affected by heat transfer, but for these calculations the zone was taken as adiabatic. The composition at the entrance to the post-flame zone region is taken to be the exit condition from a stirred reactor; in this way relaxation of a gas mixture which is out of equilibrium can be observed.

In addition to the above-described burning modes, variations in the equivalence ratio* and the level of air preheat were studied. The pressure is taken at atmospheric for all cases. These conditions, along with the burning mode, should suffice to approximate, if not exactly describe, the conditions in any particular region of a combustor.

B. SPECIES, REACTIONS, AND RATES

For the present study, the species and reaction inventory was taken from the work of Engleman et al. (1973a) as was their assignment of "best guess" suggested rates. Since the species and reaction inventory and rate assignments were proceeding concurrently with the present program, there was ample opportunity to experiment with different reaction sets which had been used by other investigators, including some reactions which were not in the 134-reaction set of Engleman et al. (1973a). These will be discussed later.

The set of species included in the present study is shown in Table 3.1. Recent experimental evidence has suggested the presence of the species C_2 in methane/air combustion [Pratt and Malte (1973)]. This species was not included in the present study.

*Defined here as $\phi = (F/A)/(F/A)_{stoichiometric}$. The equivalence ratio ϕ may be thought of as the fraction of the supplied air which would be utilized if the complete combustion were required.

Table 3.1

SPECIES INCLUDED IN THE PRESENT STUDY

CH	Methylidyne	HNO	Nitroxyl
CHN	Hydrogen cyanide	HO	Hydroxyl
CHO	Formyl	HO_2	Hydroperoxyl
CH_2	Methylene	H_2	Hydrogen, diatomic
CH_2O	Formaldehyde	H_2O	Water
CH_3	Methyl	N	Nitrogen, monatomic
CH_3O	Methoxyl	NO	Nitric oxide
CH_4	Methane	NO_2	Nitrogen dioxide
CO	Carbon monoxide	N_2	Nitrogen, diatomic
CO_2	Carbon dioxide	N_2O	Dinitrogen monoxide
CN	Cyano	O	Oxygen, monatomic
H	Hydrogen, monatomic	O_2	Oxygen, diatomic
HN	Imidogen		

All possible reactions that might occur among the species of Table 3.1 were collected by Engleman and Bartok (1973). Those reactions which appeared to be sterically improbable, spin forbidden, or not fundamental reaction steps were eliminated. This resulted in a set of 322 reactions in 25 species. Of these, 134 reactions in 25 species were taken as the master set, these being selected on the basis that their rates had been either measured or estimated by previous researchers. The master set of 134 reactions is shown in Table 3.2, along with the rates recommended by Engleman and Bartok. Of these reactions, more than half have estimated rates, i.e., the absence of experimental rate data indicates that they have never been observed, though each has received some attention in the literature. A complete accounting of the 134-reaction set is given by Engleman and Bartok. The reverse reaction rate was determined from the forward rate and thermochemical data.

Table 3.2

REACTION SET USED AS THE BASIS FOR SCREENING

Rate Coefficients* $k_f = A T^{-n} e^{-E/RT}$

Reaction Number	Reaction	A	n	E	Reference
Termolecular Reactions**					
008	CH +H =CH2	3.00E+16	.5	0.	ESTIMATE
023	CH +O =CHO	1.00E+16	.5	0.	TUNDER(1967)
026	CN +H =CHN	3.00E+16	.5	0.	TUNDER(1967)
036	CHO =CO +H	2.50E+20	1.5	16.8	BENSON(1973)
043	CH2O =CHO +H	8.00E+33	4.5	87.	BENSON(1973)
061	CH4 =CH3 +H	2.00E+17	.0	88.	HARTIG(1971)
077	CO2 =CO +O	1.00E+15	0.	100.	CLARK(1971)
079	H2 =H +H	2.00E+14	.0	96.	BAULCH(1972)
084	H2O =HO +H	3.00E+15	.0	105.	BAULCH(1972)
089	H +N =HN	3.00E+16	.5	0.	TUNDER(1967)
092	H +NO =HNO	2.00E+16	.0	0.	CLYNE(1962)
099	H +O =HO	8.00E+15	.0	0.	SCOFIELD(1973)
101	H +O2 =HO2	1.50E+15	.0	1.	BAULCH(1972)
109	HN +O =HNO	1.00E+16	.5	0.	TUNDER(1967)
112	HO +N =HNO	1.00E+15	.5	0.	TUNDER(1967)
121	HO2 =HO +O	4.00E+15	1.5	64.	BENSON(1973)
124	N2 =N +N	4.00E+21	1.6	225.	BAULCH(1973)
132	NO =N +O	4.00E+20	1.5	150.	BAULCH(1973)
138	NO2 =NO +O	1.00E+16	.0	65.	BAULCH(1973)
140	N2O =N2 +O	1.00E+14	.0	50.	ENGLEMAN(1973)
142	O2 =O +O	2.50E+19	1.0	118.7	JOHNSTON(1968)
147	CH2O =CO +H2	1.00E+12	-1.0	65.	BENSON(1973)
149	CH3O =CH2O+H	4.00E+40	7.5	22.6	BENSON(1973)
Bimolecular Reactions					
001	CH +CHN =CH2 +CN	3.00E+11	- .6	8.	TUNDER(1967)
002	CH +CHO =CH2 +CO	3.00E+10	- .7	1.	TUNDER(1967)
003	CH +CH2O=CH2 +CHO	1.00E+11	- .7	4.	TUNDER(1967)
004	CH +CH3 =CH2 +CH2	1.25E+11	- .7	5.	TUNDER(1967)
005	CH +CH4 =CH2 +CH3	2.50E+11	- .7	5.	TUNDER(1967)
006	CH +CO2 =CHO +CO	1.00E+10	- .5	6.	TUNDER(1967)
009	CH2 +N =CH +HN	6.00E+11	- .7	40.5	MAYER(1967)
011	CH +HNO =CH2 +NO	6.00E+11	- .5	0.	TUNDER(1967)
012	CH +HO =CHO +H	5.00E+11	- .5	10.	TUNDER(1967)
013	CH2 +O =CH +HO	2.00E+11	- .7	26.	MAYER(1967)
015	CH +HO2 =CHO +HO	5.00E+11	- .5	6.	TUNDER(1967)
016	CH +HO2 =CH2 +O2	1.00E+10	- .5	15.	TUNDER(1967)
017	CH2 +H =CH +H2	3.00E+11	- .7	26.	MAYER(1967)
018	CH2 +HO =CH +H2O	5.00E+11	- .5	6.	TUNDER(1967)
022	CH +O =CO +H	5.00E+11	- .5	4.	TUNDER(1967)
024	CH +O2 =CHO +O	5.00E+11	- .5	6.	TUNDER(1967)
027	CH2O+CN =CHN +CHO	1.25E+11	- .7	3.	TUNDER(1967)
028	CH3 +CN =CHN +CH2	1.00E+11	- .7	3.	TUNDER(1967)
029	CH4 +CN =CHN +CH3	3.00E+11	- .7	5.	TUNDER(1967)
030	CHO +CN =CHN +CO	2.00E+11	- .5	0.	TUNDER(1967)
031	CHN +H =CN +H2	2.50E+11	- .7	18.	TUNDER(1967)
032	CHN +HO =CN +H2O	2.00E+11	- .6	5.	TUNDER(1967)
033	CN +HN =CHN +N	1.00E+11	- .5	2.	TUNDER(1967)
034	CN +HNO =CHN +NO	4.00E+11	- .5	0.	TUNDER(1967)
035	CHN +O =CN +HO	3.00E+11	- .7	17.	TUNDER(1967)
037	CHO +CHO =CH2O+CO	1.50E+11	- .5	0.	TUNDER(1967)
038	CHO +CH2 =CH3 +CO	3.00E+10	- .7	1.	TUNDER(1967)
039	CHO +CH3 =CH2 +CH2O	1.50E+11	- .7	4.	TUNDER(1967)
040	CHO +CH3 =CH4 +CO	3.00E+11	- .5	0.	TUNDER(1967)
041	CHO +CH4 =CH2O+CH3	8.00E+11	- .6	9.	TUNDER(1967)
042	CH2 +O =CHO +H	5.00E+11	- .5	4.	TUNDER(1967)
044	CHO +H =CO +H2	3.00E+10	-1.	0.	BENSON(1973)
045	CHO +HNO =CH2O+NO	3.00E+11	- .5	0.	TUNDER(1967)
046	CH2O+O =CHO +HO	2.00E+11	-1.	4.4	DEAN(1971)
047	CHO +HO =CO +H2O	3.00E+10	-1.	0.	BENSON(1973)
048	CH2O+H =CHO +H2	1.25E+10	-1.	3.2	WESTENBERG(1972)
049	CH2O+HO =CHO +H2O	3.00E+09	-1.	1.	BENSON(1973)
050	CHO +N =CO +HN	2.00E+11	- .5	2.	TUNDER(1967)
051	CHO +NO =CO +HNO	2.00E+11	- .5	2.	TUNDER(1967)
052	CHO +O =CO +HO	3.00E+11	-1.	.5	BENSON(1973)

*Units: mole, cc, sec, °K, kcal

**The third body term, M, is understood to appear on each side of these equations.

Table 3.2 (Cont)

Reaction Number	Reaction	A	n	E	Reference
053	CH2 +CH4 =CH3 +CH3	1.25E+12	- .7	20.	TUNDER(1967)
054	CH2 +HNO =CH3 +NO	6.00E+11	- .5	0.	TUNDER(1967)
055	CH2 +HO =CH3 +O	5.00E+11	- .5	6.	TUNDER(1967)
056	CH3 +H =CH2 +H2	2.00E+11	- .7	3.	TUNDER(1967)
057	CH3 +HO =CH2 +H2O	6.00E+10	- .7	2.	TUNDER(1967)
058	CH2 +O2 =CH2O+O	5.00E+11	- .5	7.	TUNDER(1967)
059	CH3 +O =CH2O+H	2.00E+12	- .5	- .3	MORRIS(1973)
060	CH3 +O2 =CH2O+HO	3.00E+13	- .0	30.	BENSON(1973)
062	CH3 +HNO =CH4 +NO	5.00E+11	- .5	0.	TUNDER(1967)
063	CH4 +O =CH3 +HO	1.00E+10	-1.	8.	WESTENBERG(1969)
064	CH3 +HO2 =CH4 +O2	1.00E+11	- .5	6.	TUNDER(1967)
065	CH4 +H =CH3 +H2	5.00E+10	-1.	10.	WALKER(1968)
066	CH4 +HO =CH3 +H2O	3.00E+13	- .0	5.	WILSON(1972)
067	CN +NO =CO +N2	3.00E+11	- .0	0.	BODEN(1968)
068	CN +O2 =CO +NO	3.00E+11	- .0	0.	BASCO(1965)
069	CO +HNO =CO2 +HN	1.00E+11	- .5	7.	TUNDER(1967)
070	CO +HO =CO2 +H	4.00E+09	- .5	0.	ENGLEMAN(1973)
071	CO +HO2 =CO2 +HO	1.00E+12	- .0	12.	BENSON(1973)
072	CO2 +H2 =CO +H2O	1.00E+09	- .5	15.	TUNDER(1967)
073	CO2 +N =CO +NO	2.00E+11	- .5	25.	BENSON(1973)
074	CO +NO2 =CO2 +NO	3.00E+12	- .0	30.	JOHNSTON(1957)
075	CO +N2O =CO2 +N2	1.00E+11	- .0	23.	LIN(1969)
078	CO +O2 =CO2 +O	1.00E+13	- .0	60.	DEAN(1971)
080	H +HN =H2 +N	6.00E+11	- .5	8.	BENSON(1973)
081	H +HNO =HN +HO	2.00E+11	- .5	13.	TUNDER(1967)
082	H +HNO =H2 +NO	1.00E+13	- .0	2.5	HAMPSON(1972)
083	H +HO =H2 +O	8.00E+09	- 1.	7.	BAULCH(1972)
085	H +HO2 =HO +HO	2.50E+14	- .0	1.9	BAULCH(1972)
086	H +HO2 =H2 +O2	2.50E+13	- .0	.7	BAULCH(1972)
087	H +HO2 =H2O +O	1.00E+13	- .0	1.	LLOYD(1971)
088	HO +H2 =H +H2O	2.50E+13	- .0	5.2	BAULCH(1972)
090	HN +O =H +NO	6.00E+11	- .5	0.	BENSON(1973)
091	HO +N =H +NO	6.00E+11	- .5	8.	BENSON(1973)
093	HNO +O =H +NO2	5.00E+10	- .5	0.	TUNDER(1967)
094	H +HO2 =HO +HO	3.00E+14	- .0	1.5	BAULCH(1973)
095	HN +N =H +N2	6.00E+11	- .5	0.	BENSON(1973)
096	H +N2O =HN +NO	1.00E+11	- .5	30.	TUNDER(1967)
097	HNO +N =H +N2O	5.00E+10	- .5	3.	TUNDER(1967)
098	H +N2O =HO +N2	8.00E+13	- .0	15.	BAULCH(1973)
100	HO +O =H +O2	2.50E+13	- .0	0.	BAULCH(1972)
104	HN +HO =H2O +N	5.00E+11	- .5	2.	TUNDER(1967)
105	HNO +N =HN +NO	1.00E+11	- .5	2.	TUNDER(1967)
106	HN +NO2 =HNO +NO	2.00E+11	- .5	5.	TUNDER(1967)
107	HN +N2O =HNO +N2	1.00E+11	- .5	3.	TUNDER(1967)
108	HN +O =HO +N	6.00E+11	- .5	8.	BENSON(1973)
110	HNO +O =HN +O2	1.00E+11	- .5	7.	TUNDER(1967)
111	HO2 +N =HN +O2	1.00E+11	- .0	0.	KRETSCHMER(1963)
113	HNO +HO =H2O +NO	1.00E+12	- .0	1.	BENSON(1973)
114	HNO +NO =HO +N2O	2.00E+12	- .0	26.	WILDE(1969)
115	HNO +O =HO +NO	5.00E+11	- .5	0.	TUNDER(1967)
116	H2 +O2 =HO +HO	2.50E+12	- .0	39.	RIPLEY(1966)
117	HO +HO =H2O +O	6.00E+12	- .0	1.	BAULCH(1972)
118	HO +HO2 =H2O +O2	1.00E+13	- .0	1.	LLOYD(1971)
120	HO2 +NO =HO +NO2	1.00E+12	- .0	3.	BENSON(1973)
122	HO2 +O =HO +O2	5.00E+13	- .0	1.	LLOYD(1971)
125	N +NO =N2 +O	1.50E+13	- .0	0.	BAULCH(1973)
127	N +NO2 =NO +NO	4.00E+12	- .0	0.	PHILLIPS(1965)
128	N +NO2 =N2 +O+O	1.50E+12	- .0	0.	PHILLIPS(1965)
129	N +NO2 =N2 +O2	1.00E+12	- .0	0.	PHILLIPS(1965)
130	N +NO2 =N2O +O	5.00E+12	- .0	0.	PHILLIPS(1965)
131	N +N2O =NO +N2	5.00E+08	- .0	10.	BORTNER(1963)
133	N +O2 =NO +O	6.00E+09	- 1.	6.3	BAULCH(1973)
135	N2O +O =NO +NO	1.00E+14	- .0	28.	BAULCH(1973)
136	NO +NO2 =N2O +O2	1.00E+12	- .0	60.	BORTNER(1963)
137	NO +N2O =NO2 +N2	2.00E+12	- .0	40.	KAUFMAN(1955)
139	NO2 +O =NO +O2	1.00E+13	- .0	1.	BAULCH(1970)
141	N2O +O =N2 +O2	1.00E+14	- .0	28.	BAULCH(1973)
143	CHO +O2 =CO +HO2	8.00E+12	- .0	0.	PEETERS(1973)
148	CH3 +O2 =CH3O+O	2.50E+09	-1.	28.5	BENSON(1973)
150	CN +O =CO +N	1.00E+12	- .0	0.	BODEN(1968)
151	CH +HN =CHN +H	1.00E+11	.5	4.73	ESTIMATE

In the course of the present study, some reactions for which rate data was not available from Engleman et al. were hypothesized and are included in the set [reactions (8), (140), and (151), see Table 3.1)]. The rates for these reactions were determined by the methods shown in Appendix B. It was necessary to generate such data for the species methoxyl (CH_3O) which is not available in the JANAF Tables (1971). The procedure and results are shown in Appendix C. These calculations are in reasonable agreement with some sparse data which are recently available.

C. SCREENING CRITERIA

1. General

The screening is accomplished by elimination of those reactions whose contribution to the production or destruction rate of any particular species participating in that reaction is less than some specified percentage at each integration step. The specified percentage is the screening criterion.

In the present application of methane combustion in air with pollutant formation, some "key" species were assigned more stringent criteria than the other species. It is useful to use different criteria for different species because the same accuracy or relative importance is not attached to all species.

2. Screening for Pollutant Formation (Key species NO, O, CO)

Screening reactions for their importance in pollutant formation can be accomplished by placing stringent criteria on the pollutants of interest (NO and CO). Since intermediate radicals such as O-atoms affect NO formation, a criterion is also placed on one of the intermediate radicals (HO or H or O). It is not necessary to place criteria on all radicals since they are safely assumed to be interrelated through the O-H chain mechanism. For example, our studies show that the ratio $(O_2)(H)/(O)(OH)$ takes its equilibrium value for combustion around $T \approx 2000^{\circ}K$.

3. Screening for Heat Release (Key species CH_3, CO, H_2O)

Screening reactions for their importance in heat release is done by placing criteria on the three groups of species in the hydrocarbon breakdown scheme: main reactants, key intermediates, and products. The key species are thus chosen from the following chart:

Reactants	Intermediates	Products
CH, CH_3, O_2	CO; OH, H, O	CO_2, H_2O

It was presumed that we need only place a criterion on two of the three groups, since they are necessarily related by conservation of carbon atoms (e.g., if the main reactants and key intermediates are known then the products are known).

Originally two key oxidation species were selected, these were CH_4 and CO, reflecting a key reactant and intermediate product. The key reactant was switched from CH_4 to CH_3 and this switch had little effect on computed species concentrations. The temperatures computed with screened reaction sets were quite sensitive to the choice of CH_4 vs. CH_3 as key species. In an attempt to screen on the heat release per se, we designated H_2O as a key species, since H_2O production is closely related to the heat release. The addition of H_2O as a key species increased the resulting reaction set by a few reactions, but greatly improved the heat release authenticity.

4. Stringency of Retention Criterion

The 5%/10% criterion was adopted, where the first digit indicates the criterion on the "key" species and the second digit gives the criterion for all other species considered. It was felt that this was conservative but not overly so

Several different computer runs for WSR ($\phi = 1$) case were carried out in order to examine the effect of the retention criterion. Three criteria were examined: these are noted as 5%/10%, 5%/25%, and 10%/25%. Recall that the reaction screening is carried out by elimination of any reaction whose percentage contribution to the production or destruction rate of the particular species is less than the criterion.

Case I. Key Species: CH_3, CO, NO, O

The following reactions were screened out with a 10%/25% criterion but retained with a 5%/25% criterion:

(47)	CHO + HO	=	CO + H_2O
(99)	HO + M	=	H + O + M

Case II. Key Species: CH_4, CO, H_2O, NO, O

The following reactions were screened out with a 5%/25% criterion but retained for a 5%/10% criterion:

(12)	CHO + H	=	CH + HO
(22)	CO + H	=	CH + O
(68)	CO + NO	=	CN + O_2
(83)	H_2 + O	=	H + HO
(118)	H_2O + O_2	=	HO + HO_2
(143)	CO + HO_2	=	CHO + O_2

Accordingly, the more stringent 5%/10% criterion was adopted. Reactions (83), (143), and (99) ended up in the final controlling set (see Table 6.1, p. 52). Reaction (68) was restored in order to match predictions with data on fuel-rich stirred reactors (see Table 7.4, p.66).

IV. RESULTS FOR PERFECTLY-STIRRED COMBUSTION

A. STOICHIOMETRIC ($\phi = 1$) PERFECTLY-STIRRED REACTOR

1. The WSR ($\phi = 1$) Case History--An Illustration of the Screening Methods

It is instructive to summarize the specific steps taken to determine the controlling mechanisms for the WSR ($\phi = 1$) case before documenting the results of the reaction screening and elimination of species in more detail. A 22 reaction 16 species mechanism was derived from the original reaction set of 134 reactions and 25 species. Table 4.1 shows how the reduced set evolved.

Table 4.1

SELECTED TEST CASES FOR WSR ($\phi = 1$)

Purpose of Run	Orig. Run#	REACTIONS No.	REACTIONS Remarks	SPECIES No.	SPECIES Remarks	RESULTS NO ppm	RESULTS T °K	RESULTS Comments
To establish reference solution	1,13	134	Master set	25	Master set	34	2064	
To apply 5%/10% screening criteria and confirm validity of screened set	3,14	53	Only those reactions satisfying 5%/10% criteria	25	Master set	33	2050	81 reactions eliminated Temperature somewhat low (see Table 4.2)
Attempt to remove more reactions	4	46	Remove seven more reactions which were (a) marginal (screened out by 5%/25% criteria (b) important to gross production but not to net production	25	Master set	34	2050	Changes appear to be permissible
Compute Jacobian to identify marginal species	6	46	Same as above	25	Master set	34	2050	Nine marginal species identified: CH, CN, NO_2, CH_2, HN, N_2O, CH_3O, CHN, HNO
Explore validity of removing eight species	5	26	Remove reactions associated with insignificant species: 10 reax involving CN, HN, CHN, HNO; 5 reax involving CH, CH_2; 4 reax involving NO_2, N_2O	17	Based on above, remove eight species: NO_2, CH, CN, CHN, N_2O, CH_2, HN, HNO (retain CH_3O)	33	2050	Changes appear to be permissible
Explore validity of removing 10 species (2 add'l over Run #5)	8	18	Same as above; also remove six reax involving HO_2 and two reax involving CH_3O	15	Same as above; also remove HO_2 and CH_3O	32	2038	• CH_3O insignificant • HO_2 significant (intolerable temperature error)
Attempt to reproduce temperature of reference	12	33	Starting with 46 reax of Run #4, remove 14 reax involving CN, NO_2, N_2O, and CH_3O. Also restore O+H+M = OH + M (screened out by Runs #3,14)	21	Remove CN, NO_2, N_2O, CH_3O	32	2058	Better agreement with reference temperature
Final reduced set	15	22	Starting with 18 reax of Run #8, retained O+H+M = OH+M and retained three HO_2 reactions	16	Remove nine species: NO_2, CH, CN, CHN, N_2O, CH_2, HN, HNO, CH_3O (HO_2 retained)	33	2059	Predictions appear to be more accurate than Run #3 (see Table 4.2)

2. Application of Screening Criteria

The master set of 134 reactions in 25 species were screened with a retention criterion of 5% on the key species and 10% on all the others. The key species were taken as CH_4, CO, H_2O, O, and NO. After the screening there remained 53 reactions in 25 species. The results are compared in Table 4.2, and show excellent agreement except for CH_3O (10^{-10} vs 10^{-20}).

Table 4.2

COMPARISON OF RESULTS
FOR WSR (ϕ = 1) CASE

Species	Reference Case 134 reax; 25 sp Mass Fraction	After Removing Insignificant Reactions 53 reax; 25 sp Mass Fraction	After Removing Insignificant Reactions [except reax (99)] and Species 22 reax; 16 sp Mass Fraction
CH	5.448525E-08	4.468482E-08	---
CHO	1.097949E-06	1.259693E-06	1.163810E-06
CH2O	8.556080E-06	9.838586E-06	2.348705E-05
CH3O	1.288174E-10	3.816257E-20	---
CN	1.724417E-14	8.056930E-17	---
CO2	1.099303E-01	1.091302E-01	1.095881E-01
HN	1.989306E-09	1.914627E-09	---
HO	5.137354E-03	5.255954E-03	5.204020E-03
H2	8.505206E-04	8.859799E-04	8.601249E-04
N	1.004477E-08	9.653278E-09	8.782269E-09
NO2	1.866735E-09	1.672654E-09	---
N2O	1.737365E-07	1.809567E-07	---
O2	1.990988E-02	2.044295E-02	2.009116E-02
CHN	8.627687E-12	3.992004E-14	---
CH2	1.822494E-07	1.552852E-07	---
CH3	1.724471E-05	1.606675E-05	1.692448E-05
CH4	4.123362E-05	3.968808E-05	3.768075E-05
CO	2.595048E-02	2.646327E-02	2.616152E-02
H	1.848635E-04	2.025506E-04	1.917879E-04
HNO	2.537763E-08	2.800732E-08	---
HO2	8.859533E-07	9.473626E-07	1.203319E-06
H2O	1.114248E-01	1.108918E-01	1.112415E-01
NO	3.461712E-05	3.267976E-05	3.331709E-05
N2	7.249837E-01	7.249846E-01	7.249844E-01
O	1.524071E-03	1.641728E-03	1.563503E-03
T, °K	2064	2050	2059

Comparing the results of the 53 reaction set to the 134 reaction set in Table 4.2, it was felt that the observed temperature difference was too large. The deleted reactions were examined individually for the dual properties of having been marginally deleted as well as having a large heat of release. The reaction

(99) $HO + M = H + O + M, \qquad \Delta H = 102.229$ kcal/mole

failed to meet the 5% criteria because it contributed 4% of the destruction of O-atoms (and less than 3% to the net production of HO and H). Its restoration in the reaction set increased temperature from 2050°K to 2058°K (compared with 2064°K for the complete reaction set).

3. Determination of Insignificant Species

After the first screening, the Jacobian elements of the set of ordinary differential equations, viz.,

$$\frac{\partial}{\partial(C_j)} \frac{dC_i}{dt}$$

(where C_i can represent concentration or temperature)

were calculated and displayed for i = CH_4, CO, H_2O, O, and NO, and temperature. This Jacobian matrix is examined for candidate species whose influence on methane oxidation or pollutant formation is small. There were nine candidate species: CH, CH_2, CH_3O, CHN, CN, HNO, HN, NO_2, and N_2O (as shown in Table 4.3) which were examined individually for their influence.

Table 4.3

MARGINAL SPECIES
[WSR ($\phi = 1$)]

Species i	Relative Influence of j Compared to Influence of Important Species	Variable Most Affected by i	Remarks
CH_3O	10^{-6}	---	
CH_2	10^{-2}	T	[potentially important for $\phi > 1$ (see Chap VII)]
CH	10^{-4}	T	
CHN	10^{-4}	---	[potentially important for $\phi > 1$ (see Chap VII)]
HNO	10^{-1}	NO	[found to be in a "loop"]
CN	10^{-4}	T,OH	
HN	10^{-5}	---	
NO_2	10^{-3}	NO	[exists via exchange reactions with NO]
N_2O	10^{-7}	---	[potential alternate path to NO (see Fig. 4.2)]

In some cases species may be eliminated because they occur in a chain of reactions which is of minor consequence. In other cases we are led to loops of reactions which exhibit steady state exchange of atoms with negligible net effect on hydrocarbon oxidation or pollutant formation. The species and loop screening are carried out by hand with the help of the computer output (Jacobian matrix and reaction screening) described above. Some examples are given below.

Example: Elimination of the Species Methlidyne, CH

(18) $CH_2 + HO \rightarrow CH + H_2O$

(24) $CH + O_2 \rightarrow CHO + O$

Reactions (18) and (24) in sequence constitute a path from CH_2 to CHO, with CH the intermediary competing with CH_2O. However this path is very minor: reaction (24) contributes only .13% to the production of CHO and reaction (18) destroys only 0.4% of the CH_2. These reactions were retained by the reaction screening because of their obviously large effect on CH, but can be neglected because they do not affect the principal CH_4 oxidation scheme.

Example: Elimination of HNO and its Effect on NO-Formation

This loop concerns the conversion of nitric oxide to nitroxyl (HNO) and then back to nitric oxide.

	Reaction	Rate based on 100 moles/sec Production rate of NO
(92)	$NO + H + M \rightarrow HNO + M$	-43
(115)	$HNO + O \rightarrow HO + NO$	+23
(82)	$HNO + H \rightarrow H_2 + NO$	+11
(113)	$HNO + OH \rightarrow H_2O + NO$	+ 3
(69)	$HNO + CO \rightarrow HN + CO_2$	+ 4
(90)	$HN + O \rightarrow H + NO$	
		- 2 net

The net destruction rate of NO due to these reactions is 4% of the net production of NO due to all sources (48 units--see Figure 4.2). Moreover, the concentration of HNO is of the order of 25 ppb. On these bases, these reactions and the HNO species were deleted.

Proceeding in the manner indicated above for species and loop screening, all of the species CH, CH_2, CH_3O, CHN, CN, HN, HNO, NO_2, and N_2O were eliminated for the case WSR ($\phi = 1$), resulting in 22 reactions in 16 species. The results from this reduced set were actually closer to the reference solution than the 53 reaction set discussed previously, as may be seen in Table 4.2. The only noticeable deviations are in CH_4 (9% lower), HO_2 (30% higher), and CH_2O (higher by X 2.3).

4. Reduced Set of 22 Reactions

The resultant reaction subset for the case WSR ($\phi = 1$) is shown in Table 4.4.

Table 4.4

SCREENED REACTION SET (22 REAX) FOR STOICHIOMETRIC STIRRED REACTOR WSR ($\phi = 1$)

Termolecular Reactions		
036	CHO + M	= CO + H + M
077	CO2 + M	= CO + O + M
084	H2O + M	= HO + H + M
099	H + O + M	= HO + M
101	H + O2 + M	= HO2 + M
Bimolecular Reactions		
046	CH2O + O	= CHO + HO
047	CHO + HO	= CO + H2O
052	CHO + O	= CO + HO
059	CH3 + O	= CH2O + H
063	CH4 + O	= CH3 + HO
065	CH4 + H	= CH3 + H2
066	CH4 + HO	= CH3 + H2O
070	CO + HO	= CO2 + H
083	H + HO	= H2 + O
085	H + HO2	= HO + HO
088	HO + H2	= H + H2O
091	HO + N	= H + NO
100	HO + O	= H + O2
117	HO + HO	= H2O + O
125	N + NO	= N2 + O
133	N + O2	= NO + O
143	CHO + O2	= CO + HO2

5. Critical Paths for Methane Oxidation

Figure 4.1 shows the principal paths identified for methane pyrolysis and oxidation. This figure shows the progressive oxidation sequence $CH_4 \rightarrow CH_3 \rightarrow CH_2O \rightarrow CHO \rightarrow CO$. The number above each path indicates the relative rate of carbon transfer by that reaction path. The major initiating reaction is $CH_4 + OH \rightarrow CH_3 + H_2O$, presumably because OH is prevalent under backmixed conditions. Surprisingly, the initiating reactions

$$(61) \quad CH_4 + M = CH_3 + H + M$$
$$(64) \quad CH_4 + O_2 = CH_3 + HO_2$$

are of no consequence and are omitted. Indeed, this turns out to be true under lean and rich conditions as well. Three paths from CH_3 to CHO were found and are discussed below.

a. Formaldehyde Path

The principal path from methyl (CH_3) to formyl (CHO) is by a series of simple oxidations through formaldehyde (CH_2O). This accounts for 35% of CHO formation.

b. Methylene Path

A large percentage goes through reactions of the form $CH_n + CH_2O \rightarrow CHO + CH_{n+1}$. These reactions involve methylene (CH_2). This path becomes increasingly more important with increasing equivalence ratio (fuel rich conditions). This loop has only a net 1% effect on the destruction of CH_3; however, it has a very substantial effect on CHO formation. Since the rate of $CH_2 + CH_2O \rightarrow CHO + CH_3$ is quite uncertain, and since parallel path (a) was available and gave nearly identical WSR concentrations, we arbitrarily eliminated CH_2 and path (b) from the set, saving three reactions.

c. Methoxyl Path

Another path for the destruction of CH_3 is through the radical methoxyl (CH_3O), through the reactions

Figure 4.1

METHANE OXIDATION PATHS
WSR ($\phi = 1$)

COMPLETE MECHANISM
(Based on 134 reactions)

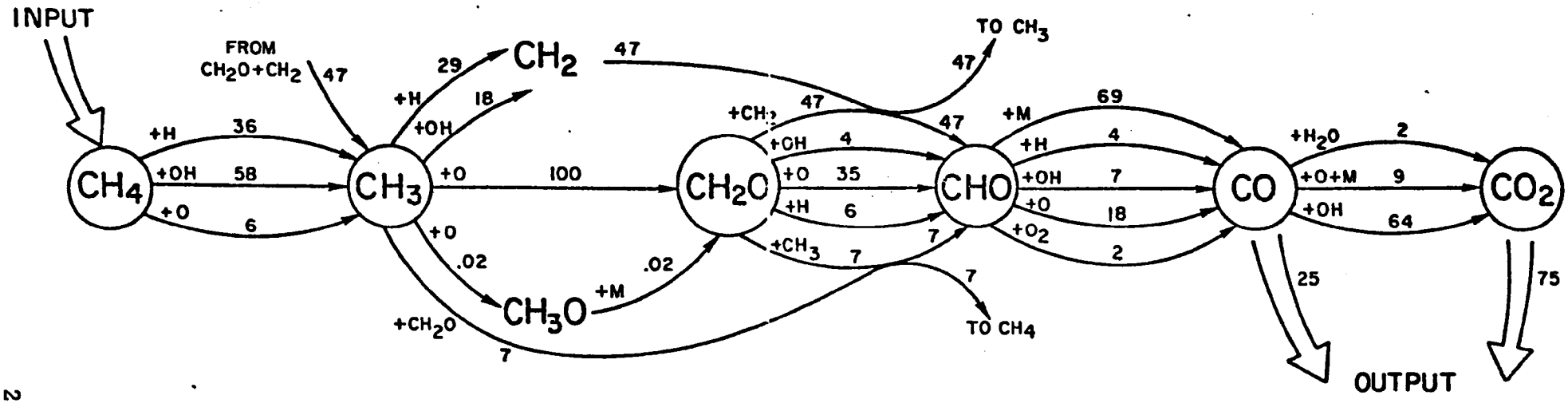

Rate numbers based on
100 mole/sec production
of ($CO + CO_2$)

SIMPLIFIED MECHANISM
(22 reactions)

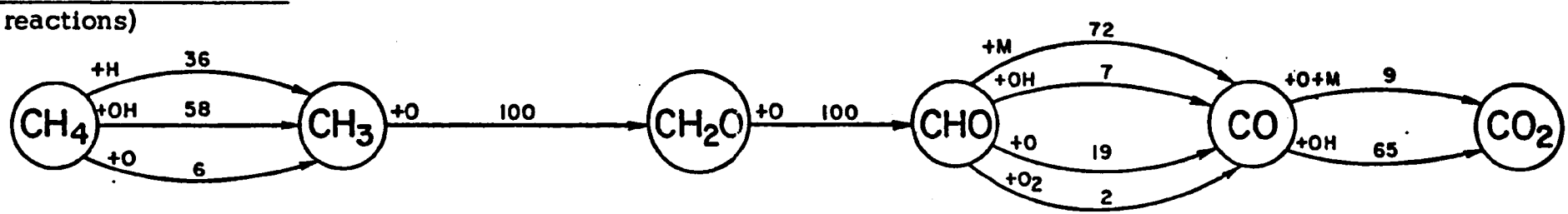

$$(148) \quad CH_3 + O_2 = CH_3O + O$$
$$(149) \quad CH_3O + M = CH_2O + O + M$$

but these turn out to be too slow to have an appreciable effect on the CH_3, so they can be safely omitted from the scheme.

d. Oxidation of Formyl

It is seen in Figure 4.1 that there are five parallel paths for the conversion of formyl to carbon monoxide; of these,

$$(143) \quad CHO + O_2 = CO + HO_2$$

is not important in the methane breakdown scheme but is in HO_2 production.

6. Critical Paths for Nitric Oxide Formation

The detailed pollutant formation mechanism is shown in Figure 4.2. The bottleneck in the rate of NO formation is the process of breaking up molecular nitrogen, and for this there are three alternatives. N_2 can collide with O atoms, giving NO + N (the Zeldovich mechanism); N_2 can combine with O in a three-body reaction to form N_2O; or N_2 can collide with an active hydrocarbon radical such as CH_2. For the 134-reaction set considered here, we see that of all possible paths to NO, only the extended Zeldovich mechanism, viz.,

$$(125) \quad O + N_2 = NO + N$$
$$(133) \quad N + O_2 = NO + O$$
$$(91) \quad OH + N = NO + H$$

survives the screening process. Other reactions of the type $R + N_2 = RN + N$ (not in the 134-reaction set) may also be important (see Chapter VII). Without these reactions, the master set indicates that 99.4% of the non-N_2 nitrogen ends up as NO, rather than in the form of HN, HNO, N_2O, NO_2, or CHN.

The potential importance of N_2O can be seen from Figure 4.2 which shows that N_2 destruction to form N_2O nearly equals the rate of reaction (125) shown above. While most of this N_2O returns to N_2, about 1% of the NO is formed by reaction (135):

Figure 4.2

NITRIC OXIDE FORMATION PATHS
WSR ($\phi = 1$)

COMPLETE MECHANISM
(Based on 134-reaction set for CH_4/air)

Numbers based on 100 moles/sec production rate of NO (48 of which is output)

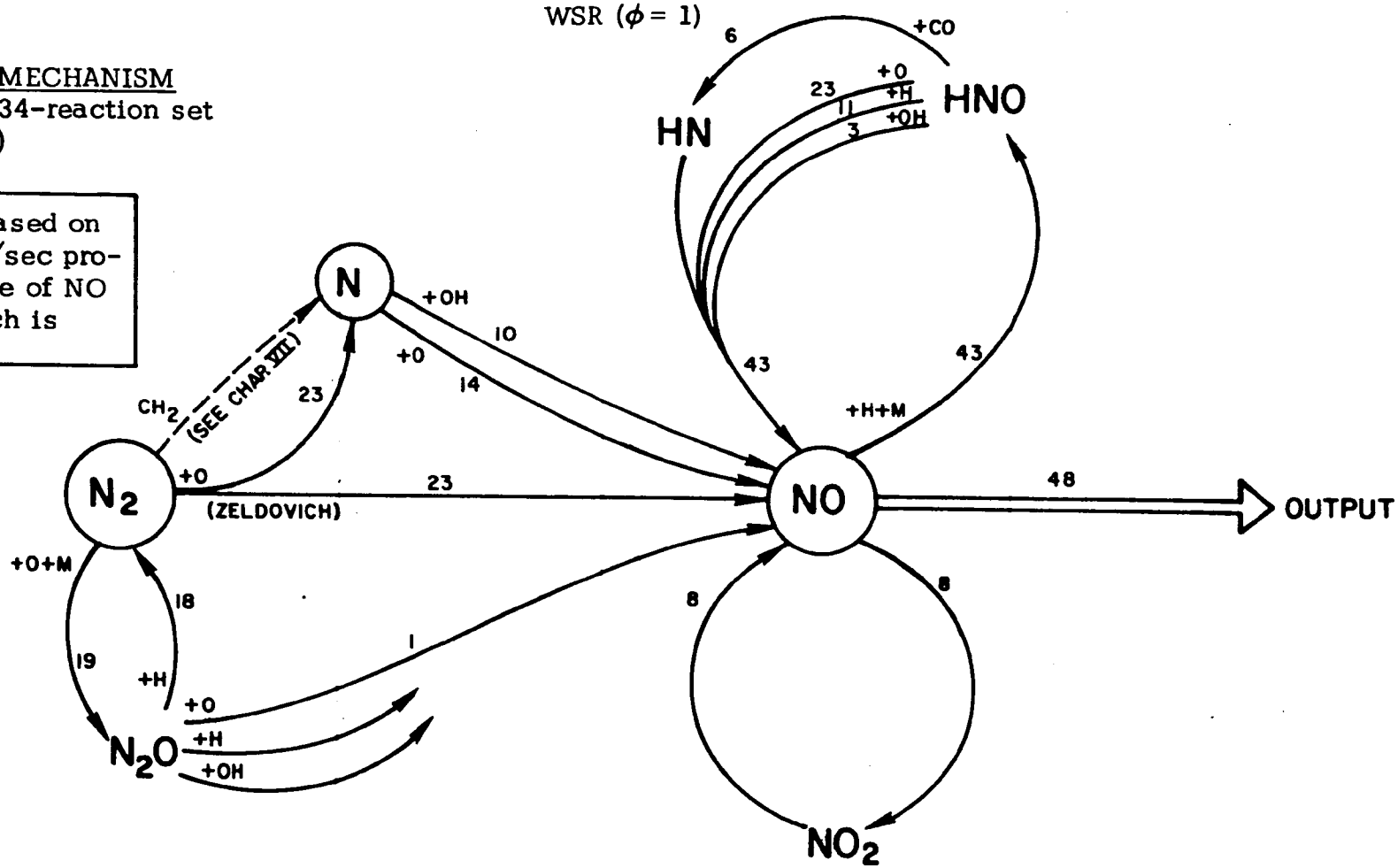

SIMPLIFIED MECHANISM
(22-reaction set for CH_4/air)

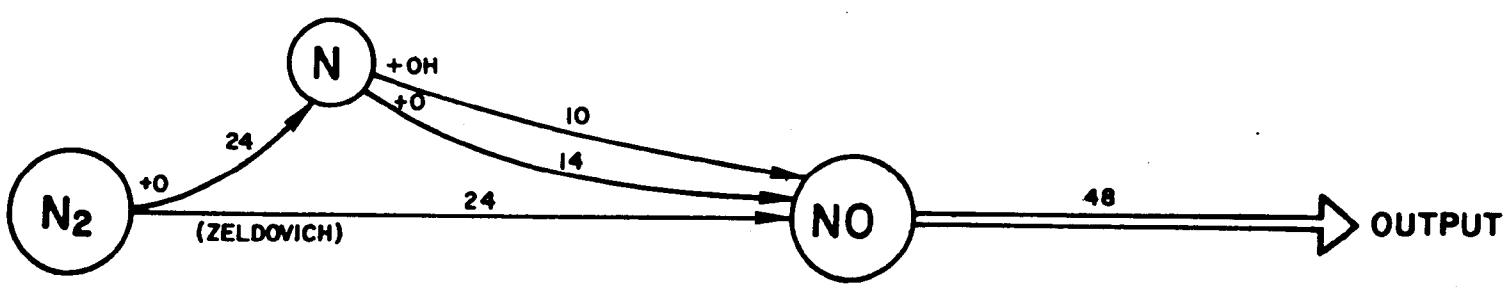

$$(135) \quad N_2O + O \rightarrow NO + NO$$

Because of the potential importance of N_2O, the rates of the following reactions should be better established:

$$(140) \quad N_2 + O + M \rightarrow N_2O + M$$
$$(98) \quad N_2O + H \rightarrow N_2 + OH$$
$$(135) \quad N_2O + O \rightarrow NO + NO$$
$$(96) \quad N_2O + H \rightarrow NH + NO$$
$$(114) \quad N_2O + OH \rightarrow NO + HNO$$

In this regard, the rate of reaction (140) seems uncertain to a factor of X 10^4. Compared to the rate used in this study, Barton and Dove (1969) recommend a rate 10^3 faster, whereas Olschewski, Troe, and Wagner (1967) list a rate of X 200 slower.

These nitrogen oxide reactions are coupled to the hydrocarbon oxidation reactions through the O-H chain reactions. Methane breakdown generates radicals which then react with nitrogen.

B. FUEL RICH (ϕ = 1.25) PERFECTLY STIRRED REACTOR

1. Application of Screening Criteria

As in the WSR (ϕ = 1) case, the residence time is 2 msec here. However, in order to explore the effect of preheat the WSR (ϕ >1) case was run at a specified temperature of 3960°R as opposed to the 3700°R adiabatic temperature of the ϕ = 1 case. The reaction screening reduced the original set of 134 reactions to 48 reactions.

2. Elimination of Insignificant Species

Following the procedures previously discussed, we were able to eliminate the following eight species: CH, CH_3O, CHN, CN, HN, HNO, NO_2, and N_2O. In addition, methylene (CH_2) was eliminated due to uncertainties over the existence and the rates of the following reactions:

$$(56) \quad CH_3 + H = CH_2 + H_2$$
$$(57) \quad CH_3 + HO = CH_2 + H_2O$$
$$(39) \quad CH_2 + CH_2O = CH_3 + CHO$$

Although the numerical results indicate that these reactions are an important path from CH_3 to CHO, we arbitrarily replaced them by an alternate formaldehyde (CH_2O) route from CH_3 to CHO:

$$(59) \quad CH_3 + O = CH_2O + H$$
$$(46) \quad CH_2O + O = CHO + HO$$

The resulting WSR ($\phi > 1$) concentrations were essentially unchanged, which means that NO formation and CH_4 oxidation are insensitive to the $CH_3 \rightarrow CHO$ path under these conditions. Nevertheless, the three methylene reactions (56), (57), and (39) are singled out as being potentially important in pyrolysis of methane. Furthermore, when additional reactions of the form $R + N_2 \rightarrow RN + N$ are added to the 134-reaction set, CH_2 may become important (see Chapter VII). The explanation of measured NO and CHN in jet-stirred reactors at $\phi > 1$ also indicates that CH_2 may be important.

3. Controlling Reaction Set

The subset of reactions controlling the fuel-rich stirred reactor contains 21 reactions in 16 species. These are shown in Table 4.5.

Table 4.5

SCREENED REACTION SET (21 REAX)
FOR FUEL-RICH STIRRED REACTOR [WSR ($\phi > 1$)]

Termolecular Reactions			Bimolecular Reactions					
036	CHO + M	= CO + H + M	044	CHO + H	= CO + H2	083	H + HO	= H2 + O
077	CO2 + M	= CO + O + M	046	CH2O + O	= CHO + HO	085	H + HO2	= HO + O
084	H2O + M	= HO + H + M	047	CHO + HO	= CO + H2O	088	HO + H2	= H + H2O
099	H + O + M	= HO + M	052	CHO + O	= CO + HO	091	HO + N	= H + NO
101	H + O2 + M	= HO + H + M	059	CH3 + O	= CH2O + H	100	HO + O	= H + O2
			065	CH4 + H	= CH3 + H2	117	HO + HO	= H2O + O
			066	CH4 + HO	= CH3 + H2O	125	N + NO	= N2 + O
			070	CO + HO	= CO2 + H	143	CHO + O2	= CO + HO2

4. Critical Paths in Methane Oxidation

The differences in the methane breakdown scheme between $\phi > 1$ and $\phi = 1$ can be seen in Figures 4.3 vs. 4.1. We observe the following:

1. The fuel rich conditions rule out the initiating reaction $CH_4 + O = CH_3 + HO$ and causes a substantial shift from reaction (66) ($CH_4 + HO = CH_3 + H_2O$) to reaction (65) ($CH_4 + H = CH_3 + H_2$).

2. The methylene path is favored over the formaldehyde path. A larger percentage of CH_3 goes to CH_2 in preference to CH_2O. The main path to CHO in the fuel rich case is through the reaction $CH_2 + CH_2O = CH_3 + CHO$, rather than by reaction (46). However, CH_2 and the methylene path were arbitrarily deleted for reasons described above.

3. The remainder of the chain is essentially the same, the principal reactions being

$$(36) \quad CHO + M \rightarrow CO + H + M$$

$$(70) \quad CO + HO \rightarrow CO_2 + H$$

5. Critical Paths of NO Formation

The NO-formation reactions are even simpler than in the stoichiometric case. The oxygen-deficient conditions cause a slow rate of formation of NO and the second Zeldovich reaction

$$(133) \quad N + O_2 = NO + O$$

is screened out upon application of the 5%/10% screening criterion. Likewise the reaction

$$(135) \quad N_2O + O \rightarrow NO + NO$$

producing only .16% of the NO, is screened out for the rich case. Just as in the WSR ($\phi = 1$) case, N_2O is formed from N_2 at a rate comparable to the Zeldovich rate (in this case in 1:3 proportions) but all N_2O returns to N_2 via $N_2O + H$ [reaction (98)].

COMPLETE MECHANISM
(Based on 134 reactions)

Figure 4.3

METHANE OXIDATION PATHS FOR
FUEL-RICH STIRRED REACTOR [WSR ($\phi > 1$)]

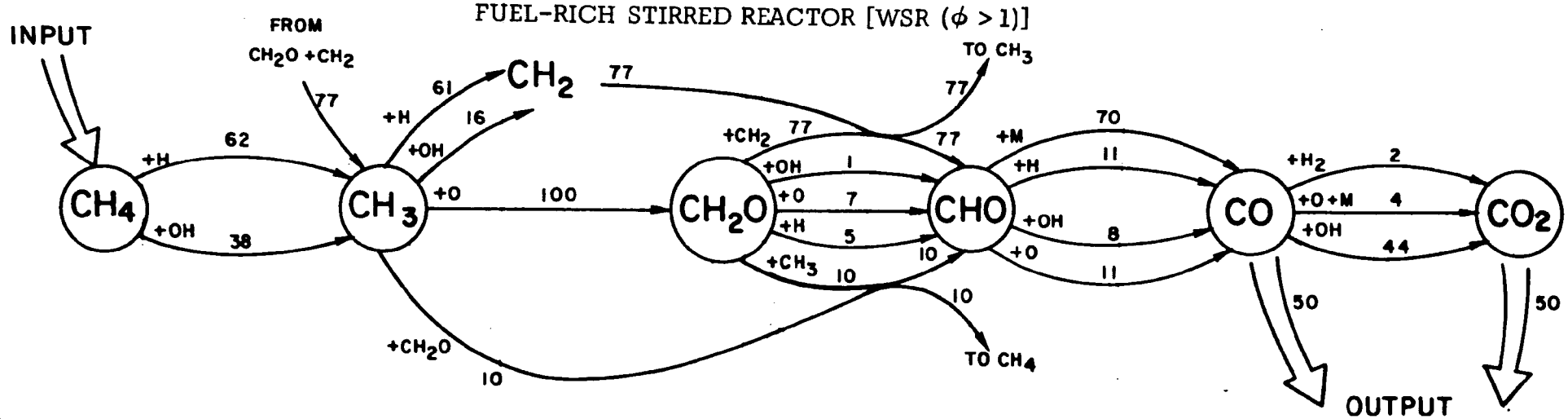

Rate numbers based on
100 mole/sec production
of ($CO + CO_2$)

SIMPLIFIED MECHANISM
(Based on 21 Reactions)

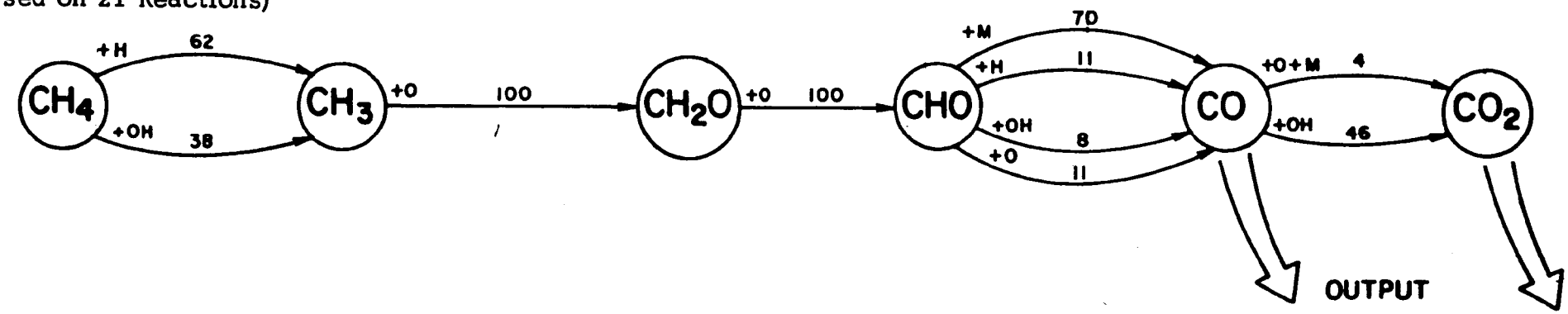

Thus, essentially all of the NO is formed by the two reactions

$$(125) \quad O + N_2 = NO + N$$
$$(91) \quad HO + N = NO + H \quad .$$

It should be emphasized that these results are only as valid as the original 134-reaction set. In Chapter VII we suggest additions to the set of the form $R + N_2 \rightarrow RN + N$ which seem needed to explain fuel-rich NO data, for which the altered Zeldovich mechanism [(125), (91)] is entirely inadequate.

C. FUEL LEAN ($\phi = 0.8$) PERFECTLY STIRRED REACTOR

1. Application of Screening Criteria

The residence time of this adiabatic stirred reactor is again taken at 2 msec. The reaction screening reduced the original 134-reaction set to 48 reactions. The reaction

$$(99) \quad H + O + M = HO + M$$

was restored to the set as an important source of heat release, even though the 5%/10% screening criteria indicated it had less than a 5% influence.

2. Elimination of Insignificant Species

Following the procedures of the $\phi = 1$ and $\phi > 1$ well-stirred reactors, the eight species CH, CH_2, CH_3O, CHN, CN, HN, HNO, and NO_2 were eliminated, thus resulting in 23 reactions. In this case N_2O must be retained as explained below in paragraph 5.

3. Reduced 23-Reaction Set for WSR ($\phi < 1$)

The resultant set of 23 reactions is shown in Table 4.6.

Table 4.6

SCREENED REACTION SET (23 REAX)
FOR FUEL-LEAN STIRRED REACTOR [WSR ($\phi < 1$)]

Termolecular Reactions		
036	CHO + M	= CO + H + M
077	CO2 + M	= CO + O + M
084	H2O + M	= HO + H + M
099	H + O + M	= HO + M
101	H + O2 + M	= HO2 + M
140	N2O + M	= N2 + O + M
Bimolecular Reactions		
046	CH2O + O	= CHO + HO
052	CHO + O	= CO + HO
059	CH3 + O	= CH2O + H
063	CH4 + O	= CH3 + HO
065	CH4 + H	= CH3 + H2
066	CH4 + HO	= CH3 + H2O
070	CO + HO	= CO2 + H
085	H + HO2	= HO + HO
088	HO + H2	= H + H2O
091	HO + N	= H + NO
098	H + N2O	= HO + N2
100	HO + O	= H + O2
117	HO + HO	= H2O + O
125	N + NO	= N2 + O
133	N + O2	= NO + O
135	N2O + O	= NO + NO
143	CHO + O2	= CO + HO2

4. Critical Paths for Methane Oxidation

The methane breakdown scheme in the lean case is shown in Figure 4.4. The results obtained here are not unlike those obtained for the $\phi = 1$ case.

The following observations are made in comparing the lean with the stoichiometric case:

1. In the lean case, the high oxygen concentration leads to an increased importance of the oxygen-bearing species in the initiation reactions (CH_4 + O and CH_4 + OH).

Figure 4.4

COMPLETE MECHANISM
(Based on 134 reaction set)

METHANE OXIDATION PATHS FOR
FUEL-LEAN STIRRED REACTOR [WSR ($\phi < 1$)]

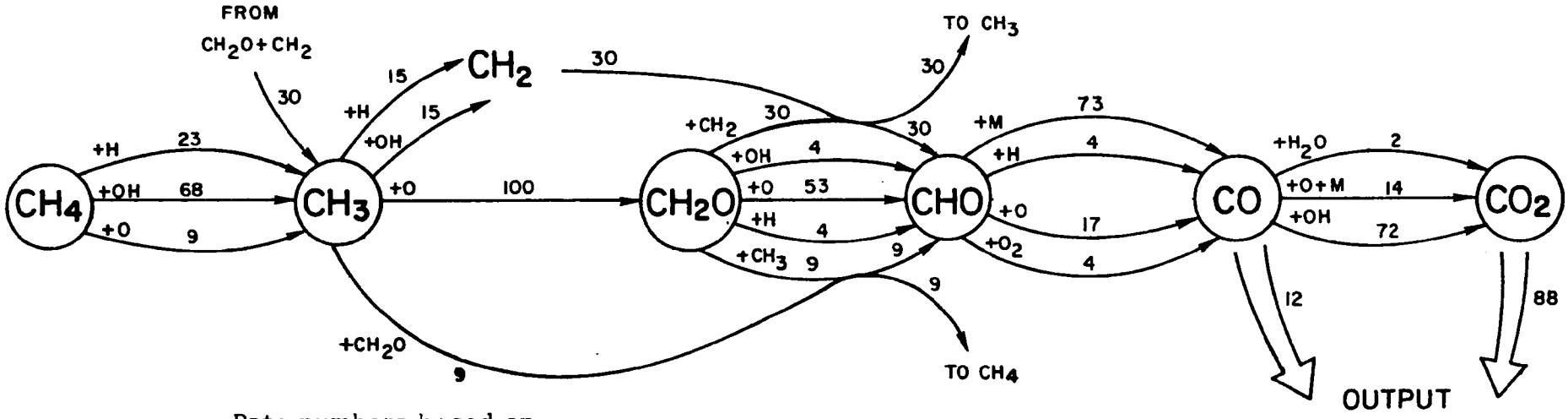

Rate numbers based on 100 moles/sec net production of ($CO + CO_2$)

SIMPLIFIED MECHANISM
(Based on 23-reaction set)

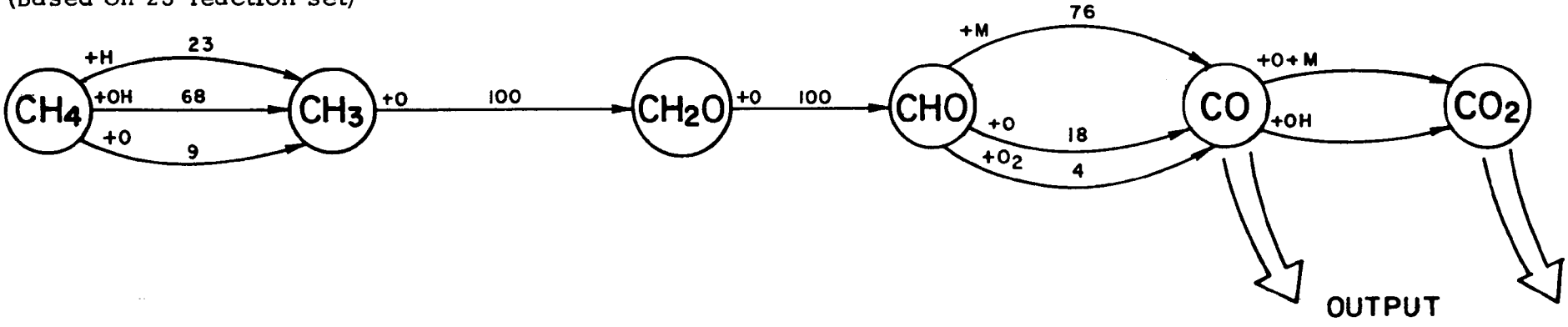

2. The methylene (CH_2) reactions are suppressed by the rapid consumption of CH_3 by the reaction $CH_3 + O = CH_2O + H$. Unlike the $\phi = 1$ and $\phi > 1$ cases, one need not overrule the numerical computation in discarding the CH_2 reactions.

The remainder of the scheme is approximately the same as the stoichiometric and fuel-rich cases.

5. Critical Paths to NO Formation

The major path to NO is through the conventional Zeldovich mechanism, with N + OH providing 19% of the fast second step (as opposed to 78% at $\phi > 1$):

$$\left.\begin{array}{lll} (125) & O + N_2 & \rightarrow NO + N \\ (133) & N + O_2 & \rightarrow NO + O \text{ (81\% of N)} \\ (91) & N + OH & \rightarrow NO + H \text{ (19\% of N)} \end{array}\right\} \text{86\% of net NO}$$

In addition, an N_2O mechanism provides the remaining 14% of the NO. It was found that reaction (140), the recombination of $N_2 + O + M \rightarrow N_2O + M$, is four times as active as reaction (125). Although 96% of the N_2O returns to N_2 (via $N_2O + H$), the remaining N_2O can lead to increased NO by the following competing reaction:

$$(135) \quad N_2O + O \rightarrow NO + NO \quad .$$

Since the rate of reaction (140) is unknown, this result should be explored with further studies. The nitrous oxide reactions are unimportant in the stoichiometric and fuel-rich cases because the NO-producing step $N_2O + O \rightarrow NO + NO$ is less important in their O-atom deficient atmospheres. The importance of reactions involving N_2O in lean systems has also been suggested by Pratt and Malte (1973).

D. SIMPLIFICATIONS TO THE METHANE OXIDATION MECHANISM

Consider the following mechanism for $CH_3 \rightarrow CHO$ conversion:

	Step 1: Consume CH3	Step 2: Form CHO
Path 1: Direct Two-Step Through CH_2O	$CH_3 + O = CH_2O + H$	$CH_2O + O = CHO + H$
Path 2: Parallel Through CH_2	$CH_3 + H = CH_2 + H_2$ $CH_3 + OH = CH_2 + H_2O$	$CH_2 + CH_2O = CHO + CH_3$
	Single Step CH_3 to CHO	
Path 3: Formaldehyde Bypass	$CH_3 + O = CHO + H_2$	

In the conversion of CH_3 to CHO, the direct two-step route through formaldehyde gives over to the parallel route through methylene (CH_2), as the equivalence ratio is increased. Nevertheless it appears permissible to use simpler path (1) instead of path (2) without incurring error. Both path (1) and path (2) are presumably equal in terms of radical generation. In both cases we notice that the Step 1 reactions are all chain terminating (one radical product for two radical reactants), while the Step 2 reactions are all chain branching (two radical products for one radical reactant).

Compare paths (1) and (2) with what might be called the formaldehyde-bypass reaction (path 3), which is an alternative route from methyl to formyl, viz.,

$$(144) \qquad CH_3 + O = CHO + H_2 \quad .$$

This reaction goes directly from methyl to formyl, omitting the intermediate CH_2O, and is probably not elementary. It has been used to simplify methane oxidation schemes because the second step of the two-step process $CH_3 + O \rightarrow CH_2O + H \rightarrow CHO + H_2$ is fast. This reaction is chain terminating, as opposed to the net chain carrying effect of the two-step routes discussed. The effect of using the bypass reaction was to reduce the O-atom concentration and hence reduce the NO. However, in substituting path (1) for path (2), no such difficulties accrue.

V. RESULTS FOR PYROLYSIS, IGNITION, AND POST-FLAME REACTIONS

A. PYROLYSIS AND IGNITION AT STOICHIOMETRIC ($\phi = 1$)

1. Application of the Screening Criterion

We attempted to simulate the ignition conditions of a combustor, wherein the premixed reactants are visualized to mix with hot products of combustion just before ignition (see Figure 5.1). For the purpose of this computation, this ignition condition was represented by a 70/30 mixture of reactants to equilibrated combustion products at a mixed temperature of 1200°K. These figures are, of course, arbitrary, but it is hoped that they are representative of the actual situation.

Figure 5.1

SCHEMATIC OF IGNITION MODEL

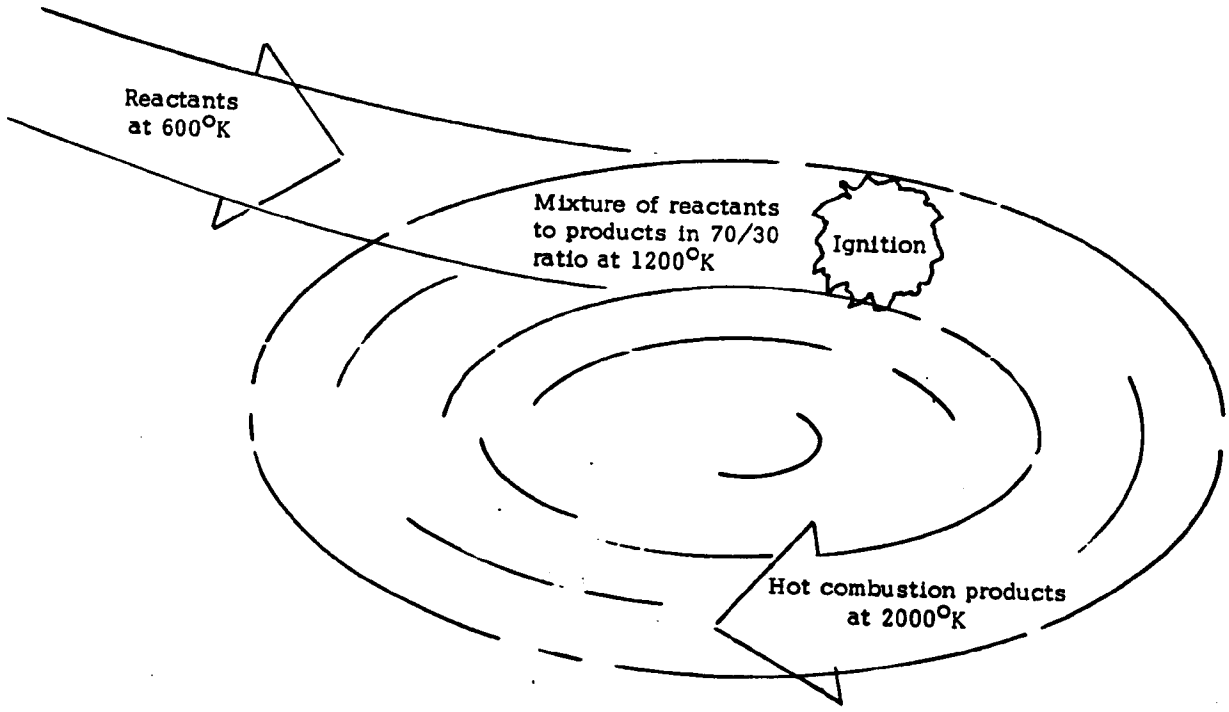

As in the plug flow simulation of the post-flame region, the screening criterion is applied continuously during the ignition process. Again, experience demonstrated that the reaction screening criteria could be relaxed from 5%/10% to 5%/25%. Two regimes are readily apparent:

- Pyrolysis (1200 - 1500°K)
- Combustion (T > 1500°K)

In the combustion regime, once the incubation period is complete, what is important is the species histories during the ignition phenomenon. However, the ignition delay is of great interest in the pyrolysis regime.

The reaction screening on the original 134 reactions brings the set to 69 reactions in 25 species.

2. Elimination of Insignificant Species

As a first try at species screening, it was decided to follow the example of the other screening cases and eliminate seven species: CH, CHN, CN, HNO, HN, NO_2, and N_2O. This brought the set to 27 reactions/18 species. The predicted temperature and concentration histories were in fair agreement. For combustion conditions (T > 1500°K), it was possible to eliminate five more reactions and one more species (CH_3O) and still reproduce the ignition profiles. This 22 reaction/18 species mechanism is given in Table 5.2, p. 40.

However, at low temperatures (T < 1500°K), five other reactions had to be added, otherwise the set predicted excessive CH_2O and reduced ignition delay.

3. Special Reactions for Pyrolysis (T < 1500°K)

Some detective work was necessary to correct the excessive CH_2O and short ignition delay. As a result the following five reactions were added:

(41) $CH_2O + CH_3 = CHO + CH_4$

(60) $CH_3 + O_2 = CH_2O + HO$

(64) $CH_3 + HO_2 = CH_4 + O_2$

(58) $CH_2 + O_2 = CH_2O + O$

(61) $CH_3 + H + M = CH_4 + M$

However, none of the seven species (CH, CHN, CN, HNO, HN, NO_2, or N_2O) needed to be restored. In what follows we present the details of the analysis.

a. Adjustments to Recover Reference CH_2O Profile

CH_2O builds up to huge concentrations prior to ignition, as can be seen in Figure 5.2 where it is compared with the correct result (from the 69 reaction/25 species set). With respect to this early buildup of CH_2O, there were five reactions containing CH_2O which were deleted from the reaction set. Of these, we restored the reaction

$$(41) \qquad CH_2O + CH_3 \rightarrow CHO + CH_4 \quad ,$$

which is an important destroyer of CH_2O at early times, accounting for as much as 95% of the term $d(CH_2O)/dt$. The improvement from this change [combined with restoring reactions (58), (60), (61), and (64) discussed in c. below] is apparent from Figure 5.2.

Figure 5.2

COMPARISON OF FORMALDEHYDE PROFILES
FOR IGN (ϕ = 1)

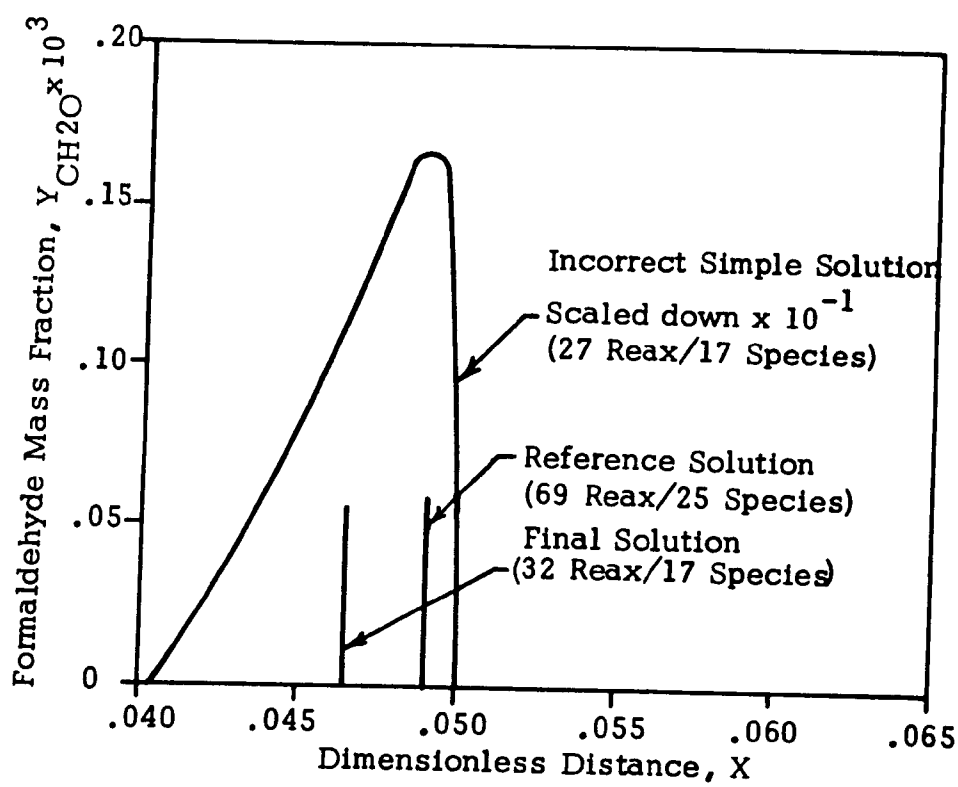

b. Additional Reactions Added for Pyrolysis ($T < 1500^{o}K$ only)

There are additional reactions whose omission could increase the ignition delay by suppressing early radical buildup. We restored the reaction

$$(60) \quad CH_3 + O_2 = CH_2O + HO$$

which as a chain carrier is responsible for 32% of the production rate of CH_2O at small times. Its inclusion should reduce the chain terminating effect of reaction (59), $CH_3 + O = CH_2O + H$, and thus reduce the ignition delay. We also restored the reaction

$$(64) \quad CH_3 + HO_2 \rightarrow CH_4 + O_2 \quad ,$$

which affects O_2 at small times.

There is still room for some improvement; with (41), (60), and (64), ignition occurs too early, though the main criticism of the previous screening, the formaldehyde production, has been corrected. Seeking an even better reaction set, the following reactions were restored to the set:

(58) $CH_2 + O_2 = CH_2O + O$. At very small times, this reaction accounts for only 1.1% of the production of CH_2O, but its omission changes the sign of the net production of CH_2O. Its inclusion should improve both CH_2 and CH_2O, as well as O-production rates.

(61) $CH_3 + H + M = CH_4 + M$. Omission of this reaction was determined to be responsible for a methyl destruction rate which was too low.

The effect of the above-described corrections is seen for formaldehyde, Figure 5.2, based on a set of 32 reactions/17 species. The results compare favorably.

An additional path for methyl decomposition is the formation and subsequent dehydrogenation of ethane, which is known to exist at temperatures as high as $1500^{o}K$ in methane flames [Dryer (1974)]. In this case, the scheme would be $CH_3 + CH_3 + M \rightarrow C_2H_6 + M$, followed by $C_2H_6 \rightarrow C_2H_5 \rightarrow C_2H_4 \rightarrow CH_2$. Since ethane was not considered in the species list for the present study, the significance of this ethane path was not explored.

c. Effect of Methoxyl (CH_3O) on Ignition Delay

In searching for mechanisms for increasing the ignition delay to its reference value, it was decided to examine, in particular, the effect of the species methoxyl (CH_3O) on the ignition. It had originally been suggested by Benson and co-workers (1972) that this species was potentially important in methane combustion in the temperature and stoichiometry range of interest. In fact, methoxyl had been screened out of every other case [i.e., WSR for all ϕ and PFR ($\phi = 1$)]. In the ignition case, however, the reaction screening output indicated that the reaction

$$(148) \quad CH_3 + O_2 \rightarrow CH_3O + O$$

is a marginal producer of O-atoms (responsible for as much as 7% of d[O]/dt) at low temperatures and so can have a small but measurable effect on the ignition delay interval. The effect of the species CH_3O on the ignition phenomenon are shown in Figure 5.3. In this figure are plotted the temperature and O-atom concentration as a function of distance for the 69-reaction screened set and the same set less the two reactions containing methoxyl, viz.,

$$(148) \quad CH_3 + O_2 \rightarrow CH_3O + O$$
$$(149) \quad CH_3O + M \rightarrow CH_2O + H + M \quad .$$

As can be seen in the figure the effect of the methoxyl is very small indeed. There is a slight shift in the ignition but if the curves were overlayed it would be seen that the O-atom concentration curves are identical while the temperature profiles are identical for $T \geq 1400^{\circ}K$. There is a slightly larger gradient for $T < 1400^{\circ}K$ when the methoxyl is present. On the basis of this comparison and the previous screening studies it seems reasonable to conclude that methoxyl-containing reactions are not of importance in methane combustion for temperatures in excess of $1500^{\circ}K$. Nevertheless these reactions are included at low temperatures ($T < 1500^{\circ}K$) and fuel-rich conditions.

Figure 5.3
EFFECT OF METHOXYL (CH_3O) ON IGNITION DELAY [IGN (ϕ = 1)]
(Temperature and Oxygen Mass Fraction)

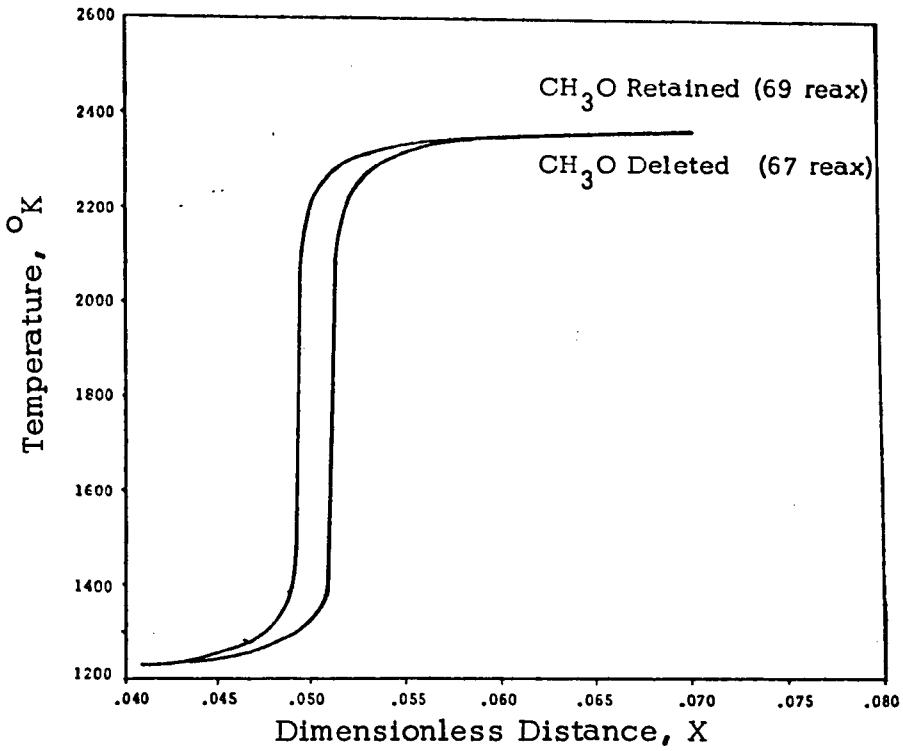

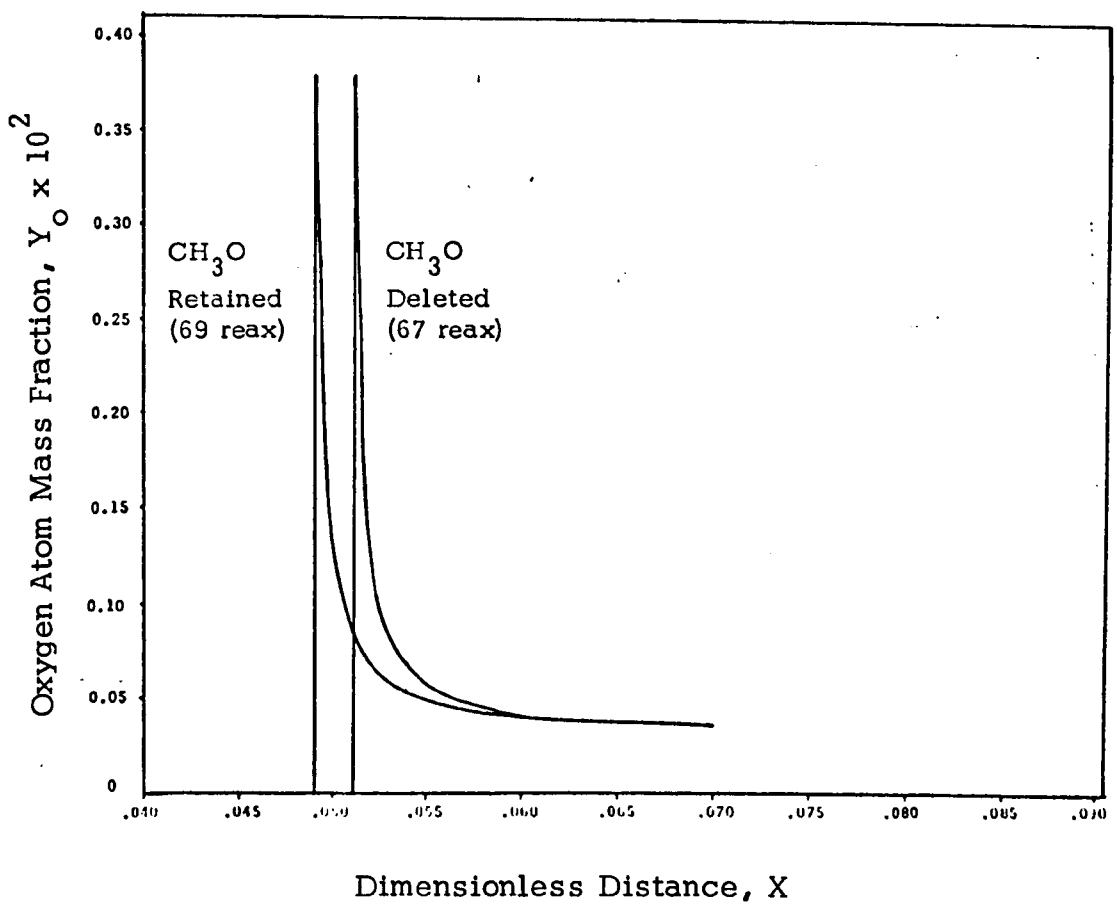

4. Controlling Reaction Sets for Ignition (22 Reax) and Pyrolysis (32 Reax)

With these reactions we have a set of 32 reactions in 17 species, listed in Table 5.1. The results are essentially indistinguishable from the baseline case (69 reactions/25 species).

TABLE 5.1

CONTROLLING REACTION SETS FOR IGNITION CASE [IGN (ϕ = 1)]

CONTROLLING REACTION SET (22 REAX/15 SPECIES) FOR IGNITION CASE [IGN (ϕ = 1)] (Sufficient for T > 1500°K)

CONTROLLING REACTION SET (32 REAX/17 SPECIES) FOR METHANE PYROLYSIS (Needed to describe ignition delay, T ≤ 1500°K)

Termolecular Reactions

36	CHO + M	= CO + H + M
77	CO2 + M	= CO + O + M
84	H2O + M	= HO + H + M
99	H + O + M	= HO + M
101	H + O2 + M	= HO2 + M

Bimolecular Reactions

44	CHO + H	= CO + H2
46	CH2O + O	= CHO + HO
47	CHO + HO	= CO + H2O
52	CHO + O	= CO + HO
59	CH3 + O	= CH2O + H
63	CH4 + O	= CH3 + HO
65	CH4 + H	= CH3 + H2
66	CH4 + HO	= CH3 + H2O
70	CO + HO	= CO2 + H
83	H + HO	= H2 + O
88	HO + H2	= H + H2O
91	HO + N	= H + NO
100	HO + O	= H + O2
117	HO + HO	= H2O + O
125	N + NO	= N2 + O
133	N + O2	= NO + O
143	CHO + O2	= CO + HO2

Pyrolysis Reactions

39	CHO + CH3	= CH2 + CH2O
41	CHO + CH4	= CH2O + CH3
56	CH3 + H	= CH2 + H2
57	CH3 + HO	= CH2 + H2O
58	CH2 + O2	= CH2O + O
60	CH3 + O2	= CH2O + HO
61	CH4 + M	= CH3 + H + M
64	CH3 + HO2	= CH4 + O2
148	CH3 + O2	= CH3O + O
149	CH3O + M	= CH2O + H + M

It is worthwhile noting that ten of the reactions discussed above are important only at small times, i.e., at low temperatures. As such, these may be classified as pyrolysis reactions which may be discarded for temperatures in excess of $1500^{o}K$. In order to verify this, a special set of 22 reactions in 16 species was extracted from the 32 reaction/17 species set by eliminating the pyrolysis reactions [including those involving CH_2 which were discussed in connection with the WSR ($\phi > 1$) case]. This reaction set is shown in Table 5.1 and appears to be valid to describe ignition <u>following</u> ignition delay. The agreement found for the temperature and each of the species concentrations is good to excellent, for temperatures greater than $1500^{o}K$. Of course, the ignition delay predicted by the smaller reaction set is meaningless.

5. Critical Paths of Methane Oxidation

The methane breakdown mechanism is shown at three specific times during ignition (in Figure 5.4). Bearing in mind the purpose of this investigation is to characterize the heat release and pollutant formation. We have analyzed processes at ignition, at maximum O-atom concentration and at maximum rate of nitric oxide formation. Notice that the times involved differ by only a fraction of a millisecond, yet this time difference is larger than the chemical runaway time. One important feature which distinguishes ignition from the stirred reactor and post flame cases is the recombination of CO + H to form CHO:

$$(36) \qquad CO + H + M \rightarrow CHO + M$$

This is probably attributable to the high CO-overshoot which occurs with the runaway, arising because the main CO_2-producing reactions are too slow to keep up with the rapid production of CO.

A qualitative picture of the ignition phenomenon can be gained by examining the history of key heat release constituents (CO and H_2O), radicals (HO and O), pollutant (NO), and hydrocarbon intermediate (CH_2O, chosen because it is the only stable molecule in the sequence). The results are shown in Figure 5.5. The temperature and O-atom concentration profiles

Figure 5.4

METHANE OXIDATION PATHS FOR IGNITION ($\phi = 1$)

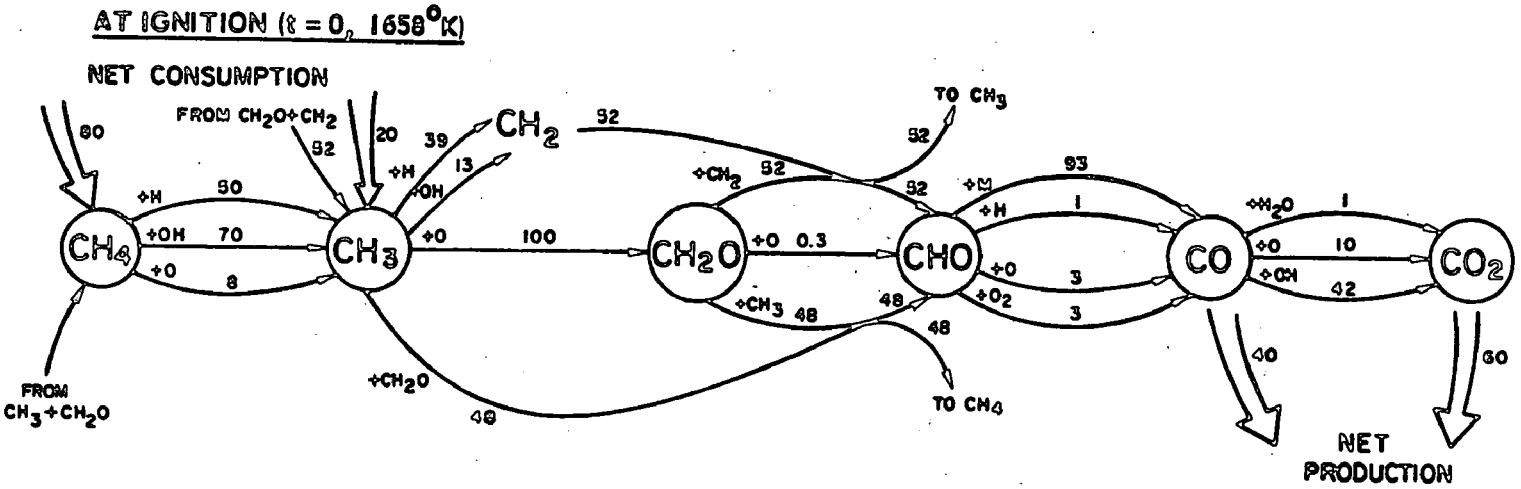

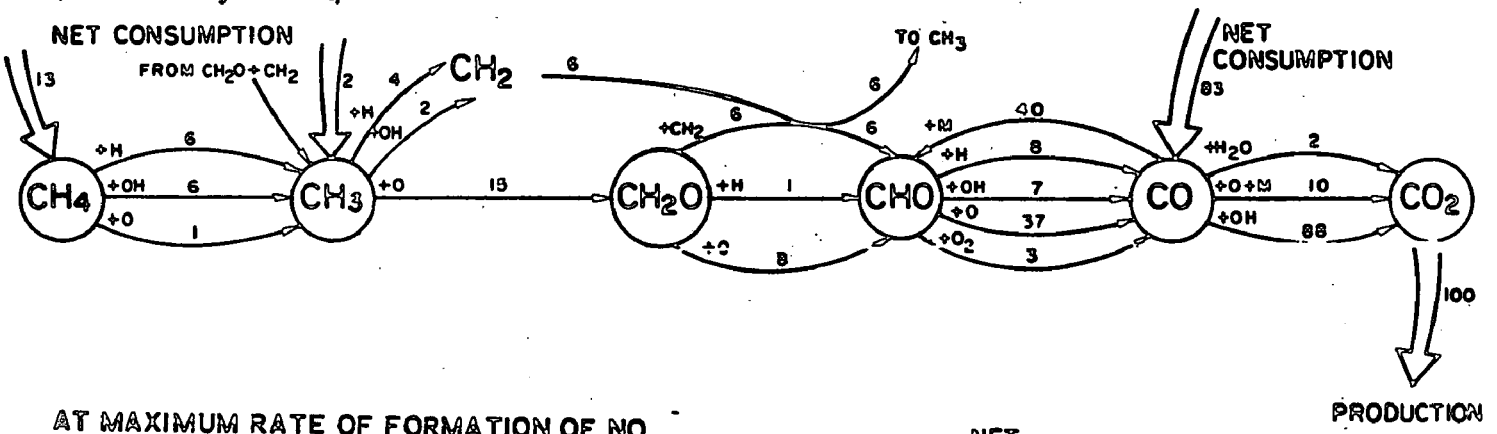

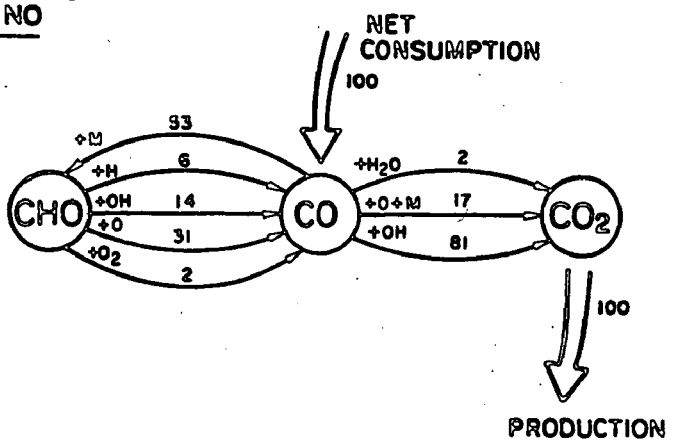

All rate numbers based on 100 mole/sec net production of ($CO + CO_2$)

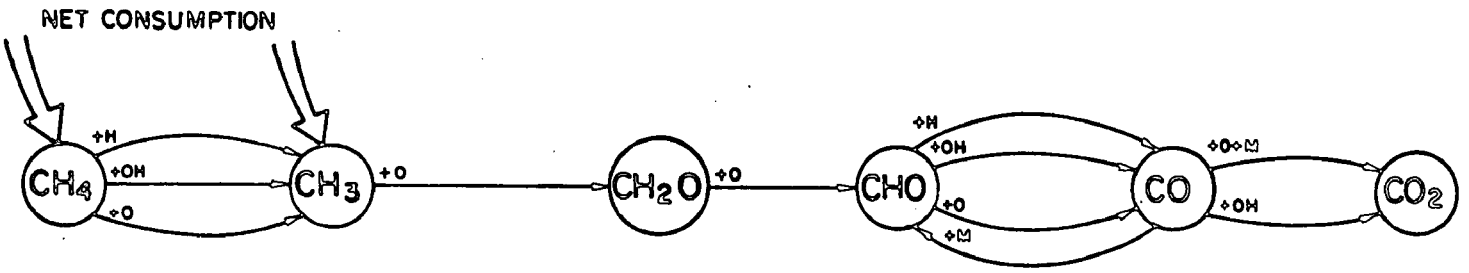

have already been seen in Figure 5.3. The radicals behave in the same way as CO, exhibiting a very sudden rise and overshoot then gradually relaxing to equilibrium. The water behaves much like the temperature, rising monotonically to its equilibrium value. The formaldehyde comes into existence suddenly during the runaway and disappears as quickly as it appeared.

Figure 5.5

MASS FRACTION PROFILES FOR IGNITION
[IGN ($\phi = 1$)]

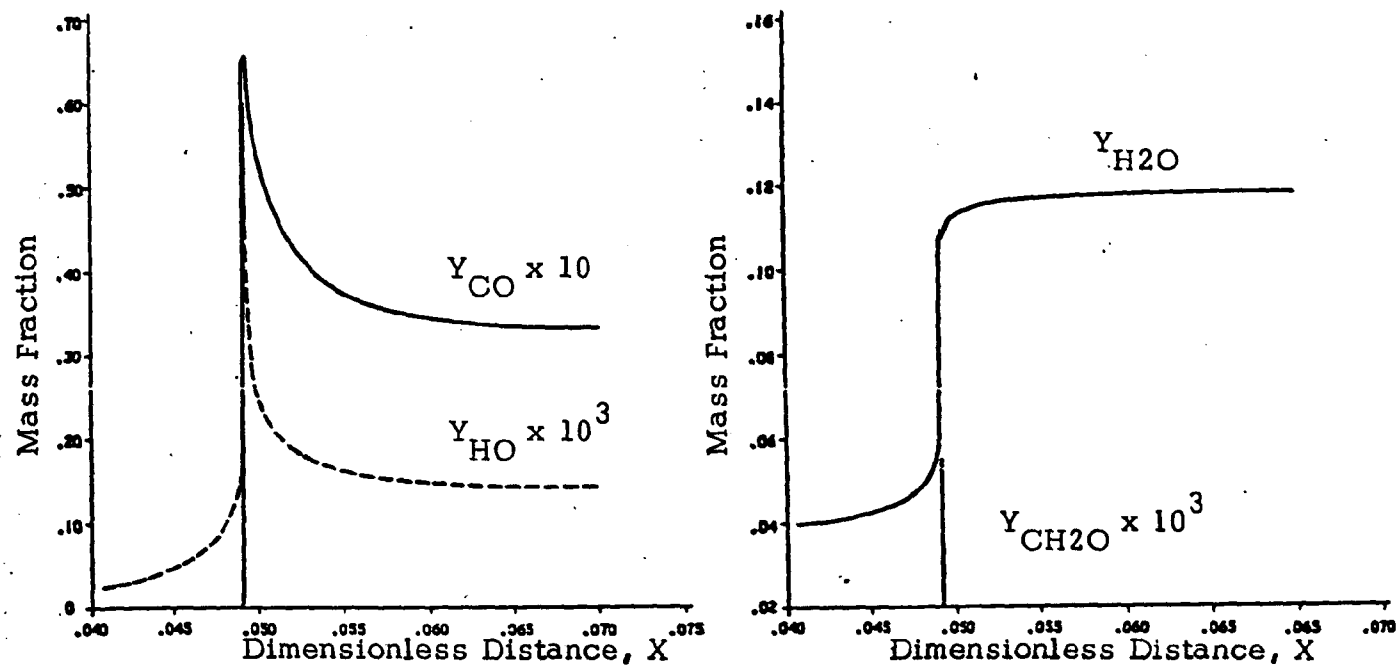

(a) Carbon Monoxide and Hydroxyl Histories

(b) Water and Formaldehyde Histories

6. Critical Paths for Nitric Oxide Formation

Thus far, we have confined our attention in this case IGN ($\phi = 1$) to the hydrocarbon sequence and no mention has been made of NO. Figure 5.6 shows the NO concentration for the 69 reaction/25 species case, which allowing for differences in the ignition delay, is reproduced faithfully by the controlling 22-reaction set. This brings up the question of prompt NO which is currently of interest.

In spite of an oxygen atom overshoot of 11 times equilibrium, there is negligible prompt NO formed. The NO-formation actually begins after the runaway, if we interpret the runaway to occur during the rise and fall of formaldehyde.

Figure 5.6

NITRIC OXIDE PROFILE FOR IGNITION OF PREHEATED REACTANTS ($\phi = 1$)

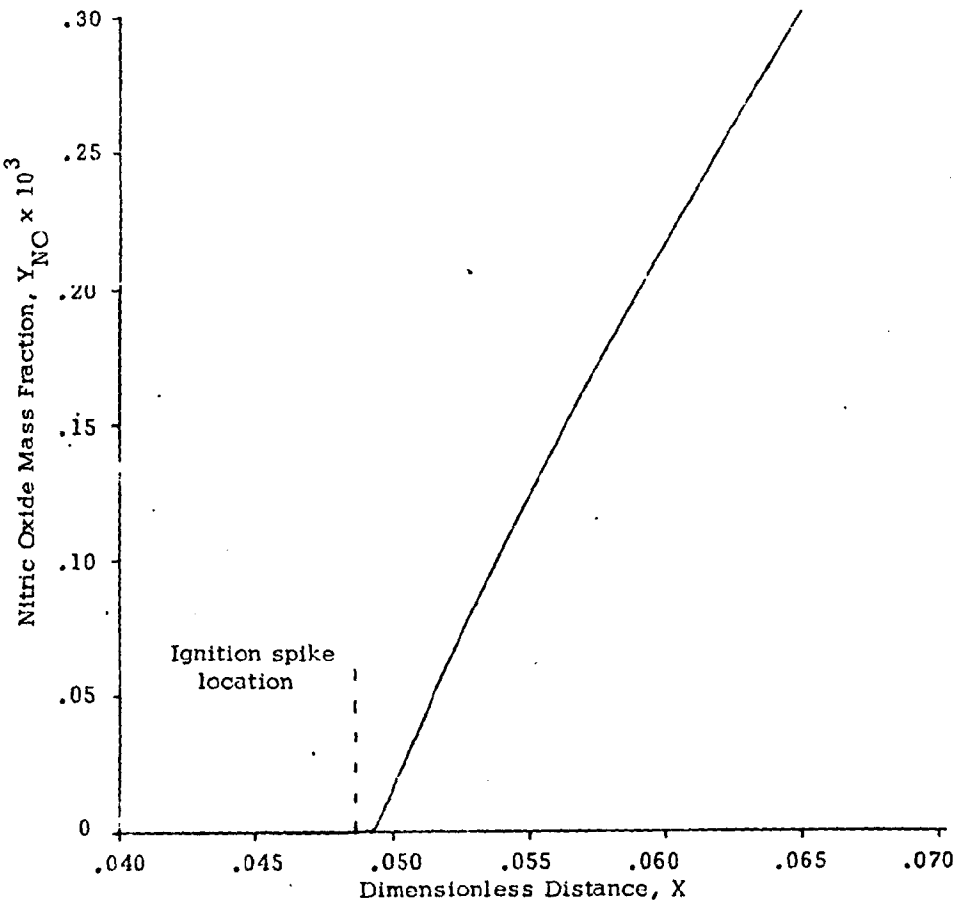

In fact, while the NO-formation rates themselves are potentially very high during the O-atom overshoot, the temporal duration is so short and the temperature is so low as to preclude the possibility of forming substantial NO. Figure 5.7 shows a blow-up of the runaway. The O-atom overshoot duration is only 150 microseconds. $(O)/(O)_{eq}$ has fallen to 1.5 before the temperature reaches 2000°K, the temperature at which the NO-formation rate becomes significant. NO production from O-atom overshoot cannot be ruled out in real flames, however, since with backmixing the high O-atom concentrations would be free to diffuse to adjacent high temperature regions.

An alternate possibility for prompt NO is the reaction $R + N_2 \rightarrow RN + N$. For example, if R is CH, RN is CHN. Indeed CHN has been observed in flat flames [Eberius et al. (1973)]; however, none is predicted for the present 134-reaction master set. Chapter VII describes how CHN and "prompt" NO would be predicted if the reaction $CH_2 + N_2 \rightarrow CHN + N$ were added to the 134-reaction set.

Figure 5.7

DETAILED STRUCTURE OF IGNITION RUNAWAY

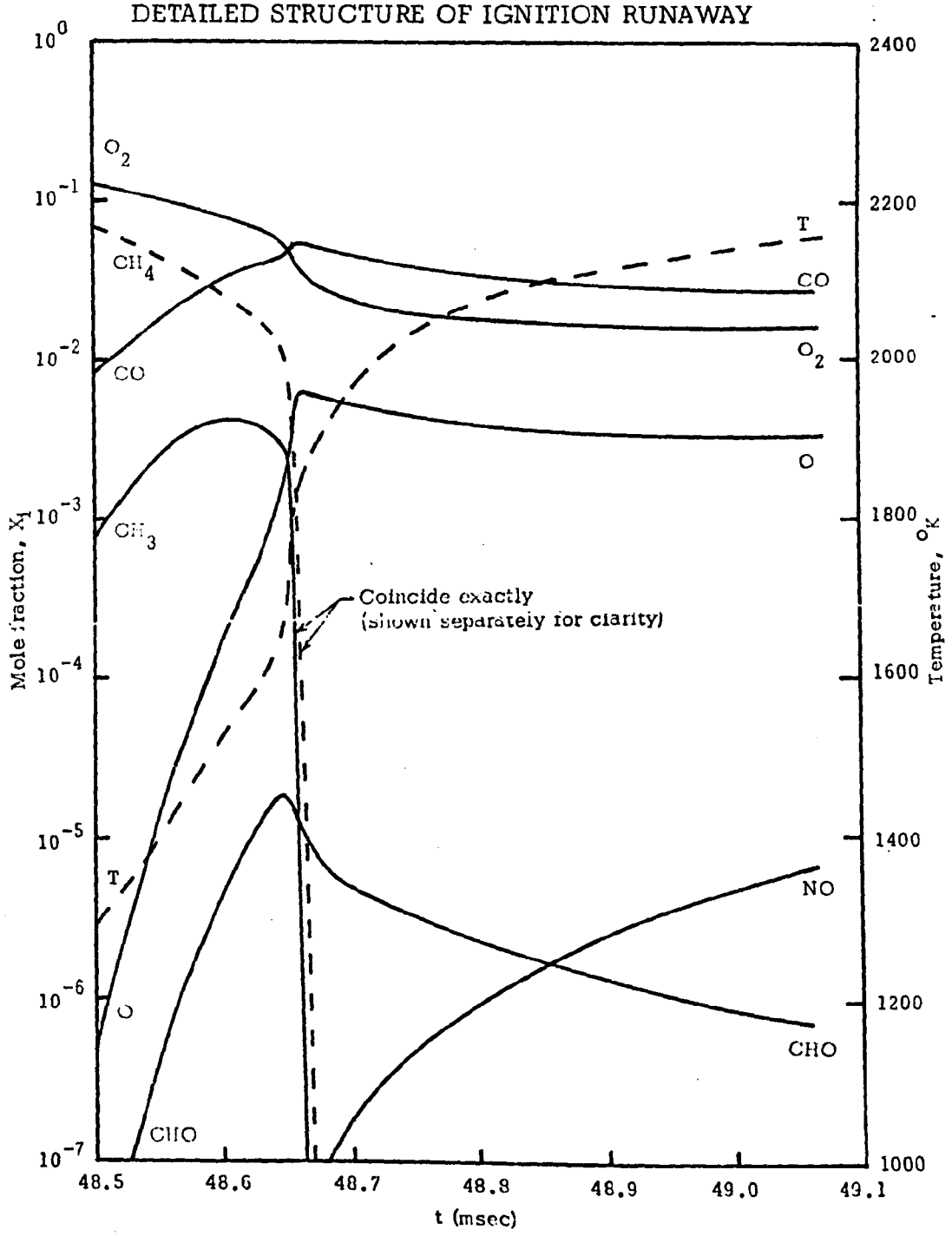

B. POST-FLAME REACTIONS AT STOICHIOMETRIC ($\phi = 1$)

1. Application of Screening Criterion

A plug flow case was set up to represent the after-burning region of a combustor, where the hot products such as CO equilibrate on longer time scales than the main heat release zone. The initial composition was specified as the WSR ($\phi = 1$) output, and the case was constrained to be adiabatic.

The reaction screening on 134 reactions reduced the number to 61, and the histories of key species and temperature are shown in Figure 5.8.

Figure 5.8

PROFILES FOR POST-FLAME CASE
(Plug Flow, $\phi = 1$)

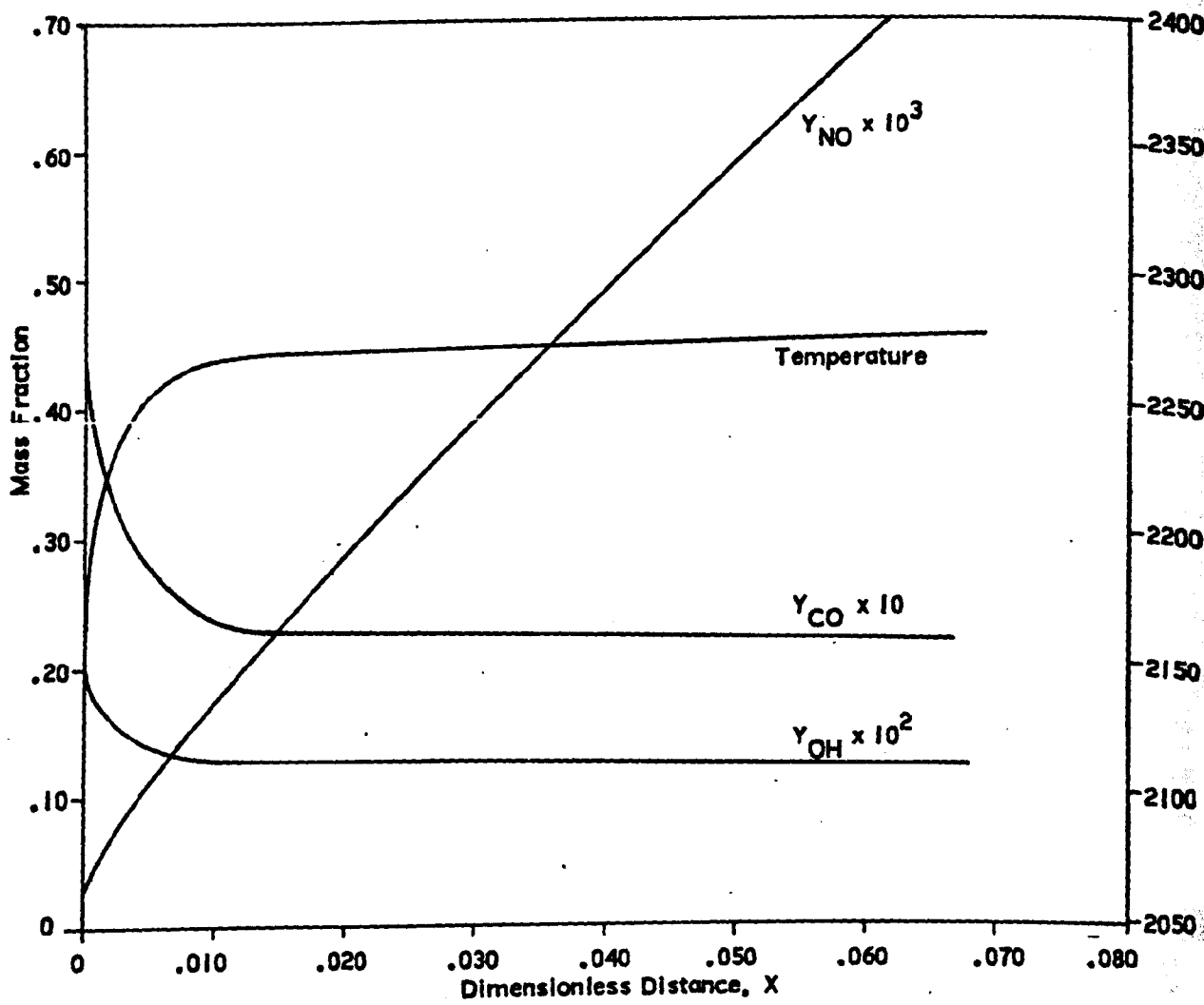

2. Elimination of Insignificant Species

Following the examples suggested by the stirred reactor runs, it was found that the nine species CH, CH_2, CHN, CH_3O, CN, HN, HNO, NO_2, and N_2O could be eliminated.

3. Reduced Reaction Set for PF ($\phi = 1$)

This resulted in 23 reactions in 16 species; these are shown in Table 5.2. The predictions of this set compared favorably with the 61-reaction set.

Table 5.2

SCREENED REACTION SET (23 REAX) FOR ADIABATIC PLUG FLOW REACTOR ($\phi = 1$)

Termolecular Reactions

36	CHO + M	= HO + H + M
77	CO2 + M	= CO + O + M
84	H2O + M	= HO + H + M
99	H + O + M	= HO + M
101	H + O2 + M	= HO2 + M

Bimolecular Reactions

44	CHO + H	= CO + H2
46	CH2O + O	= CHO + HO
47	CHO + HO	= CO + H2O
52	CHO + O	= CO + HO
59	CH3 + O	= CH2O + H
63	CH4 + O	= CH3 + HO
65	CH4 + H	= CH3 + H2
66	CH4 + HO	= CH3 + H2O
70	CO + HO	= CO2 + H
83	H + HO	= H2 + O
85	H + HO2	= HO + HO
88	HO + H2	= H + H2O
91	HO + N	= H + NO
100	HO + O	= H + O2
117	HO + HO	= H2O + O
125	N + NO	= N2 + O
133	N + O2	= NO + O
143	CHO + O2	= CO + HO2

4. Critical Paths of Oxidation

Oxidation paths are shown in Figure 5.9 for various elapsed times in the simulated post flame region. Oxidation of the intermediates CH_2O and CHO in the earliest stages is somewhat artificial because of the initial condition (in a real combustor the post-flame region would not start literally with such a nonequilibrium WSR case). Therefore we direct the analysis to the oxidation mechanisms occurring no sooner than 2 msec after the initial condition. After 3 milliseconds, the methane, methyl, and formaldehyde are totally consumed, and the main phenomenon is conversion of CO to CO_2 by reaction (70), $CO + OH \rightarrow CO_2 + H$, sustained by exchange reactions with CO. The temperature has gone up from 2064 to 2251°K.

After 64 milliseconds, the CO has all been converted to CO_2 and the temperature is equilibrated to a value 216°K above the starting condition. Also the radicals O, H, and OH have equilibrated. For the remainder of the residence time in the reactor only the slower NO-formation reactions are still active and NO is being produced at a uniform rate (NO concentration increasing linearly with time), as shown in Figure 5.10.

5. Paths of Nitric Oxide Formation

Because of the large residence time (60 msec) and the high adiabatic temperature, cumulative NO_x was relatively high compared to the WSR cases. In fact the N-O reactions were the only reactions significantly out of equilibrium for t > 10 msec. But since products quickly cool by turbulent entrainment in a real boiler, no inference can be made about the actual relative NO production in primary vs. post-flame.

Figure 5.9

METHANE OXIDATION MECHANISMS
IN SIMULATED POST FLAME CONDITIONS
PFR ($\phi = 1$)

EARLY POST FLAME (t = 0)

Same as WSR ($\phi = 1$)

T = 2064°K

NO = 24 ppm

Rates ≈ 10^{-5} mole/cc-sec

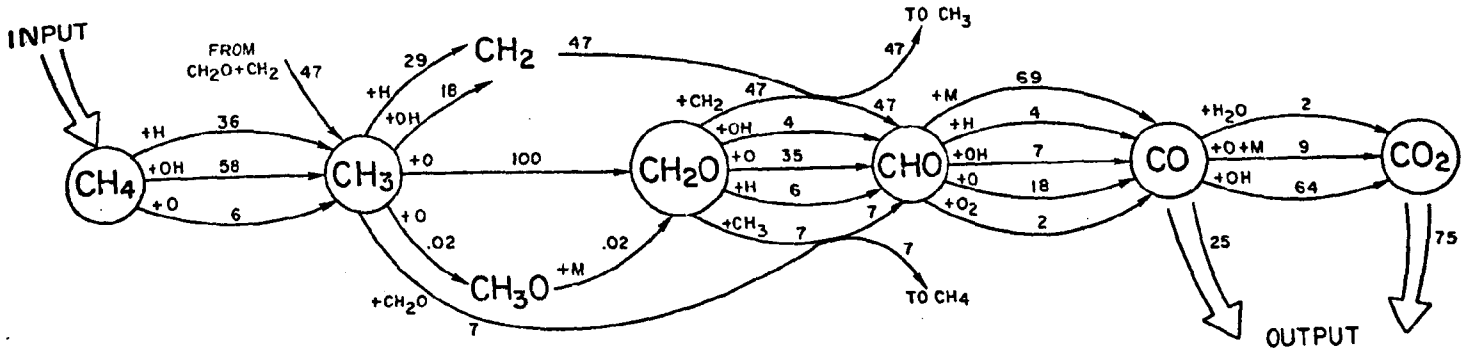

RELAXATION (t = 3.3 msec)

T = 2251°K

NO = 80 ppm

Rates ≈ 10^{-7} mole/cc-sec

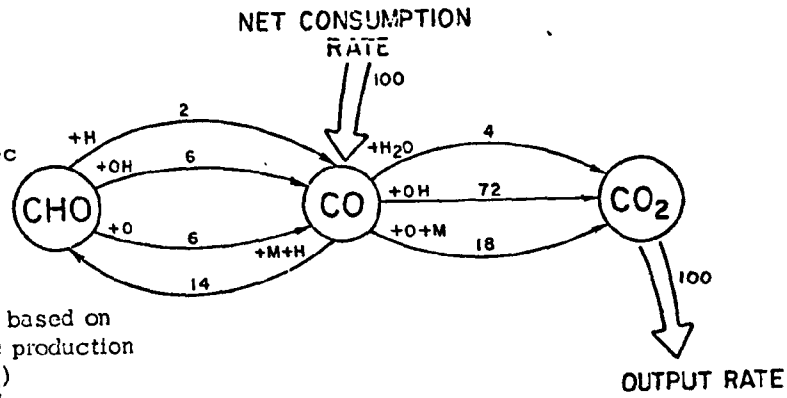

Rate numbers based on
100 mole/sec production
of ($CO + CO_2$)

NEAR EQUILIBRATION (t = 64.5 msec)

T = 2280°K

NO = 712 ppm

Rates ≈ 10^{-10} mole/cc-sec

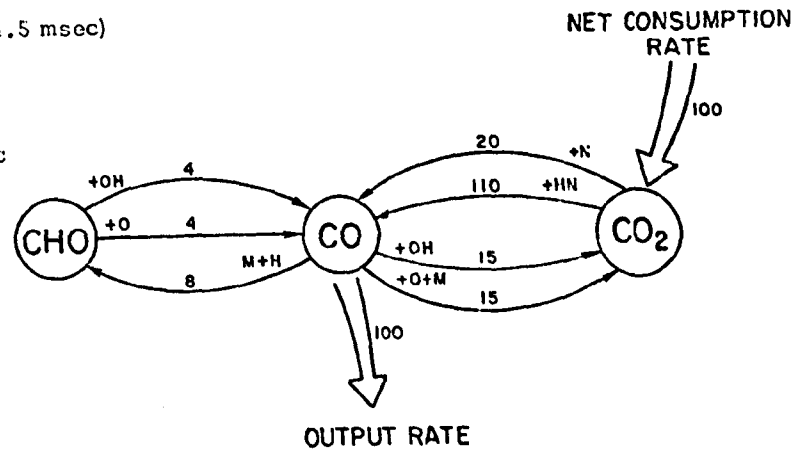

The $O + N_2 \rightarrow$ mechanism [reaction (125)] controls N_2 break up in the plug flow region, as shown in Figure 5.10.

Four paths compete for the N-atoms produced by this N_2 break up:

(133)	$N + O_2 \rightarrow NO + O$	32%
(91)	$N + OH \rightarrow NO + H$	26%
(104)	$N + H_2O \rightarrow HN + OH \rightarrow \ldots \rightarrow NO$	26%
(73)	$N + CO_2 \rightarrow NO + CO$	6%

The $N_2O + O \rightarrow NO + NO$ path is of minor importance. Presumably if heat loss had been simulated, $NO \rightarrow NO_2$ would have been observed at lower temperatures.

Figure 5.10

NITRIC OXIDE MECHANISM IN SIMULATED POST FLAME CASES
PFR (ϕ = 1)

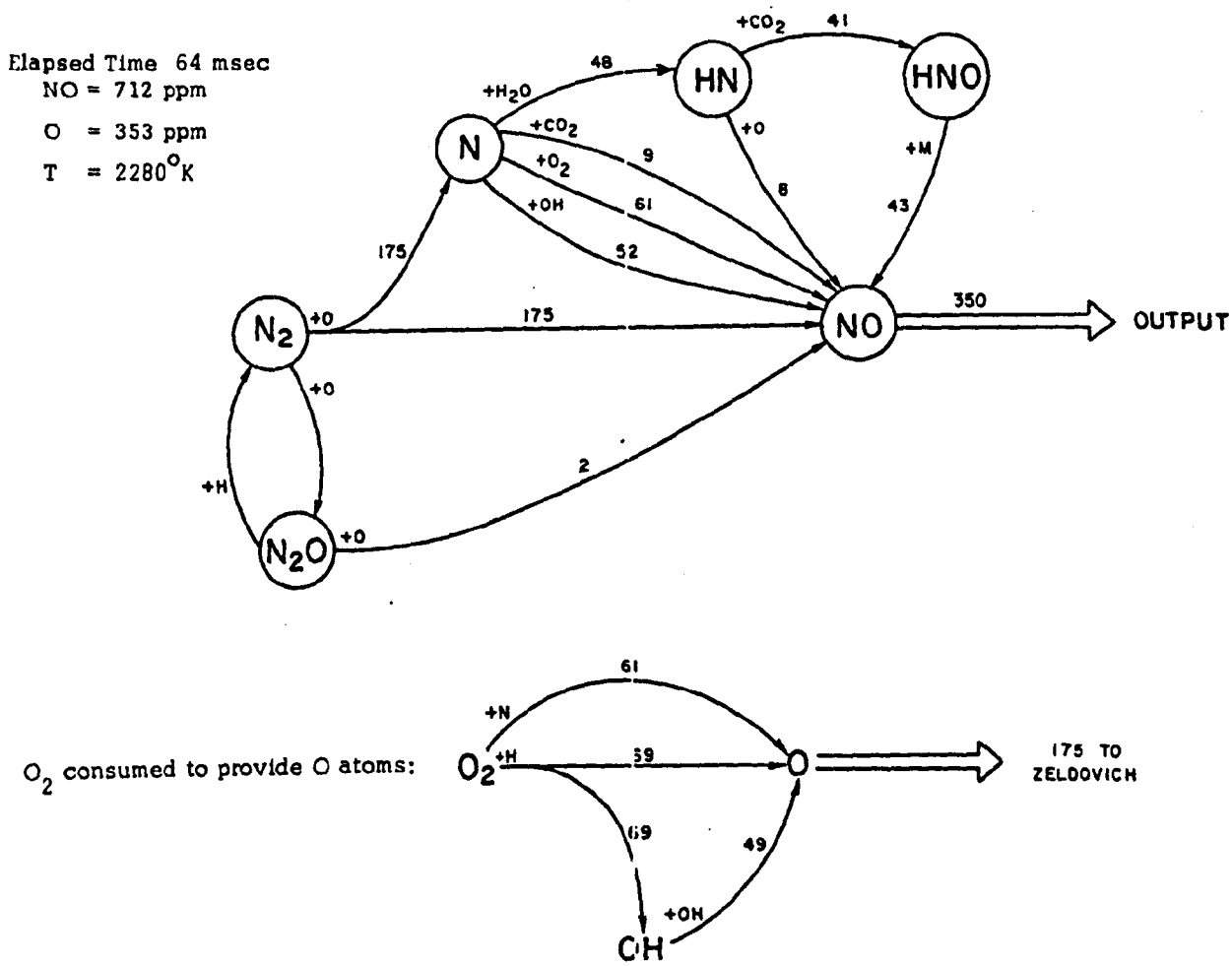

VI. SYNTHESIS OF THE SCREENED REACTION SET

A. UNION REACTION SET FOR FIVE TEST CASES

Because limiting cases have been included, the union of the five reaction sets obtained in the sections IV and V hopefully represents most of the reactions necessary and sufficient to describe methane combustion and pollutant formation under the conditions

$$p = 1 \text{ atm}$$

$$1500^{\circ}K < T < 2500^{\circ}K$$

$$0.8 < \phi < 1.25$$

The reactions are summarized in Table 6.1, where the union is seen to consist of 26 reactions in 16 species. Of these, 12 are related to the methane breakdown, 8 are in the O-H chain, and 6 are related to the pollutant formation (i.e., nitric and nitrous oxide). Table 6.2 compares this union set with reactions selected by previous investigators.

B. CORROBORATION WITH THREE NEW CASES

To confirm the predictive validity of the reaction set, the following cases were run using the 134-reaction master set and then repeated with the 26 reaction set:

IGN ($\phi > 1$):	Ignition of methane/air at an equivalence ratio of 1.25. As with IGN ($\phi < 1$), a 70/30 ratio of reactants to equilibrated products was permitted to ignite at 1200°K.
PFR ($\phi < 1$):	The output concentration from a well-stirred reactor at $\phi = 0.8$ was permitted to approach equilibrium adiabatically.
PFR ($\phi > 1$):	The output concentrations of a stirred reactor at $\phi = 1.25$ was permitted to approach equilibrium through a region with a T^4 heat loss.

Table 6.1

UNION OF CONTROLLING REACTION SETS

Rate Coefficients* $k_f = A T^{-n} e^{-E/RT}$

Reaction Number	Reaction	A	n	E	Reference	Conditions for Which Reaction is Needed
	CH4 Partial Oxidation					
036	CHO +M=CO +H +M	2.50E+20	1.5	16.8	BENSON(1973)	All
044	CHO +H =CO +H2	3.00E+10	-1.	0.	BENSON(1973)	$\phi < 1$
046	CH2O+O =CHO +HO	2.00E+11	-1.	4.4	BENSON(1973)	All
047	CHO +HO =CO +H2O	3.00E+10	-1.	0.	BENSON(1973)	$\phi < 1$
052	CHO +O =CO +HO	3.00E+11	-1.	.5	BENSON(1973)	All
059	CH3 +O =CH2O+H	2.00E+12	- .5	- .3	MORRIS(1973)	All
063	CH4 +O =CH3 +HO	1.00E+10	-1.	8.	WESTENBERG(1969)	$\phi \leq 1$
065	CH4 +H =CH3 +H2	5.00E+10	-1.	10.	WALKER(1968)	All
066	CH4 +HO =CH3 +H2O	3.00E+13	- .0	5.	WILSON(1972)	All
143	CHO +O2 =CO +HO2	8.00E+12	- .0	0.	PEETERS(1973)	All
	CO Oxidation					
070	CO +HO =CO2 +H	4.00E+09	- .5	0.	ENGLEMAN(1973)	All
077	CO2 +M=CO +O +M	1.00E+15	0.	100.	CLARK(1971)	All
	O-H Reactions					
083	H +HO =H2 +O	8.00E+09	- 1.	7.	BAULCH(1973)	$\phi \geq 1$
084	H2O +M=HO +H +M	3.00E+15	.0	105.	BAULCH(1972)	All
085	H +HO2 =HO +HO	2.50E+14	- .0	1.9	BAULCH(1972)	IGN
088	HO +H2 =H +H2O	2.50E+13	- .0	5.2	BAULCH(1972)	All
099	H +O +M=HO +M	6.00E+15	.0	0.	SCOFIELD(1973)	All
100	HO +O =H +O2	2.50E+13	- .0	0.	BAULCH(1972)	All
101	H +O2+M=HO2 +M	1.50E+15	.0	1.	BAULCH(1972)	All
117	HO +HO =H2O +O	6.00E+12	- .0	1.	BAULCH(1972)	All
	NO Formation					
091	HO +N =H +NO	6.00E+11	- .5	8.	BENSON(1973)	All
098	H +N2O =HO +N2	8.00E+13	- .0	15.	BAULCH(1973)	$\phi < 1$
125	N +NO =N2 +O	1.50E+13	- .0	0.	BAULCH(1973)	All
133	N +O2 =NO +O	6.00E+09	- 1.	6.3	BAULCH(1973)	$\phi \leq 1$
135	N2O +O =NO +NO	1.00E+14	- .0	28.	BAULCH(1973)	$\phi < 1$
140	N2O +M =N2 +O +M	1.00E+14	.0	50.	ENGLEMAN(1973)	$\phi < 1$
	Low Temperature Pyrolysis					
039	CHO +CH3 =CH2 +CH2O	1.50E+11	- .7	4.	TUNDER(1967)	T < 1500°K
041	CHO +CH4 =CH2O+CH3	8.00E+11	- .6	9.	TUNDER(1967)	T < 1500°K
056	CH3 +H =CH2 +H2	2.00E+11	- .7	3.	TUNDER(1967)	T < 1500°K
057	CH3 +HO =CH2 +H2O	6.00E+10	- .7	2.	TUNDER(1967)	T < 1500°K
058	CH2 +O2 =CH2O+O	5.00E+11	- .5	7.	TUNDER(1967)	T < 1500°K
060	CH3 +O2 =CH2O+HO	3.00E+13	- .0	30.	BENSON(1973)	T < 1500°K
061	CH4 +M=CH3 +H +M	2.00E+17	.0	88.	HARTIG(1971)	T < 1500°K
064	CH3 +HO2 =CH4 +O2	1.00E+11	- .5	6.	TUNDER(1967)	T < 1500°K
148	CH3 +O2 =CH3O+O	2.50E+09	-1.	28.5	BENSON(1973)	T < 1500°K
149	CH3O +M=CH2O+H +M	4.00E+40	7.5	22.6	BENSON(1973)	T < 1500°K

*Units: cc, mole, sec, °K, kcal

Table 6.2

COMPARISON OF CONTROLLING REACTION SET WITH THOSE OF PREVIOUS INVESTIGATORS

REFERENCE	Ultra (1974)	Mellor (1972)	Sterrling & Wendt (1972)	Bowman & Seery (1972)	Bowman (1970, 1971)	Pratt & Malte (1973)	Benson et al. (1973)
APPLICATION	Atm Burner	Gas Turbine	Atm Burner	Shock Tube	Shock Tube	Atm Burner	Atm Burner
REACTIONS							
I. Low Temperature Pyrolysis of CH4							
39 CHO + CH3 = CH2 + CH2O	•						
41 CHO + CH4 = CH2O + CH3	•						
56 CH3 + H = CH2 + H2	•						
57 CH3 + HO = CH2 + H2O	•						
58 CH2 + O2 = CH2O + O	•						
60 CH3 + O2 = CH2O + HO	•		•		•		
61 CH4 + M = CH3 + H + M	•	•	•	•	•	•	•
64 CH3 + HO2 = CH4 + O2	•		•		•		•
148 CH3 + O2 = CH3O + O	•						•
149 CH3O + M = CH2O + H + M	•						•
II. CH4 Decomposition and Partial Oxidation							
63 CH4 + O = CH3 + HO	•	•	•	•	•	•	•
65 CH4 + H = CH3 + H2	•	•	•	•	•	•	•
66 CH4 + HO = CH3 + H2O	•	•	•	•	•	•	•
59 CH3 + O = CH2O + H	•		•		•		•
145 CH3 + O = CHO + H2				•			
144 CH3 + O2 = CHO + H2O		•		•	•	•	
46 CH2O + O = CHO + HO	•						•
48 CH2O + H = CHO + H2							•
49 CH2O + HO = CHO + H2O			•		•		•
36 CHO + M = CO + H + M	•	•	•	•	•	•	•
44 CHO + H = CO + H2	•						
47 CHO + HO = CO + H2O	•	•	•	•	•	•	•
52 CHO + O = CO + HO	•						
143 CHO + O2 = CO + HO2	•						
III. CO Oxidation							
70 CO + HO = CO2 + H	•	•	•	•	•	•	•
77 CO + O + M = CO2 + M	•					•	•
78 CO + O2 = CO2 + O						•	
IV. O-H Bimolecular Propagation							
83 H + HO = H2 + O	•	•	•	•	•	•	
85 H + HO2 = HO + HO	•		•				
86 H + HO2 = H2 + O2			•				•
88 HO + H2 = H + H2O	•	•	•	•	•	•	
100 HO + O = H + O2	•	•	•	•	•	•	•
116 H2 + O2 = HO + HO		•				•	
117 HO + HO = H2O + O	•	•	•	•	•	•	
118 HO + HO2 = H2O + O2			•				•
122 HO2 + O = HO + O2			•				
V. O-H Termolecular Termination							
79 H2 + M = H + H + M		•	•			•	
84 H2O + M = HO + H + M	•	•	•	•	•	•	
99 H + O + M = HO + M	•	•				•	
101 H + O2 + M = HO2 + M	•		•				•
142 O + O + M = O2 + M		•	•		•	•	
NA H + OH + H2O = H2O + H2O			•				
NA H + O2 + H2O = HO2 + H2O			•				
VI. NO Formation							
91 HO + N = H + NO	•	•	•	•	•	•	
124 N + N + M = N2 + M			•				
125 O + N2 = NO + N	•	•	•	•	•	•	
132 NO + M = N + O + M		•			•	•	
133 N + O2 = NO + O	•	•	•	•	•	•	
134 NO + NO = N2 + O2		•					
146 N2 + OH = NO + HN		•			•		
VII. Involving NO2							
127 N + NO2 = NO + NO		•			•		
129 N + NO2 = N2 + O2		•			•		
136 NO + NO2 = N2O + O2			•			•	
138 NO2 + M = NO + O + M		•				•	
139 NO2 + O = NO + O2		•				•	
NA NO2 + M = O2 + N + M		•				•	
VIII. Involving N2O							
98 H + N2O = NO + N2	•	•	•			•	
135 N2O + O = NO + NO	•	•	•			•	
137 NO + N2O = NO2 + N2			•				
140 N2O + M = N2 + O + M	•		•			•	
141 N2O + O = N2 + O2		•	•			•	

*Ultrasystems Pyrolysis Reactions

For the ignition case, IGN ($\phi > 1$), an additional run was made with the union reaction set plus the ten pyrolysis reactions (for a total of 36 reactions in 18 species). In all cases the comparisons were made graphically and the results were generally excellent. A few exceptions did occur and these are discussed below.

In the case IGN ($\phi > 1$), the complete set with ten additional pyrolysis reactions gives excellent agreement at low temperature, whereas the 26 reaction/16 species set exhibits gross misrepresentations (e.g., formaldehyde) during preignition. It was also observed that HO radical concentrations were about 50% greater with the 26-reaction set than with the more complete one.

The reference solution for PFR ($\phi > 1$) with heat loss predicted NO slightly decreasing downstream, whereas with the reduced set NO tends to remain constant. (See Figure 6.1) The change in NO concentration, amounting to about 1% of original NO in 20 msec, was determined to be due to the following reaction sequence

$$CHO + NO \rightarrow CO + HNO \rightarrow CO_2 + HN$$

which was screened out of the 26 reaction set, and apparently only occurs under peculiar conditions of heat loss and composition. This numerical result suggests that NO may be reduced by injection of formaldehyde (a stable hydrocarbon which readily goes to formyl) into the post flame zone. Such scavenger techniques for reduction of NO have received only modest attention in the literature to date. This result must be treated as speculative because (a) the rates used in the calculation are unknown, (b) fuel rich conditions are rare in post flame regions of real combustors, and (c) the behavior may level off at a 2-3% reduction upon depletion of CHO.

It is felt that this agreement confirms that the union reaction set of 26 reactions in 16 species to be as good as the original 134-reaction set at describing methane combustion in the conditions previously stated.

Figure 6.1

NITRIC OXIDE DECOMPOSITION
OBSERVED FOR PFR ($\phi > 1$)

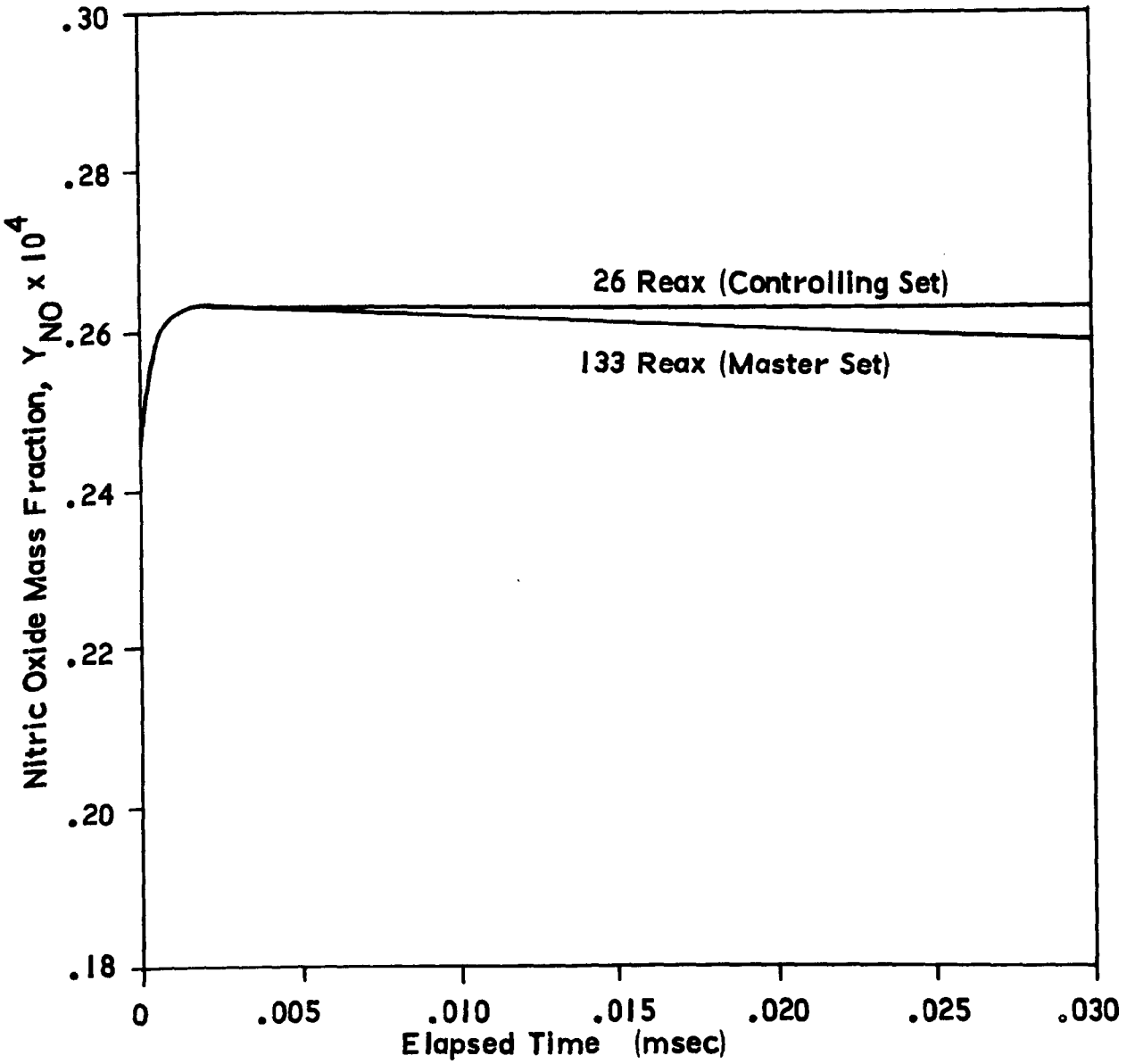

VII. EVALUATION OF REACTION SET AGAINST STIRRED REACTOR DATA

A. PURPOSE

In the foregoing sections, a kinetic model describing CH_4/air combustion was synthesized from a master set of 134 reactions with assigned rates. It was found that 26 reactions are necessary and sufficient to duplicate to $\pm 5\%$ the predictions of the master set for $.80 < \phi < 1.25$, $1500^{\circ}K < T < 2500^{\circ}K$, and $P = 1$ atm. The validity of this 26 reaction subset obviously depends on the accuracy of the original 134-reaction set in two crucial aspects:

(1) That no significant reaction was inadvertently omitted.

(2) That rate constants selected for each of the 134 reactions sufficiently describe the actual rate. Here it is recognized that the three numbers characterizing a given rate (A, n, E) are not exclusive. It is also recognized that the more significant a reaction is, the more accurately its rate must be known.

With regard to item (1), the probability of overlooking a significant reaction is not negligible, because the CHON system can support over 400 bimolecular reactions* of which only 134 have been included. With regard to item (2), whereas the rate uncertainty can be as low as a factor of X2 for well-studied reactions, some 85 of the 134 reactions had not been related to experimental measurements and required rate approximation techniques accurate in most cases to no better than $X10^3$.

Given these compounded uncertainties, any numerical screening without comparison to measured data could easily result in a subset which is partially or completely fictitious. The purpose of the comparison reported herein was to test the predictive ability of the 26-reaction subset against measurements of CH_4/air combustion systems. The system selected as a data base was the well stirred reactor, because of the ease with which it can be modelled due to minimum mixing effects; other idealized combustion systems of interest for further comparison are the shock-tube and the flat flame.

*Considering bimolecular collisions and only triatomic, diatomic, and atomic species; in addition, one includes certain more complex molecules such as CH_4, CH_2O, and CH_3 and these replace unlikely smaller molecules such as C_2O, C_2N, and HN_2.

The stirred reactor data reported by Bartok and Engleman (1972) on the CH_4/air system was selected because their Longwell reactor is rate limited, exhibiting residence times of less than 2 msec, in contrast to other devices requiring longer residence times because of greater "unmixedness" [e.g., Pratt and Malte (1973)]. This data is more reliable than the earlier data of Bartok et al. (1971) because of the use of a chemiluminescent NO_x analyzer instead of the electrochemical device which is suspect under fuel-rich conditions. In the following sections we describe how the Kinetic Analysis Program (KAP) was adapted to model the Longwell reactor, present the comparison with the numerically screened set, and finally suggest specific explanations which could be considered to bring data and theory into agreement:

(1) Revised reactions and rates

(2) Experimental errors due to probe and analyzer phenomena.

(3) Model deficiencies due to imperfect mixing or inadequate representation of heat loss.

B. REPRESENTATION OF EXPERIMENTAL CONDITIONS WITH KAP

The jet-stirred reactor shown in Figure 7.1 and described by Bartok and Engleman (1972) is represented by a perfectly stirred (homogeneous) reactor using the KAP program (see Appendix A).

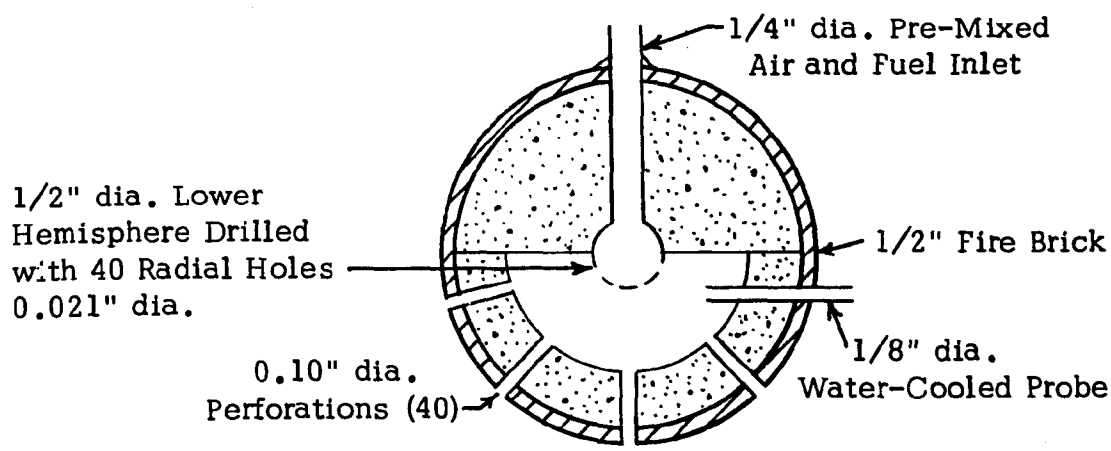

Figure 7.1

JET-STIRRED REACTOR
[Bartok and Engleman (1972)]

Needed as input to KAP are the inlet temperature, pressure, and reactant concentration, heat loss coefficient (cal/sec-^{o}K), reactor volume, and mass throughput rate (gm/sec). These were taken as follows [Bartok and Engleman 1972)]:

	Fuel Rich (ϕ = 1.41)	Stoichiometric (ϕ = 1)	Fuel Lean (ϕ = .79)
Y_{O_2}	.215	.220	.233
Y_{N_2}	.709	.725	.733
Y_{CH_4}	.076	.055	.044
T_0	375°F	375°F	375°F
P	1 atm	1 atm	1 atm
$\overline{H}$	.028 cal/sec^{o}K	.028 cal/sec^{o}K	.028 cal/sec^{o}K
V	14.5 cm^3	14.5 cm^3	14.5 cm^3
$\dot{m}$	1.22 g/sec	1.20 g/sec	1.19 g/sec

In accordance with the experimental data, variations in fuel/air ratio were obtained by holding air flow constant and varying fuel flow. This accounts for the slight increase in $\dot{m}$ with ϕ, and resulted in a slight variation in residence time.

Because the reported 14.5 cm^3 reactor volume is slightly larger than the volume calculated from the dimensions in Figure 7.1 [Bartok and Engleman (1972) seem to have neglected the injection hemisphere of 0.6 cm^3 displacement], we consider the volume of the reactor to be uncertain to about $\pm$5%. This uncertainty carries over into residence time and therefore significantly affects the kinetic predictions.

Perhaps the most critical uncertainty lies with the heat losses to which the kinetics predictions are sensitive. The heat transfer coefficient was estimated from four supporting calculations:

(a) From the discrepancy between calculated adiabatic flame temperature, T_{ad}, and measured flame temperature, T, Bartok and Engleman (1972) derived a value of H for each run from the energy balance:

$$H = \frac{(T_{ad} - T)}{(T - T_{\infty})} (\dot{m} C_p)$$

where T_{∞} is the temperature of the surrounding air. The authors recommend a value $\overline{H}$ (averaged over all runs) of .025 cal/sec^{o}K.

(b) Past studies of the Longwell reactor near the blowout limit have shown the heat loss to be about 10% of the chemical heat release. For the jet-stirred system operating on CO/air, this amounts to

$$H = 0.1\, \dot{m} \eta Q/(T - T_{\infty}) \approx .028 \text{ cal/sec}^{o}\text{K}$$

where $\dot{m}$ = 1 g/sec, η = .67 (conversion of CO to CO_2)*, Q = 701 cal/g-mixture, and $T - T_{\infty} \approx 1700^{o}$K.

(c) Direct calculations of the rate of heat transfer through a 1-1/2" thick hemispheric firebrick shell were carried out using the expression

$$\dot{Q} = \frac{2\pi r_i r_0}{r_i - r_0} k_c (T - T_{\infty})$$

Unfortunately the key parameter, thermal conductivity, varies over a factor of 10 for various types of firebrick (see Table 7.1). The average value of firebrick conductivity would lead to a value of $\overline{H}$ = .035 cal/sec^{o}K.

Table 7.1

THERMAL CONDUCTIVITY OF FIREBRICK
[From Babcock and Wilcox, Steam (1972) p 16-6]

Firebrick Type	Thermal Conductivity
B&W K-20	1.5 Btu-in/ft^2-hr^{o}F
B&W K-30	3.0 Btu-in/ft^2-hr^{o}F
Avg 1st Quality	9.0 Btu-in/ft^2-hr^{o}F
B&W Allmul	12.0 Btu-in/ft^2-hr^{o}F
B&W 80	15.0 Btu-in/ft^2-hr^{o}F

*$\eta \equiv X_{CO_2}/[X_{CO} + X_{CO_2}]$.

(d) Parametric studies of the KAP stirred reactor model with CO/air reactants were compared with corresponding data of Engleman et al. (1972). The results at $\phi = 1$ gave a best fit value between .015 and .030 cal/sec°K, as shown in Table 7.2 below:

Table 7.2

	Measured (unknown $\overline{H}$)	Predicted $\overline{H}$ (cal/sec°K)			
		$\overline{H}$=0	$\overline{H}$=.015	$\overline{H}$=0.30	$\overline{H}$=0.45
T	2080 ± 50°K	2131°K	2085°K	2037°K	1993°K
NO	90 ± 10 ppm	180 ppm	117 ppm	75 ppm	45 ppm
O_2	3.2 ± 0.5%	4.2%	4.1%	3.9%	3.8%
η	.78	.72	.73	.74	.75

Based on (a) - (d), the value of $\overline{H}$ = 0.28 cal/sec°K was adopted for the CH_4/air calculations. It is recommended that in future experiments the heat loss be measured directly at several locations using thin film gages.

C. PREDICTIONS BASED ON SCREENED REACTION SET

The 26-reaction set of Table 6.1 predicts concentration levels of NO which are much lower than measured values, as shown in Figure 7.2. The measured values are about X 2.5 higher in the lean and stoichiometric cases and about X40 higher in the rich case. This discrepancy exists despite rather good agreement of temperature and O_2 values, as shown below:

Case	T, °K Measured	T, °K Predicted	O_2, % Measured	O_2, % Predicted
ϕ=.79	1900 ± 60	1880	5.0 ± 0.5	4.5
ϕ=1.00	2050 ± 60	2065	1.4 ± 0.5	1.6
ϕ=1.41	1900 ± 60	1971	not avail.	not avail.

Edelman also obtained underpredictions of NO for the same stirred reactor fueled with propane [see Engleman et al. (1973)]; again the discrepancy was a factor of twenty on the fuel rich side.

Figure 7.2

COMPARISON OF EXPERIMENTAL DATA
FROM JET-STIRRED REACTOR WITH PREDICTIONS
BASED ON VARIOUS REACTION SETS

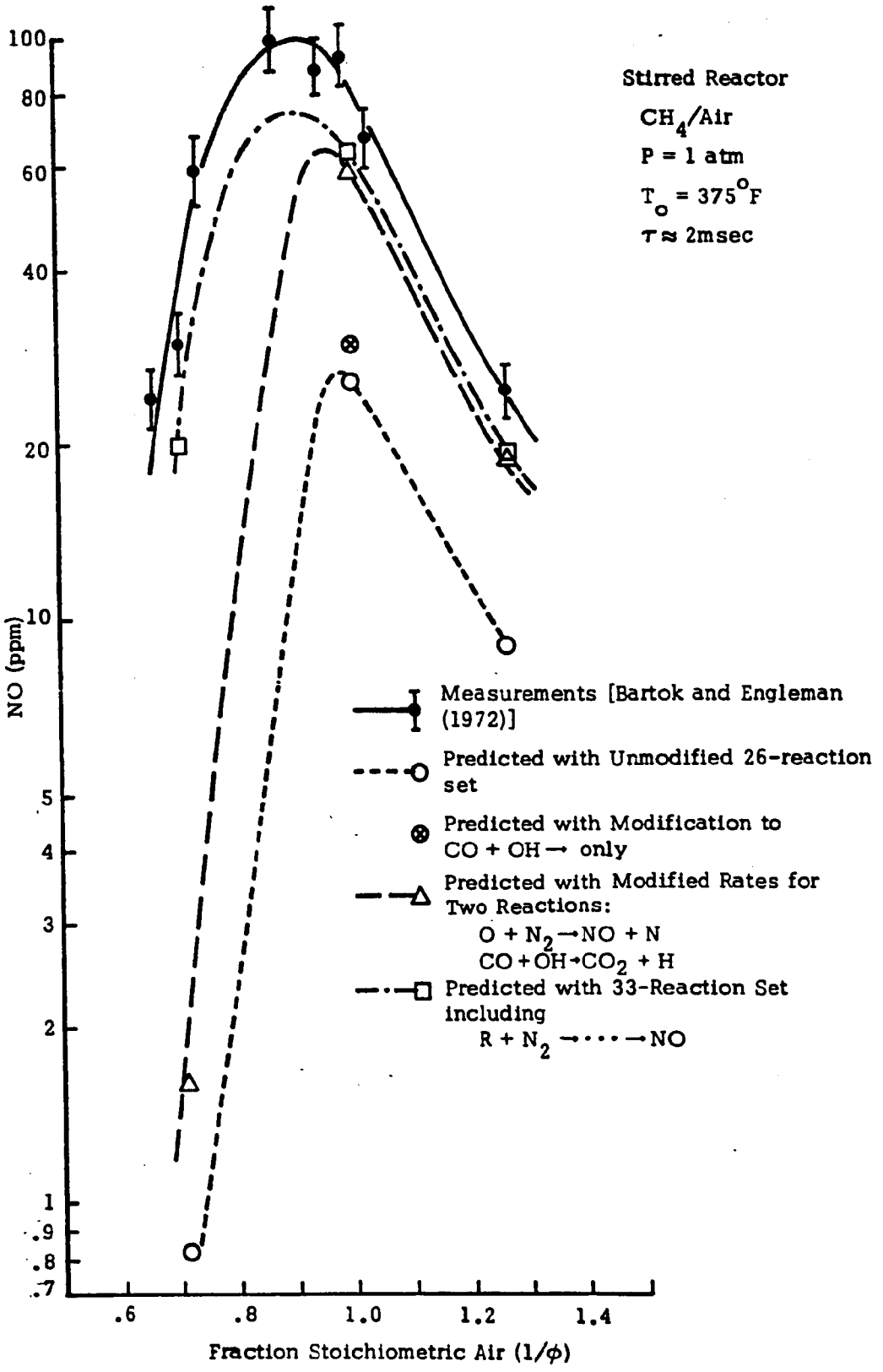

D. KINETIC REVISIONS TO RECONCILE THEORY WITH DATA

1. Rate Adjustments for Lean Combustion

The rates of two key reactions were increased:

Reaction	k (orig)	k (revised)
$CO + OH \xrightarrow{k} CO_2 + H$	$4.00 \times 10^9 T^{0.3}$	$5.6 \times 10^{11} \exp(-\frac{1.08}{RT})$
$N + NO \xrightarrow{k} N_2 + O$	1.50×10^{13}	$6.31 \times 10^{11} T^{0.5}$

Both revised rates were taken from the Leeds critical assessment of Baulch et al. (1970). At $\phi = 1$ ($T = 2065^{\circ}K$), these two changes increase the predicted NO concentration by factors of 1.23 and 1.85, respectively, as shown in Figure 7.2. Although factors of x 2 are not usually argued by kineticists, it may be useful to comment briefly on these rates.

The CO/air data of Engleman et al. (1973) support an increase in the CO + OH rate, because the measured "conversion" fraction, $\eta \equiv X_{CO_2} / (X_{CO} + X_{CO_2})$, is .78 compared to .73 predicted without revising the CO + OH rate. The revised value for CO + OH is based on Drysdale and Lloyd (1970) and agrees with the recent review by Smith and Zellner (1973) at $2000^{\circ}K$.

With respect to the Zeldovich fixation step ($O + N_2 \rightarrow$), clearly k(revised)/k(orig) ≈ 2 at $2000^{\circ}K$. Which rate is correct? With respect to the rate of Baulch et al. (1970), all of the NO predictions by Bartok et al. (1971), Newhall (1968), Bell et al. (1971), Janes (1970), and Martinez (1970) are underestimates by a factor of 2. The slower rate k(orig) quoted by these workers can be traced to shock tube studies by Glick et al. (1957) and Duff and Davidson (1959), which were later confirmed by Wray and Teare (1962).

The key to this puzzling discrepancy may lie in the energy modes of the nitrogen molecule. Of the three modes, translational, rotational, and vibrational, it can safely be assumed that the first two are in local equilibrium (T_{trans} and T_{rot} are identical to the local temperature, T). Equilibration of the vibrational mode is somewhat more sluggish, and this can markedly

affect the rate of any chemical reaction involving nitrogen: If the nitrogen is vibrationally "cold" (nonequilibrium, $T_{vib} \ll T$), the rate is much smaller than if N_2 is vibrationally "hot" ($T_{vib} = T$). In the latter case, the extra vibrational energy helps push the reaction over the activation threshold E_1.

The consensus of many engineers (who are not chemical kineticists) was to adopt the shock tube data of Glick et al. (1957), and Duff and Davidson (1959). However, this shock-tube data describes the rate of vibrationally "cold" nitrogen reacting with oxygen atoms:

$$O + N_2 \text{ (cold)} \overset{k_f}{\rightleftarrows} NO + N$$

$$k_f = 6 \times 10^{13} \exp(-E_1/RT) \quad .$$

Wray et al. (1970) re-examined the shock-tube data and determined that N_2 was indeed at least 75% out of vibrational equilibrium. However, Wray et al. concluded that the translational energy of the collision is sufficient to overcome the endothermicity of the reaction $O + N_2 + 3.3 \text{ eV} \rightarrow NO + N$ and have that reaction occur with essentially the same rate as has been measured for it when $T_V \equiv T_T$. That is, the authors suggest that if N_2 had been vibrationally "hot", the rate of NO production would not have been considerably larger.

By way of contrast, the Leeds evaluation assumed complete vibrational equilibration and recommended a value for the following reaction:

$$O + N_2 \text{ (hot)} \underset{k}{\overset{k_f}{\rightleftarrows}} NO + N$$

$$k_f = 18 \times 10^{13} \exp(-E_1/RT) \quad .$$

Under vibrational equilibrium $k_f = K_{eq}k$, where K_{eq} is the equilibrium constant. In their determination of k_f, the Leeds group used this relation and exhaustive data on the reverse rate k (which has been studied much more thoroughly than k_f). Unfortunately, the k data was obtained at low temperature

so that a lengthy extrapolation was required. The fact that the Leeds rate is three times larger may be due to this extrapolation; however, it is more likely due to participation of the vibrational modes. The Leeds group regards the shock tube data with considerable suspicion, advising that "in themselves they cannot be regarded as very accurate."

In our judgment N_2 is more likely to remain equilibrated throughout an industrial flame than behind a shock wave because of the slower thermal transients to which an element of fluid is exposed. That is, the NO formation process is system dependent. In the industrial flame, heat transfer occurs by turbulent mixing and radiation so that characteristic times are in the range 10^{-1} to 10^{-3} sec rather than the 10^{-5} to 10^{-6} sec range as characteristic of the sudden passage of a shock wave. The characteristic vibrational relaxation time for N_2-N_2 collisions is about 150 μsec [Blackman (1956)] under typical boiler conditions, and since unlike-pair collisions are up to 100 times more efficient [Vincenti and Kruger (1965)], the relaxation time in a mixture involving O_2, H_2O, and CO_2 may be on the order of 10^{-5} sec. Thus, the Leeds rate data is to be preferred as a tentative best guess for NO formation in practical combustion equipment. The rate of NO formation may be different for shock tubes than for combustion equipment; i.e., the process is system dependent.

2. Revisions for Fuel-Rich Combustion

Original-set predictions of NO on the fuel-rich side were about a factor of 50 lower than measured values. Two lines of reasoning were pursued: (a) Since, in the 26-reaction set, Zeldovich fixation ($O + N_2 \rightarrow$) governs NO formation, rate adjustments were sought to increase the O-atom concentration; (b) alternate paths to NO (via $R + N_2 \rightarrow$) were sought.

(a) Attempts to Increase O-Atom Concentration

Both O_2 and O-atoms far exceed equilibrium CHON levels (by factors of 600 and 240, respectively) because of the intense backmixing of the perfectly-stirred reactor. The predicted O-atom and O_2 concentrations were 147 ppm and

589 ppm, respectively, which constitutes an $(O)^2/O_2$ value 100 times over equilibrium at this temperature. The superequilibrium level of O-atoms needed to make Zeldovich fixation sufficient was on the order of 0.4%, fully X7000 over the CHON equilibrium value. Although 0.4% of free O-atoms was quite improbable under fuel-rich conditions, nevertheless a number of rate adjustments were attempted as shown in Table 7.3. Assuming a constant partial equilibrium value of $(O_2)(H)/(OH)(O) \approx 7$ at 2000°K, which was confirmed for many test cases, rate adjustments were sought to decrease (OH), increase (O_2), or increase (H). None of these measures increased O-atom levels more than a factor of 3.

Table 7.3

RATE REVISIONS INTENDED TO BOOST O-ATOM LEVELS

Case	Results		
	X_O	T, °K	X_{NO}
Needed to reconcile Zeldovich theory with with measured rate	4000 ppm	1900±50	35±5 ppm
Original 26-reaction set (no revision)	147 ppm	1976	0.7 ppm
Lean revisions $\left\{\begin{matrix} CO + OH \rightarrow \\ O + N_2 \rightarrow \end{matrix}\right\}$, see above	153 ppm	1990	1.6 ppm
Attempt to boost O-atoms: Replace $CH_2O + O$ by 3-reaction pyrolysis route: $\left\{\begin{matrix} CH_3 + H \rightleftarrows CH_2 + H_2 \\ CH_3 + OH \rightleftarrows CH_2 + H_2O \\ CHO + CH_3 \rightleftarrows CH_2 + CH_2O \end{matrix}\right\}$	207 ppm	1985	1.9 ppm
Attempt to boost O_2 by removing HO_2 reactions Also attempt to boost H by removing (CHO + H→) path	430 ppm	1934	2.4 ppm
Same as above, except $CH_4 + H \rightarrow$ removed to boost H-atom concentration	446 ppm	1935	2.5 ppm

(b) Alternate Paths to NO

A number of reactions conceivably could produce nitrogen-bearing radicals as an alternate to the $O + N_2 \rightarrow NO + N$ path. A partial list is given in Table 7.4 with selected comments.

Table 7.4

CANDIDATE $R + N_2 \rightarrow R \cdot N + N$ REACTIONS

Listed in Original 134-Reaction Set?	Reaction	Endothermicity (kcal/mole) at 300°K	Order of Magnitude Concentration of Species "R" in CH_4/Air Flame	Comments
No	$CH_2 + N_2 \rightarrow HCN + NH$	20.2	10^{-7}	N_2 breakup by CH_2 is possible because CH_2 is quite energetic. 4-center, probably not elementary; may go through CH_2N intermediate. Discussed by Sternling and Wendt (1972). Leads to CHN which has been observed [Bachmaier et al (1973)].
No	$C_2 + N_2 \rightarrow CN + CN$	23.0	--	Four-center. C_2 (Swan) band emission observed in hydrocarbon flames at 5165 Å.
No	$C + N_2 \rightarrow CN + N$	53.1	--	C less likely than C_2 as gaseous species
No	$HO_2 + N_2 \rightarrow HNO + NO$	40.4	10^{-6}	Sterically improbable (four-center). Also would be largest in lean instead of rich case.
No	$CH + N_2 \rightarrow HCN + N$	3.3	10^{-7}	Spin-forbidden, proposed by Fenimore (1971). CH emission bands observed at 4315 Å.
No	$H_2 + N_2 \rightarrow HN + HN$	160	10^{-2}	Sterically improbable (four-center). Also highly endothermic.
Yes	$CO + N_2 \rightarrow CN + NO$	159	10^{-2}	Highly endothermic, four center.
Yes	$H + N_2 \rightarrow HN + N$	140.9	10^{-2}	Highly endothermic.
No	$OH + N_2 \rightarrow HN + NO$	92.2	10^{-2}	Sterically improbable (four-center). Bowman (1973) suggests $k = 10^5$ to 10^8.
Yes	$OH + N_2 \rightarrow N_2O + H$	62.3	10^{-2}	Endothermic

The reaction selected was $CH_2 + N_2 \rightarrow CHN + HN$, which was followed by five reactions hypothesized to complete the path to NO:

$$NH + O \rightarrow NO + H \quad \text{(later screened out)}$$
$$NH + OH \rightarrow N + H_2O$$
$$HCN + OH \rightarrow CN + H_2O$$
$$CN + O_2 \rightarrow CO + NO$$
$$CN + O \rightarrow CO + N \quad \text{(later screened out)}$$

Two of the five reactions were later screened out as relatively unimportant, as noted. It will be more realistic in future studies to provide and screen additional reaction paths whereby HCN, NH, and CN can form molecular nitrogen, thereby giving less than 100% conversion efficiency of these species to NO.

In order to provide the CH_2 needed for the key $CH_2 + N_2$ reaction, two pyrolysis reactions were considered:

$$CH_3 + OH \rightarrow CH_2 + H_2O \quad \text{(screened out)}$$
$$CH_3 + H \rightarrow CH_2 + H_2$$

Including these reactions is by no means arbitrary since the screening runs at $\phi = 1.25$ indicated their importance (see Chapter III). It was found that H was eight times more effective than OH in producing CH_2 for the $\phi = 1.4$ case. Competing with the $CH_2 + N_2$ sink for CH_2 radicals were two key pyrolysis reactions previously shown to be important by the screening (again, see Chapter III):

$$CH_2 + O_2 \rightarrow CH_2O + O \quad \text{(screened out)}$$
$$CH_2 + CH_2O \rightarrow CHO + CH_3$$

It was found that $CH_2 + O_2$ could be screened out for the present conditions.

The rate of the key reaction $CH_2 + N_2 \rightarrow CHN + HN$ was selected by adopting the activation energy based on 28% of bond energy (41.7 kcal). Then a parameter study was conducted on predicted NO and CHN, as shown in Figure 7.3. The rates selected for all six reactions are listed below:

Figure 7.3

PARAMETER STUDY ON THE RATE OF THE REACTION $CH_2 + N_2 \rightarrow CHN + HN$

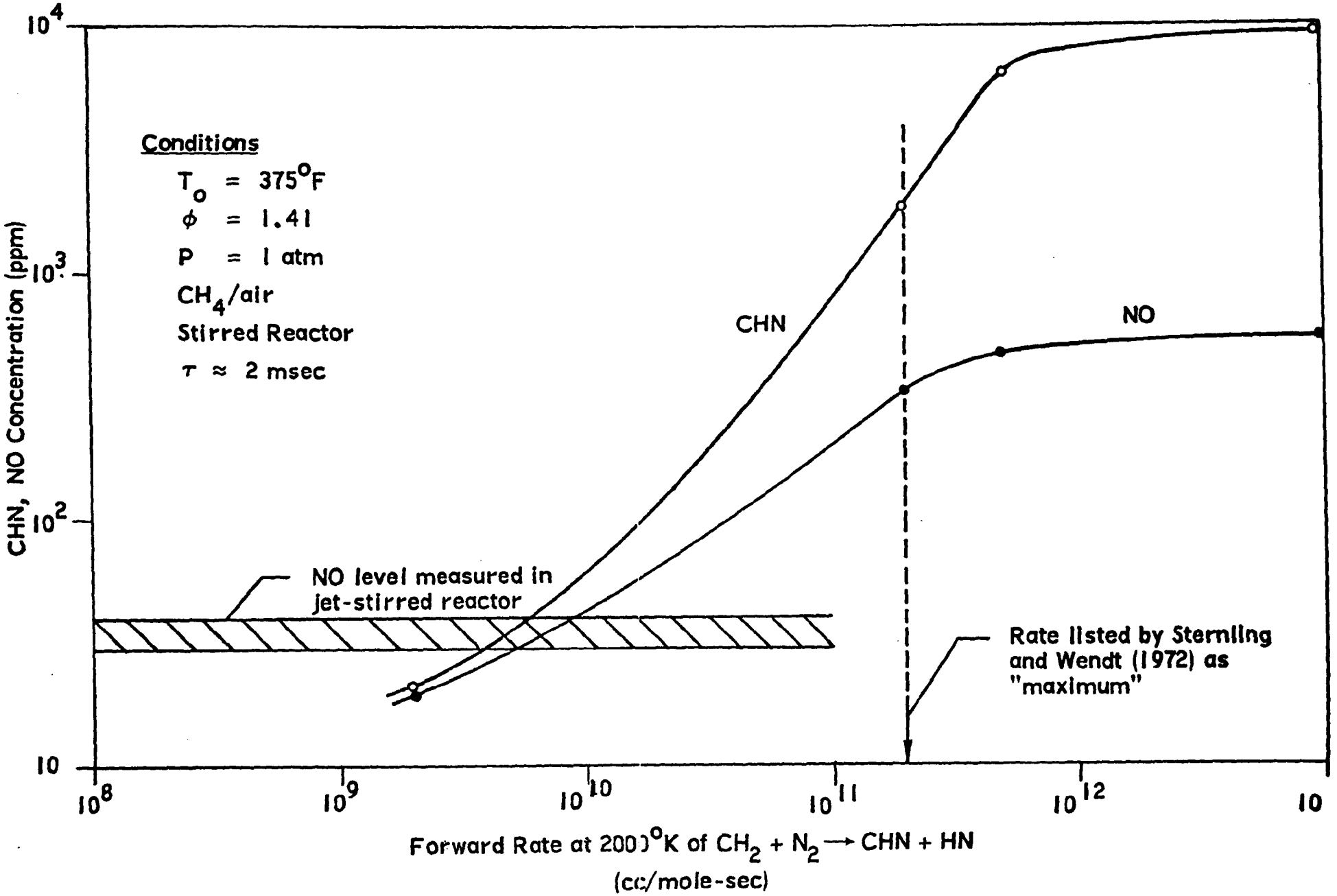

	$k_f = A\,T^{-n} \exp(-B/RT)$		
	A	n	B
CH_2 production			
$CH_3 + H = CH_2 + H_2$	2×10^{11}	-0.7	3.0
CHN and HN production			
$CH_2 + N_2 = CHN + HN$	2.04×10^{13}	0	41.7
CH_2 destruction			
$CH_2 + CH_2O = CHO + CH_3$	1.50×10^{11}	-0.7	4.0
CHN and HN conversion to NO			
$CHN + OH = CN + H_2O$	2×10^{11}	-0.6	5.0
$CN + O_2 = CO + NO$	3×10^{11}	0	0
$NH + OH = N + H_2O$	5×10^{11}	-0.5	2.0

With this set the fuel-rich predictions are brought into reasonable agreement with the data as shown in Figure 7.2. It is not claimed that the mechanism adopted is unique or corresponds to reality. However some non-Zeldovich path to NO ($R + N_2 \rightarrow R \cdot N + N$) appears mandatory for fuel-rich conditions. Iverach et al. (1973) and Fenimore (1971) have reported higher NO concentrations for fuel-rich flames than can be attributed to the Zeldovich mechanism. Bachmaier et al. (1973) measured substantial quantities of HCN (e.g. 8 ppm at $\phi = 1.3$) for fuel-rich methane/air flames.

What has been shown above is that the jet-stirred results of Bartok and Engleman (1972) corroborate these observations. The kinetic mechanism hypothesized above may indicate one conceivable explanation for all of these discrepancies between the Zeldovich mechanism and fuel-rich NO data.

3. Summary of Kinetic Revisions

Table 7.5 presents the 33-reaction set which results from forcing agreement to the jet-stirred data of Bartok and Engleman (1972).

Table 7.5

EMPIRICALLY ADJUSTED 33-REACTION SET
FOR CH_4/AIR WITH REVISIONS TO TABLE 6.1 NOTED (*)

Rate Coefficients[◊] $k_f = A\,T^{-n}\,e^{-B/RT}$

Reaction Number	Reaction	A	n	B	Reference
	Termolecular Reactions				
36	CHO = CO + H	2.50E+20	1.5	16.8	Benson (1973)
77	CO2 = CO + O	1.00E+15	0	100.	Benson (1973)
84	H2O = HO + H	3.00E+15	0	105.	Baulch (1972)
99	H + O = HO	8.00E+15	0	0	Scofield (1973)
101	H + O2 = HO2	1.50E+15	0	1.	Baulch (1972)
140	H2O = N2 + O	1.00E+14	0	50.	Estimate
	Bimolecular Reactions				
44	CHO + H = CO + H2	3.00E+10	-1.	0	Benson (1973)
46	CH2O + O = CHO + HO	2.00E+11	-1.	4.4	Benson (1973)
47	CHO + HO = CO + H2O	3.00E+10	-1.	0	Benson (1973)
52	CHO + O = CO + HO	3.00E+11	-1	.5	Benson (1973)
59	CH3 + O = CH2O + H	2.00E+12	- .5	-.3	Morris (1973)
63	CH4 + O = CH3 + HO	1.00E+10	1	8.	Westenberg (1969)
65	CH4 + H = CH3 + H2	5.00E+10	-1	10.	Walker (1968)
66	CH4 + HO = CH3 + H2O	3.00E+13	0	5.	Wilson (1972)
70	*CO + HO = CO2 + H	5.60E+11	0	1.08	Baulch (1969)
83	H + HO = H2 + O	8.00E+09	-1	7.	Benson (1973)
85	H + HO2 = HO + HO	2.50E+14	0	1.9	Baulch (1972)
88	HO + H2 = H + H2O	2.50E+13	0	5.2	Baulch (1972)
91	HO + N = H + NO	6.00E+11	- .5	8.	Benson (1973)
98	H + N2O = HO + N2	8.00E+13	0	15.	Baulch (1973)
100	HO + O = H + O2	2.50E+13	0	0	Baulch (1972)
117	HO + HO = H2O + O	6.00E+12	0	1.	Baulch (1972)
125	*N + NO = N2 + O	6.31E+11	- .5	0	Baulch (1969)
133	N + O2 = NO + O	6.00E+09	-1.	6.3	Benson (1973)
135	N2O + O = NO + NO	1.00E+14	0	28.	Baulch (1973)
143	CHO + O2 = CO + HO2	8.00E+12	0	0	Peeters (1973)
49	*CH2O + HO = CHO + H2O	1.00E+14	0	0	Benson (1973)
56	*CH3 + H = CH2 + H2	2.00E+11	- .7	3.	Tunder (1967)
39	*CHO + CH3 = CH2 + CH2O	1.50E+11	- .7	4.	Tunder (1967)
	*CH2 + N2 = CHN + HN	2.04E+13	0	41.7	Mod Sternling (1972) (see Fig. 7.3)
104	*HN + HO = H2O + N	5.00E+11	- .5	2.	Tunder (1967)
32	*CHN + HO = CN + H2O	2.00E+11	- .6	5.	Tunder (1967)
68	*CN + O2 = CO + NO	3.00E+11	0	0	Basco (1965)

◊Units: cc, mole, sec, °K, kcal

The set is not unique, and the model of perfectly stirred combustion does not precisely apply to the data of Bartok et al. Nevertheless it would appear from the analysis of this chapter that further study is warranted in the following areas:

(1) Determination of the rate of the $O + N_2 \rightarrow NO + N$ reaction to better precision, especially under conditions permitting the vibrational state of N_2 to be well characterized.

(2) Rescreening the total 134-reaction set with the addition of Zeldovich bypass reactions such as $CH_2 + H_2 \rightarrow CHN + HN$. Of the ten reactions listed in Table 7.4, five were discarded as unlikely by Engleman et al., three were within the set of 134 recommended reactions, and two were not considered by Engleman et al.

(3) Rates of the following two reactions appeared to have been underestimated by x2 and x20, respectively, in the original 134-reaction set: $CO + OH \rightarrow CO_2 + H$, $CH_2O + OH \rightarrow CHO + H_2O$. Again a rescreening is called for.

REFERENCES

Bachmaier, F., Eberius, K. H., and Just, Th. (1973). The Formation of Nitric Oxide and the Detection of HCN in Premixed Hydrocarbon-air Flames at 1 Atmosphere, Comb. Sci. Tech. 7 77.

Bahn, G. S. (1973). Approximate Thermochemical Tables for Some C-H and CHO Species, NASA CR-2178.

Bartok, W. and Engleman V. S. (1972). Definition of the Mechanism and Kinetics of the Formation of NO_x and Other Pollutants in Combustion Reactions, EPA Contract No. 68-02-0224, Status Report, p. 87-117.

Bartok, W., Engleman, V. S., de Valle, E. G. (1971). Laboratory Studies and Mathematical Modeling of NO_x Formation in Combustion Processes, Final Report, EPA Contract CPA 70-90, Phase II.

Barton, S. C. and Dove, J. E. (1969). Can. J. Chem. 47, 521.

Basco, N. (1965). Proc. Roy Soc. A283, 302.

Baulch, D. L., Drysdale, D. D., and Horne, D. G. (July 1970). Dept. of Physical Chemistry, The University, Leeds, England, High Temperature Reaction Rate Data Report No. 5.

Baulch, D. L., Drysdale, D. D., Horne, D. G., and Lloyd, A. C. (1972). Evaluated Kinetic Data for High Temperature Reactions, Vol. I., CRC Press.

Baulch, D. L., Drysdale, D. D., Horne, D. G., and Lloyd, A. C. (1973). Evaluated Kinetic Data for High Temperature Reactions, Vol. II., CRC Press.

Bell, A. W., Devolo, N. B., Breen, B. P., Bagwell, F. A., and Rosenthal, K. (1971). Combustion Control for Elimination of Nitric Oxide Emissions from Fossil Fuel Power Plants, 13th Symposium (International) on Combustion, The Combustion Institute, Pittsburgh, p. 391.

Benson, S. W. and Fueno, T. (1962). Mechanism of Atom Recombination by Consecutive Vibrational Deactivations, J. Chem. Phys. 36, 1597-1607.

Benson, S. W., Golden, D. M., and Shaw, R. (August 1973). SRI Interim Annual Report, Project PYU-2009.

Blackman, V. H. (1956). Vibrational Relaxation in Oxygen and Nitrogen, J. Fluid Mech. 1, 61.

Boden, J. C. and Thrust, B. A. (1968). Proc. Roy. Soc. A305, 107.

Bortner, M. H. (August 1963). General Electric Missile and Space Division Report No. R63SD63.

Bowman, B. R., Pratt, D. T., and Crowe, C. T. (1973). Effects of Turbulent Mixing and Chemical Kinetics on Nitric Oxide Production in a Jet-Stirred Reactor, 14th Symposium (International) on Combustion, The Combustion Institute, Pittsburgh, p. 819.

Bowman, C. T. (1970). An Experimental and Analytical Investigation of the High-Temperature Oxidation Mechanisms of Hydrocarbon Fuels, Comb. Sci. Tech. 2, 161.

Bowman, C. T. (1971). Investigation of Nitric Oxide Formation Kinetics in Combustion Processes: The Hydrogen-Oxygen-Nitrogen Reaction, Comb. Sci. Tech. 3, 37-45.

Bowman, C. T. (1973). Kinetics of Nitric Oxide Formation in Combustion Processes, 14th Symposium (International) on Combustion, The Combustion Institute, Pittsburgh, p. 729.

Bowman, C. T. and Seery, D. J. (1972). Emissions from Continuous Combustion Systems (W. Cornelius and W. G. Agnew, Eds.), Plenum Press, p. 123.

Brown, F. and Crist, R. (1941). J. Chem. Phys. 9, 840.

Chinitz, W. and Bauer, T. (1966). An Analysis of Nonequilibrium Hydrocarbon/Air Combustion, Pyrodynamics 4.

Clyne, M. A. A. and Thrush, B. A. (1962). Disc. Faraday Soc. 33, 139.

Dean, A. M. and Kistiakowsky, G. B. (1971). J. Chem. Phys. 54, 1718.

Dryer, F. (1974). Private Communication, Princeton University.

Duff, R. E. and Davidson, N. (1959). J. Chem. Phys. 31, 1018.

Eberius, K. H., Hoyerman, K., and Wagner, H. Gg. (1973). Structure of Lean Acetylene-Oxygen Flames, 14th Symposium (International) on Combustion, The Combustion Institute, Pittsburgh, p. 147.

Edelman, R. B. and Fortune, O. F. (1969). A Quasiglobal Chemical Kinetic Model for the Finite Rate Combustion of Hydrocarbon Fuels with Application to Turbulent Burning and Mixing in Hypersonic Engines and Nozzles, AIAA Paper No. 69-86.

Engleman, V. S. and Bartok. W. (1973). Definition of the Mechanisms and Kinetics of the Formation of NO_x and Other Pollutants under Normal and Combustion Modification Conditions, Progress Report No. 1 EPA Contract No. 68-02-0224, Modif. #1.

Engleman, V. S., Edelman, R. B., Bartok, W., and Longwell, J. P. (1973). Experimental and Theoretical Studies of NO_x Formation in a Jet-Stirred Combustor, 14th Symposium (International) on Combustion, The Combustion Institute, Pittsburgh, p. 755.

Fenimore, C. P. (1964). Chemistry in Premixed Flames, Topic 19: Gas Kinetics, Vol. 5, McMillan, New York.

Fenimore, C. P. (1971). Formation of Nitric Oxide in Premixed Hydrocarbon Flames, 13th Symposium (International) on Combustion, The Combustion Institute, Pittsburgh, p. 373.

Fenimore, C. P. (1972). Formation of Nitric Oxide from Fuel Nitrogen in Ethylene Flames, Comb. Flame 19, 289-296.

Frey, H. M., Nickerson, G. R., and Tyson, T. J. (1970). One-Dimensional Kinetic Nozzle Analysis Reference Computer Program, Dynamic Science Report No. CS-1-9/70.

Frey, H. M. and Nickerson, G. R. (1970). Two-Dimensional Kinetic Nozzle Analysis Reference Computer Program, Dynamic Science Paper No. CS-12-70-1.

Fristrom, R. M. and Westenberg, A. A. (1965). Flame Structure, McGraw Hill, New York.

Glick, H. S., Klein, J. J., and Squire, W. (1957). J. Chem. Phys. 27, 850.

Hammond, D. C. Jr. and Mellor, A. M. (1973). Analytic Predictions of Emissions from and Within an Allison J-33 Combustor, Comb. Sci. Tech. 6, 279-286.

Hampson, R. F. (ed) (1972). NBS Report 10-692.

Hartig, R., Troe, J. and Wagner, H. Gg. (1971). Thermal Decomposition of Methane Behind Reflected Shock Waves, 13th Symposium (International) on Combustion, The Combustion Institute, Pittsburgh, p. 147.

Hirschfelder, J. O., Curtiss, C. F., and Bird, R. B. (1954). Molecular Theory of Gases and Liquids, Wiley, New York.

Iverach, D., Basden, K. S., and Kirov, N. Y. (1973). Formation of Nitric Oxide in Fuel-Lean and Fuel-Rich Flames, 14th Symposium (International) on Combustion, The Combustion Institute, Pittsburgh, p. 767.

James, D. E. (1970). A Boiler Manufacturer's View on Nitric Oxide Formation, Presented to the Fifth Technical Meeting, West Coast Section of APCA.

JANAF Thermochemical Tables (1971). U. S. Dept. of Commerce, National Bureau of Standards Publication NSRDS-NBS 37, second edition.

Johnston, H. S. (1968). NSRDS-NBS 20.

Kaufman, F. and Kelso, J. R. (1955). J. Chem. Phys. 23, 602.

Kliegel, J. R., Gold, P. I., and Weekley, C. T. (1968). Chemical Species and Chemical Reactions of Importance in Nonequilibrium Rocket Engine Performance Calculations, Pyrodynamics 6.

Kretschmer, C. B. and Petersen, H. L. (1963). J. Chem. Phys. 39, 1772.

Leonard, P. A., Lester, T. W., Clancy, M. G., Laurendeau, N. M., and Mellor, A. M. (1973). Nitric Oxide Formation in Hydrocarbon Flames, TACOM Propulsion Systems Laboratory Technical Report No. 11816.

Lin, M. C. and Bauer, S. H. (1969). J. Chem. Phys. 50, 3377.

Lloyd, A. C. (1971). NBS Report 10 447.

Mayer, S. W., Schieler, L., and Johnston, H. S. (1967). Computation of High-Temperature Rate Constants for Bimolecular Reactions of Combustion Products, 11th Symposium (International) on Combustion, The Combustion Institute, Pittsburgh, p. 837.

Martinez, P. (1970). Formation of NO in Hydrocarbon-Air Combustion, Comb. Sci. Tech. 1, 461.

Mellor, A. M. (1972). Current Kinetic Modeling Techniques for Continuous Flow Combustors, Emissions from Continuous Combustion Systems, Plenum Press, New York, 22-53.

Morris, E. D. and Niki, H. (1973). I. J. C. K. 5, 47.

Newhall, H. K. (1968). Kinetics of Engine Generated Nitrogen Oxides and Carbon Monoxide, 12th Symposium (International) on Combustion, The Combustion Institute, Pittsburgh, p. 603.

Olschewski. H. A., Troe, J., and Wagner, H. Gg. (1967). Studies of Unimolecular Reactions of Triatomic Molecules, 11th Symposium (International) on Combustion, The Combustion Institute, Pittsburgh, p. 155.

Peeters, J. and Mahnen, G. (1973). Reaction Mechanisms and Rate Constants of Elementary Steps in Methane-Oxygen Flames, 14th Symposium (International) on Combustion, The Combustion Institute, Pittsburgh, p. 133.

Penner, S. S. (1957). Chemistry Problems in Jet Propulsion, Pergamon Press, New York.

Phillips, L. F. and Schiff, H. I. (1965). J. Chem. Phys. 42, 3171.

Pratt, D. T. and Malte, P. C. (1973). Formation of Thermal and Prompt NO_x in a Jet-Stirred Combustor, Paper No. 34b, 75th National AIChE Meeting.

Pratt, D. T. and Malte, P. C. (1974). Measurement of Atomic Oxygen and Nitrogen Oxides in Jet-Stirred Combustion, WSS/CI Paper 74-8, Pullman, Washington, Western States Section/The Combustion Institute.

Reid, R. C. and Sherwood, T. K. (1966). The Properties of Gases and Liquids--Their Estimation and Correlation, McGraw-Hill, New York, 2nd ed.

Ripley, D. L. and Gardiner, W. C. Jr. (1966). J. Chem. Phys. 44, 2285.

Schofield, K. (1967). Planetary Space Sci. 15, 643.

Shaw, R. (1973). Private communication.

Seery, D. J. and Bowman, C. T. (1970). An Experimental and Analytical Study of Methane Oxidation Behind Shock Waves, Comb. Flame 14, 37-48.

Sternling, C. V. and Wendt, J.O.L. (1972). Kinetic Mechanisms Governing the Fate of Chemically Bound Sulfur and Nitrogen in Combustion, Final Report, EPA Contract EHS-D-71-45, Task 14.

Tunder, R., Mayer, S., Cook, B., and Shieler, L. (1966). Compilation of Reaction Rate Data for Nonequilibrium Performance and Re-entry Calculations Programs, Aerospace Corporation.

Tunder, R., Mayer, S., Cook, E., and Schieler, L. (1967). Aerospace Report No. TR-1001 (9210-02)-1, Aerospace Corporation Thermochemistry Research Department.

Tyson, T. J. and Kliegel, J. R. (1968). An Implicit Integration Procedure for Chemical Kinetics, AIAA 6th Aerospace Sciences Meeting, Paper No. 68-180.

Vincenti, W. G. and Kruger, C. H. Jr. (1965). Introduction to Physical Gas Dynamics, J. Wiley, New York, p. 204.

Walker, R. W. (1968). J. Chem. Soc. (A) 1968, 2391.

Westenberg, A. A. and Dehaas, N. (1969). J. Chem. Phys. 50, 2512.

Wilde, K. A. (1969). Comb. Flame 13, 173.

Wilson , W. E. (1972). J. Phys. Chem. Ref. Data 1, 535.

Wray, K. L., Feldman, E. V., and Lewis, P. F. (1970). Shock Tube Study of the Effect of Vibrational Energy of N_2 on the Kinetics of the $O + N_2 \rightarrow NO + N$ Reaction, J. Chem. Phys. 53, 4131. [See also Wray, K. L. and Teare, J. D. (1962), Shock-Tube Study of the Kinetics of Nitric Oxide at High Temperatures, J. Chem. Phys. 36, 2582.]

APPENDIX A

DESCRIPTION OF THE NUMERICAL PROGRAM

1. BACKGROUND

The computer program used in this study is based on analysis carried out previously at Ultrasystems for the purpose of predicting delivered specific impulse, including the effect of kinetic losses, for liquid propellant rocket engines. These applications were reported by Tyson and Kliegel (1968) and Frey et al. (1970). The method of solution consists of integrating the one-dimensional conservation equations in a form such that gas phase chemical reactors of a general type can be included. This computer program also permits input of functions defining mass, momentum, and energy addition. Both pressure defined and area defined chemically reacting systems may be analyzed. Solid or liquid phase products are not considered.

A special screening option permits evaluation of the contribution of each chemical reaction on the production or destruction of any specified species at each integration step. The program will automatically delete any reaction whose contribution to the net production or destruction of the particular species is less than a specified amount. The calculation is then repeated if desired, to see the effect of the deleted reaction(s).

In the course of the present research effort some improvements were made to the numerical program. In particular, an improved truncation error control procedure was derived and implemented to allow for more efficient control of the integration step size.

A version of the program compatible with IBM equipment was prepared by Ultrasystems (the original was designed for CDC equipment) and set up on EPA computers in Research Triangle Park, North Carolina.

2. CONSERVATION EQUATIONS

The conservation equations governing the inviscid flow of reacting gas mixtures have been given by Hirschfelder et al. (1954), Penner (1957), and others. The following basic assumptions are made in the derivation of these equations.

- Addition rates for mass ($\dot{m}$), species ($\dot{s}$), momentum ($\dot{M}$), and energy ($\dot{H}$) are defined for the system.
- The gas is inviscid.
- Each component of the gas is a perfect gas.
- The internal degrees of freedom of each component of the gas are in equilibrium.
- The flow is one dimensional.

Based on these assumptions, the conservation of species, mass, momentum, and energy for the system can be expressed by Eqs. (1), (2), (3) and (4) below*:

$$\frac{d}{dx}\left[(1+\bar{m})\,c_i\right] = \dot{s}_i + (1+\bar{m})\,\frac{\dot{\omega}_i r^*}{\rho V} \tag{1}$$

$$\frac{d}{dx}(1+\bar{m}) = \dot{m} \tag{2}$$

$$\frac{d}{dx}\left[(1+\bar{m})\,V\right] = \dot{M} - \frac{(1+\bar{m})}{\rho V}\frac{dP}{dx} \tag{3}$$

$$\frac{d}{dx}\left[(1+\bar{m})\,h_T\right] = \dot{H}, \quad \text{where } h_T = \sum_{i=1} c_i h_i + V^2/2, \tag{4}$$

c_i are mass fractions, $\dot{w}_i$ are net production rates, and h_i are specific enthalpies of species i. Equations (1) - (4) can be written as

$$\frac{dc_i}{dx} = \frac{\dot{s}_i - \dot{m}\,c_i}{1+\bar{m}} + \frac{\dot{\omega}_i r^*}{\rho V} \tag{5}$$

$$\frac{dV}{dx} = \frac{\dot{M} - \dot{m}V}{1+\bar{m}} - \frac{1}{\rho V}\frac{dP}{dx} \tag{6}$$

*The independent variable, x, is taken as unitless with r^* as the conversion factor to units. The quantity $1+\bar{m}$ represents the streamtube mass flux normalized by the initial streamtube mass flux, i.e., $1+\bar{m} = (\rho Va)/(\rho Va)_0$.

$$\frac{dT}{dx} = \frac{1}{C_p}\left[\frac{\dot{H} - \dot{m}h_T}{1+\overline{m}} - \frac{V(\dot{M} - \dot{m}V)}{1+\overline{m}} + \frac{1}{\rho}\frac{dP}{dx} - \sum_{i=1} h_i \frac{dc_i}{dx}\right] \tag{7}$$

$$\frac{d\rho}{dx} = \left[\frac{1}{P}\frac{dP}{dx} - \frac{1}{T}\frac{dT}{dx} - \frac{1}{R}\left(\sum_{i=1} R_i \frac{dc_i}{dx}\right)\right]\rho \tag{8}$$

where

$$C_p = \sum_{i=1} c_i C_{pi}, \quad \gamma = \frac{C_p}{(C_p - R)} \tag{9,10}$$

$$h_i = \int_0^T C_{pi}\, dT + h_{i0}, \quad R = \sum_{i=1} c_i R_i \tag{11,12}$$

The perfect gas relation

$$P = \rho RT$$

has been used to obtain the above equations.

3. CHEMISTRY

The method by which the net species production rate, $\dot{\omega}_i$, is determined is described below.

A chemical reaction can be written in terms of its stoichiometric coefficients (ν_{ij} and ν'_{ij}) as

$$\sum_{i=1} \nu_{ij} \overline{M}_i \rightleftarrows \sum_{i=1} \nu'_{ij} \overline{M}_i \tag{13}$$

where $\overline{M}_i$ represents the ith chemical species name and j represents the jth reaction.

Given a system of chemical reactions, the net species production rate $\dot{\omega}_i$ for each species (component) is calculated from

$$\dot{\omega}_i = (mw)_i \sum_{j=1} \rho^{\sum \nu_{\ell j}} (\nu'_{ij} - \nu_{ij})\, X_j \tag{14}$$

Here mw_i is the molecular weight, where

$$X_j = \left[K_j \prod_{i=1} \bar{c}_i^{\,\nu_{ij}} - \rho^{\lambda_j} \prod_{i=1} \bar{c}_i^{\,\nu'_{ij}} \right] k_j M_j \tag{15}$$

The reaction rate, k_j, is from right to left (reverse) in Equation (13) and is represented by the Arrhenius form

$$k_j = a_j T^{-n_j} \exp(-b_j/RT)$$

where

a_j is the pre-exponential coefficient

n_j is the temperature dependence of the pre-exponential factor

b_j is the activation energy.

The equilibrium constant, K_j, is

$$K_j = \exp(-\Delta F/RT) \; (RT)^{-\lambda_j}$$

where

$$\Delta F = \sum_{i=1} f_i \, \nu_{ij} - \sum_{i=1} f_i \, \nu'_{ij}$$

and the integer, λ_j, is determined for a given reaction from the stoichiometric coefficients

$$\lambda_j = \sum_{i=1} (\nu'_{ij} - \nu_{ij})$$

The term M_j in Eq. (15) is provided so that the reaction rate can be modified for individual third body species by calculating the general third body term (M_j) as

$$M_j = \sum_{i=1} a_{ij}/a_{kj} \, \bar{c}_i \quad \text{for reactions requiring a third body} \tag{16}$$

$$M_j = 1 \quad \text{for all other reactions}$$

where the a_{kj}'s are the individual pre-exponential coefficients.

4. SOLUTION OF THE WELL-STIRRED REACTION EQUATIONS IN KINETIC ANALYSIS PROGRAM

The conservation equations discussed in the previous section can be manipulated through appropriate choice of the mass, momentum, species, and energy addition functions to give the well-stirred reactor solution in the steady limit of the one-dimensional flow. Conceptually, one starts with a vessel containing reactants in any concentration and adds into the vessel (at each time increment) reactants having a composition, c_i^I, and energy h_T^I, corresponding to the stirred reactor inlet conditions. At the same time, fluid products are removed at the same rate as the input ($\overline{m} = 0$) so that as we proceed in time the conditions in the vessel approach more closely the conditions in a stirred reactor. For $\overline{m} = 0$ (no mass accumulation), $\dot{M} = \dot{m}V$, $\dot{H} = \dot{m}h_T^I$, $\dot{s} = \dot{m}c_i^I$ and $dP/dx = 0$, equations (5)-(8) then become:

$$\frac{dc_i}{dx} = \dot{m}c_i^I - \dot{m}c_i + \frac{\dot{\omega}_i r^*}{\rho V}$$

$$\frac{dV}{dx} = 0$$

$$\frac{dT}{dx} = \frac{1}{C_p}\left[\dot{m}h^I - \dot{m}h_T^I - \sum_{i=1}^{n} h_i \frac{dc_i}{dx}\right]$$

$$\frac{d\rho}{dx} = \rho\left[-\frac{1}{T}\frac{dT}{dx} - \frac{1}{R}\left(\sum R_i \frac{dc_i}{dx}\right)\right]$$

In the limit as $d/dx \rightarrow 0$, i.e., steady state:

$$\dot{m}\,(c_i^I - c_i) + \frac{\dot{\omega}_i r^*}{\rho V} = 0$$

where V = constant

$\dot{m}\,(h^I - h) = 0$

ρ = constant

For reference, the stirred reactor residence time is $\tau = r^*/\dot{m}V$.

5. NUMERICAL METHOD

It has been shown [Tyson and Kliegel (1968)] that explicit methods of numerical integration are unstable when applied to relaxation equations [such as Eqs. (5), (6), (7), and (8)] unless the integration step size is of the order of the characteristic relaxation distance. Since in the near equilibrium flow regime the characteristic relaxation distance is typically many orders of magnitude smaller than the characteristic physical dimensions of the system of interest, the use of explicit methods to integrate relaxation equations often result in excessively long computation times. An implicit integration method which is inherently stable in all flow situations (whether near equilibrium or frozen) is therefore used by the computer program. With this method, step sizes which are of the order of the physical dimensions of the system of interest can be used, reducing the computation time per case several orders of magnitude when compared with conventional explicit integration methods.

Equations (5)-(8) constitute N first order simultaneous differential equations

$$\frac{dy_i}{dx} = f_i\,(x, y_i, \ldots, y_N) \qquad i = 1, 2, \ldots, N$$

with known partial derivatives (i.e., the Jacobian for the system)*

$$\alpha_i = \frac{\partial f_i}{\partial x} \quad , \quad \beta_{i,j} = \frac{\partial f_i}{\partial y_j}$$

The following implicit difference equations are used by the computer program to determine the $y_{i,n+1}$ (the subscript n denotes the nth integration step)

$$y_{i,n+1} = y_{i,n} + \Delta y_{i,n+1} \quad , \quad h = x_{n+1} - x_n$$

where the Δy increment $\Delta y_{i,n+1}$ is solved implicitly from one of the following three recipes

$$\Delta y_{i,n+1} = \left[f_{i,n} + \alpha_{i,n}\, h + \sum_{j=1}^{N} \beta_{i,j,n} \Delta y_{j,n+1} \right] \cdot h$$

*The computer program uses analytic expressions for calculation of the partial derivatives α_i, $\beta_{i,j}$. These may be printed with the output, if desired.

for the initial step and for restart (first order),

$$\Delta y_{i,n+1} = \frac{1}{3}\left[\Delta y_{i,n} + 2\left(f_{i,n} + \alpha_{i,h}\, h + \sum_{j=1}^{N} \beta_{i,j,n}\Delta y_{j,n+1}\right) \cdot h\right]$$

for equal steps (second order with h = previous h)

$$\Delta y_{i,n+1} = \frac{h_{n+1}^2}{(2h_{n+1} + h_n)\cdot h_n}\left[\Delta y_{i,n} + \left(f_{i,n} + \alpha_{i,n}\, h_{n+1} + \sum_{j=1}^{N} \beta_{i,j,n}\Delta y_{j,n+1}\right) \cdot \frac{h_n}{h_{n+1}}\left(h_{n+1} + h_n\right)\right]$$

for unequal steps (second order with h $\neq$ previous h).

If the flow is frozen, the explicit form of the above equations can be used ($\alpha_i = 0$, $\beta_{ij} = 0$), i.e. the implicit difference equations given above are each reduced from an NXN system of linear simultaneous equations to N explicit equations (N = 3 + no. of species).

Control of the integration step size, h, is provided by calculating estimates for the truncation error and comparing these to an input criterion, δ. The step size is halved if for any i = 1, 2, ..., N: $E_i > \delta$. The step size is doubled if for all i = 1, 2, ..., N: $E_i < \delta/10$

where

$$E_i = \left|\frac{\Delta y_{i,n+1} - 2\Delta y_{i,n} + \Delta y_{i,n-1}}{3\Delta y_{i,n+1} - \Delta y_{i,n}}\right|$$

The above expression for E_i is derived in Ref. 2.

APPENDIX B

APPROXIMATION TECHNIQUES FOR ARRHENIUS RATE COEFFICIENTS

When no other resources are available for rate determination, the following estimates prove to be useful. For rate constants represented by an Arrhenius equation,

$$k = AT^{-n} \exp(-B/RT)$$

where T is the absolute temperature, R is the gas constant, B is the activation energy, and N determines the pre-exponential temperature dependence, approximations have been made as follows:

(1) Exothermic, termolecular reactions

$$B + C + M \rightleftarrows BC + M \quad , \quad k = 3 \times 10^{16}\, T^{-0.5}$$

(2) Exothermic, bimolecular reactions with triatomic transition states

$$B + CD \rightleftarrows BC + D \quad , \quad k = 5 \times 10^{11}\, T^{0.5} \exp(-B/RT)$$

where E = 5.5% of the CD bond energy

(3) Exothermic, bimolecular reactions with transition states of more than three atoms

$$BC + DE \rightleftarrows BCD + E \quad , \quad k = 1 \times 10^{11}\, T^{0.5} \exp(-B/RT)$$

where E = 5.5% of the DE bond energy

(4) Exothermic, bimolecular, binary exchange reactions

$$BC + DE \rightleftarrows BD + CE \quad , \quad k = 1 \times 10^{10}\, T^{0.5} \exp(-B/RT)$$

where B = 28% of the sum of the BC and DE bond energies.

The above method of estimating exothermic reaction rates are similar to those used by Tunder et al. (1966).

The bond dissociation energy, D, for molecule BC was taken as

$$D = (\Delta H_f^0 \text{ of B}) + (\Delta H_f^0 \text{ of C}) - (\Delta H_f^0 \text{ of BC})$$

where the heats of formation are at 298.15°K. These ΔH_f^0 are given in Table B.1 for the species used in this study. The species are listed in alphanumeric order. The heat of reaction is taken as the sum of the $\Delta H^o_{f_{298}}$ of the products (RHS) minus the sum of $\Delta H^o_{f_{298}}$ of the reactants (LHS). Thus, if the sign is positive then the reaction is endothermic left to right, while if the sign is negative then the reaction is exothermic left to right. The heats of formation used in this study were taken from the JANAF Tables (1971).

Table B.1

BOND DISSOCIATION ENERGIES

Estimates from JANAF
(D kcal/mole)

D_{H-H}	=	104.2
D_{N-H}	=	85.9
D_{N-N}	=	226.0
D_{N-O}	=	151.0
D_{O-H}	=	102.3
D_{O-O}	=	119.2

APPENDIX C

THERMOCHEMICAL PROPERTIES OF METHOXYL, CH_3O

The thermochemical properties of methoxyl (CH_3O, free radical on the O-atom) are not tabulated in the JANAF Tables (1971) , nor are they in the more recent compilation by Bahn (1973). The necessary data can all be computed from the specific heat which can be calculated from the Meghreblian, Crawford, and Parr method [Reid and Sherwood (1966)] from the equation

$$C_p^o = 4R + \Sigma q_i C_{\nu_i} + \frac{3n - 6 - \Sigma q_i}{\Sigma q_i} \Sigma q_i C_{\delta_i} = A + BT + CT^2$$

where

C_p^o = ideal-gas heat capacity at constant pressure
= $C_\nu^o + R$, cal/gm-mole°K

4R = 3/2R (for translation) + 3/2R (for external rotation) + R

n = number of atoms in the molecule

q_i = number of bonds of the ith type

C_{ν_i}, C_{δ_i} = Einstein function, i.e., $RX^2 e^x/(e^x - 1)^2$

X = $h\nu/kT$ or $h\delta/kT$

h = Planck's constant, 1.58×10^{-34} cal-sec/molecule

ν = characteristic frequency for stretching vibrations, sec^{-1}

δ = characteristic frequency for bending vibrations, sec^{-1}

k = Boltzmann's constant, 3.29×10^{-29} cal/molecule°K

T = Temperature, °K

The following data are taken from Table 5-3 of Reid and Sherwood (1966):

Bond i	q_i for CH_3O	ω_ν, wave number, cm^{-1}	Stretching, $C_{\nu i}$			ω_δ, wave number, cm^{-1}	Bending, $C_{\delta i}$		
			A	$B \times 10^3$	$C \times 10^6$		A	$B \times 10^3$	$C \times 10^6$
C-H	3	3000	-0.139	0.168	0.447	1050	-0.579	3.741	-1.471
C-O	1	1030	-0.458	3.722	-1.471	1120	-0.665	3.757	-1.449

With these values we find

$$A = 4.0705$$
$$B = 22.951 \times 10^{-3}$$
$$C = -7.4575 \times 10^{-6}$$

The representation for the specific heat

$$C_p^o = A + BT + CT^2$$

is valid only up to some value T^* determined from

$$\frac{d C_p^o}{dT}(T^*) = 0 \longrightarrow T^* = \frac{-B}{2C}$$

$$C_{p\,max}^o = A - \frac{B^2}{4C} \text{ at } T = T^*$$

For $T \geq T^*$ we have $C_p = C_{p\,max}^o$ (fully excited, electronic contributions are not included). For methoxyl,

$$T^* = 1539^oK$$

$$C_{p\,max}^o = 21.729 \text{ cal/gm-mole}^oK$$

Once the specific heat is determined, the enthalpy, entropy, and free energy functions are determined from classical thermodynamics, viz.,

$$\left(\frac{\partial H^o}{\partial T}\right)_p = C_p^o \rightarrow H^o = \Delta H_f^o + \int_{T_o}^{T} C_p^o \, dT$$

$$\left(\frac{\partial S^o}{\partial T}\right)_p = \frac{C_p^o}{T} \rightarrow S^o = S_{T_o}^o + \int_{T_o}^{T} \frac{C_p^o}{T} \, dT$$

$$F^o = H^o - TS^o$$

These equations can be interpreted and expressed in terms of the parameters A, B, and C and finally tabulated in the same fashion as presented in the JANAF Tables (1971). (This form is necessary for inclusion in the KAP program.) The results are shown in Table C.1.

Table C.1

THERMODYNAMIC FUNCTIONS FOR METHOXYL (CH_3O)

$T, {}^oK$	C_p^o, $\frac{cal}{mole\text{-}{}^oK}$	$H^o-H^o_{298}$, $\frac{kcal}{mole}$	$-(F^o-H^o_{298})/T$, $\frac{cal}{mole\,{}^oK}$
100	6.2910	1.0514	7.0265
200	8.3624	2.5853	38.3951
300	10.2846	3.5189	43.3452
400	12.0577	4.6373	46.6839
500	13.6816	5.9255	49.2922
600	15.1564	7.3686	51.4880
700	16.4820	8.9518	53.4178
800	17.6585	10.6600	55.1596
900	18.6858	12.4785	56.7599
1000	19.5640	14.3922	58.2477
1100	20.2930	16.3863	59.6430
1200	20.8729	18.4459	60.9595
1300	21.3036	20.5559	62.2073
1400	21.5852	22.7016	63.3939
1500	21.7176	24.8680	64.5252
1600	21.7288	27.0407	64.9663
1700	21.7288	29.2136	65.0543
1800	21.7288	31.3865	65.2037
1900	21.7288	33.5594	65.4008
2000	21.7288	35.7323	65.6355
2100	21.7288	37.9052	65.8995
2200	21.7288	40.0780	66.1866
2300	21.7288	42.2509	66.4917
2400	21.7288	44.4238	66.8108
2500	21.7288	46.5967	67.1405
2600	21.7288	48.7696	67.4783
2700	21.7288	50.9425	67.8221
2800	21.7288	53.1154	68.1700
2900	21.7288	55.2882	68.5207
3000	21.7288	57.4611	68.8731
3100	21.7288	59.6340	69.2260
3200	21.7288	61.8069	69.5788
3300	21.7288	63.9798	69.9308
3400	21.7288	66.1527	70.2815
3500	21.7288	68.3255	70.6304
3600	21.7288	70.4984	70.9771
3700	21.7288	72.6713	71.3215
3800	21.7288	74.8442	71.6631
3900	21.7288	77.0171	72.0019
4000	21.7288	79.1900	72.3377
4100	21.7288	81.3629	72.6704
4200	21.7288	83.5357	72.9998
4300	21.7288	85.7086	73.3260
4400	21.7288	87.8815	73.6488
4500	21.7288	90.0544	73.9682
4600	21.7288	92.2273	74.2843
4700	21.7288	94.4002	74.5969
4800	21.7288	96.5730	74.9062
4900	21.7288	98.7459	75.2121
5000	21.7288	100.9188	75.5146

TECHNICAL REPORT DATA
(Please read Instructions on the reverse before completing)

1. REPORT NO. EPA-650/2-74-045	2.	3. RECIPIENT'S ACCESSION NO.
4. TITLE AND SUBTITLE Kinetic Mechanism of Methane/Air Combustion with Pollutant Formation		5. REPORT DATE June 1974
		6. PERFORMING ORGANIZATION CODE
7. AUTHOR(S) C. H. Waldman, R. P Wilson, Jr., and K. L. Maloney		8. PERFORMING ORGANIZATION REPORT NO.
9. PERFORMING ORGANIZATION NAME AND ADDRESS Ultrasystems, Inc 2400 Michelson Drive Irvine, CA 92664		10. PROGRAM ELEMENT NO. 1AB014; ROAP 21ADG-10
		11. CONTRACT/GRANT NO. 68-02-0270
12. SPONSORING AGENCY NAME AND ADDRESS EPA, Office of Research and Development NERC-RTP, Control Systems Laboratory Research Triangle Park, NC 27711		13. TYPE OF REPORT AND PERIOD COVERED Final
		14. SPONSORING AGENCY CODE
15. SUPPLEMENTARY NOTES		

16. ABSTRACT

The report gives results of the evaluation of a large set of chemical reactions describing methane/air combustion to determine the significant reactions at atmospheric pressure, at temperatures of 1500-2500K, and at equivalence ratios of 0.8-1.25. The reactions were screened to eliminate: reactions with negligible net contribution to heat evolution or pollutant formation, species with no discernible effect on major species or temperature, and groups of reactions constituting only species exchange loops. A set of 26 reactions/17 species was derived which can duplicate within 5 percent the predictions of the 134-reaction/25-species master set. Ten additional pyrolysis reactions are cited for low-temperature and fuel-rich applications. The Zeldovich mechanism is the principal route to NO for stoichiometric combustion, but under lean conditions, a path to NO involving N2O is also active. For fuel-rich conditions, comparison with stirred reactor data suggests that NO formation cannot be explained by the Zeldovich mechanism alone: an alternate path involving species of the type RN may be of importance. Finally, prompt NO arising from oxygen-atom overshoot was not predicted for an idealized plug flow ignition case.

17. KEY WORDS AND DOCUMENT ANALYSIS

a. DESCRIPTORS	b. IDENTIFIERS/OPEN ENDED TERMS	c. COSATI Field/Group
Air Pollution	Air Pollution Control	13B, 07D
Reaction Kinetics	Methane/Air	12A
Mathematical Models	Chemical Heat Release	21B
Combustion		07B
Nitrogen Oxide (NO)		
Nitrogen Oxide (N2O)		07C
Methane		

18. DISTRIBUTION STATEMENT Unlimited	19. SECURITY CLASS *(This Report)* Unclassified	21. NO. OF PAGES 102
	20. SECURITY CLASS *(This page)* Unclassified	22. PRICE

EPA Form 2220-1 (9-73)